UNIVERSITY OF WOLLONGONG AUSTRALIA

University of Wollongong - Research Online

Thesis Collection

Title: Preliminary ion mobility mass spectrometric studies on fullerenyl bisadducts

Author: Qing Xiang Zhang

Year: 2009

Repository DOI:

Copyright Warning
You may print or download ONE copy of this document for the purpose of your own research or study. The University does not authorise you to copy, communicate or otherwise make available electronically to any other person any copyright material contained on this site.
You are reminded of the following: This work is copyright. Apart from any use permitted under the Copyright Act 1968, no part of this work may be reproduced by any process, nor may any other exclusive right be exercised, without the permission of the author. Copyright owners are entitled to take legal action against persons who infringe their copyright. A reproduction of material that is protected by copyright may be a copyright infringement. A court may impose penalties and award damages in relation to offences and infringements relating to copyright material.
Higher penalties may apply, and higher damages may be awarded, for offences and infringements involving the conversion of material into digital or electronic form.

Unless otherwise indicated, the views expressed in this thesis are those of the author and do not necessarily represent the views of the University of Wollongong.

Research Online is the open access repository for the University of Wollongong. For further information contact the UOW Library: research-pubs@uow.edu.au

University of Wollongong Thesis Collections

University of Wollongong Thesis Collection

University of Wollongong *Year* 2009

Preliminary ion mobility mass spectrometric studies on fullerenyl bisadducts

Qing Xiang Zhang
University of Wollongong

Zhang, Qing Xiang, Preliminary ion mobility mass spectrometric studies on fullerenyl bisadducts, Master by Reseach thesis, School of Chemistry, University of Wollongong, 2009. http://ro.uow.edu.au/theses/3101

This paper is posted at Research Online.

NOTE

This online version of the thesis may have different page formatting and pagination from the paper copy held in the University of Wollongong Library.

UNIVERSITY OF WOLLONGONG

COPYRIGHT WARNING

You may print or download ONE copy of this document for the purpose of your own research or study. The University does not authorise you to copy, communicate or otherwise make available electronically to any other person any copyright material contained on this site. You are reminded of the following:

Copyright owners are entitled to take legal action against persons who infringe their copyright. A reproduction of material that is protected by copyright may be a copyright infringement. A court may impose penalties and award damages in relation to offences and infringements relating to copyright material. Higher penalties may apply, and higher damages may be awarded, for offences and infringements involving the conversion of material into digital or electronic form.

Preliminary Ion Mobility Mass Spectrometric Studies on Fullerenyl Bisadducts

A thesis submitted in fulfillment of the requirements for the award of the degree

Master by Research

from

University of Wollongong

by

Qing Xiang Zhang

Supervisor: Assoc. Prof. Paul Keller
Prof. Stephen Pyne

School of Chemistry

2009

Declaration

I declare that this thesis, submitted in fulfillment of the requirements for the award of the degree of Master by Research, in the School of Chemistry, Faculty of Sciences, University of Wollongong, does not contain any material which has been accepted for the award of any degree or diploma in this or any other academic institution and to my best knowledge and belief contains no material in any previous publication except where due reference has been acknowledged.

Qing Xiang Zhang

November, 2009

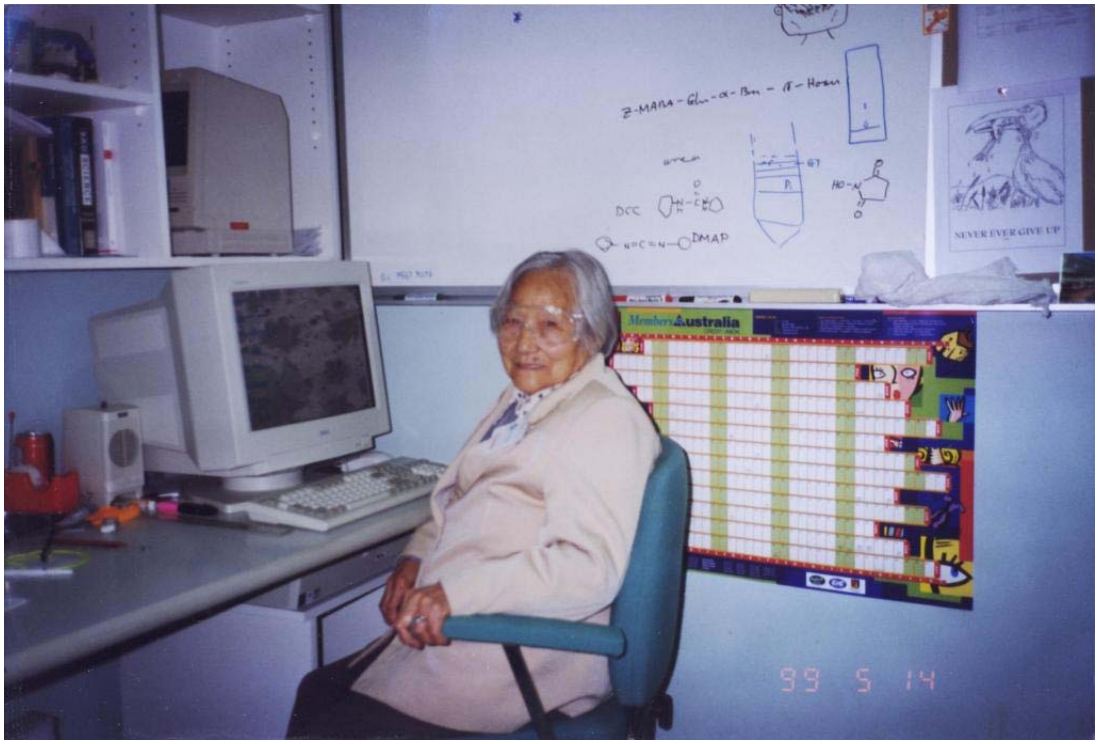

in the memory of my dear granny…

Table of Contents

List of Figures

List of Schemes

List of Tables

List of Abbreviations

°C	degree celsius
^{13}C-NMR	carbon nuclear magnetic resonance
^{1}H-NMR	proton nuclear magnetic resonance
2-D	two dimensional
3-D	three dimensional
Ac	acetate
Ar	aromatic
Bu	butyl group
C	coulomb
C	carbon
cm	centimeter
CPE	coulometrically controlled potential electrolysis
d	doublet
DBU	1,8-diazabicyclo[5.4.0]undec-7-ene
dd	doublet of doublets
DNA	deoxyribonucleic acid
dt	doublet of triplets
E	electronic field strength
equiv.	equivalence
ESI	electronspray ionisation
ESR	electron spin resonance
Et	ethyl
eV	electron volt
g	gram
g·cm^{-3}	gram per cubic centimeter

h	hour
HIV	human immunodeficiency virus
HIV-1	type one of Human immunodeficiency virus
HIVP	HIV-1 protease
HOMO	highest occupied molecular orbital
HPLC	high performance liquid chromatography
Hz	Hertz
IMMS	ion mobility mass spectrometry
IMS	ion mobility spectrometry
IPR	isolated pentagon rule
IR	infrared
J	coupling constant (Hz)
K	degree Kelvin
kJ	kilojoule
kV	kilovolt
L	liter
LUMO	lowest unoccupied molecular orbital
LUMO + 1	second lowest unoccupied molecular orbital
m	multiplet
m	*meta*
m/s	meter per second
m/z	mass to charge ratio
mbar	millibar
MCPBA	*m*-chloroperoxybenzoic acid
Me	methyl
mg	milligram
MHz	megahertz
ml	milliliter

mmol	millimole
mol	mole
Mpa	Megapascal
MS	mass spectrometry
ms	millisecond
nm	nanometer
NMR	nuclear magnetic resonance
ns	nanosecond
o	*ortho*
p	*para*
P	pressure
PBMC	peripheral blood mononuclear cells
pm	picometre
ppm	part per million
q	ion charge
Ref.	reference
RG	reactive group
rt	room temperature
s	second
s	singlet
SAM	self-assembled monolayers
T	absolute temperature
t	triplet
t	tertiary
TBA^+	tetra-*n*-butyl ammonium cation
t_d	drift time
TDAE	tetrakis(dimethylamino)ethylene
tert	tertiary

THF	tetrahydrofuran
TMS	tetramethylsilane
TOF	time of flight
TOFMS	time-of-flight mass spectrometer
Torr	millimeter of mercury
UV	ultraviolet
UV-Vis	ultraviolet-visible
V	volt
V_d	drift velocity
δ_c	chemical shift on ^{13}C-NMR spectra
μs	microsecond

Acknowledgements

On completion of my thesis I would like to thank

- ✓ Paul and Steve for their frequent discussion and help throughout the period of my study, which will always be appreciated;
- ✓ Wilford for NMR training and help with interpretation, as well as all kinds of non-academic conveniences and advices he has provided to me;
- ✓ Mohammed, Ari and Kittya for their friendly companies during lab work time;
- ✓ Andrew, Steve Wales and all other members of Keller's group for their help and support;
- ✓ Marc Bouillon in Pyne's group for his kind advices on lab work skills such as TLC staining, as well as generous donation of solvents such as toluene, when Keller's group was temporarily short of them;
- ✓ Steve Blanksby and Thitima for their MS and IMMS work and discussions;
- ✓ Many thanks to Dr. Xin Wei for his online assistances.

Abstract

In this study, four selected regioisomeric tetraethyl bismethano[60]fullerenyl tetracarboxylates (*trans-4*, *e*, *cis-2* and *cis-3* symmetry patterns) were prepared through the chemical methods reported in the literature with satisfactory yields and purities. They were subsequently analysed by ion mobility mass spectrometry (IMMS) to examine the potential of this method to resolve fullerenyl bisadduct regioisomers of the same molecular weights based on their different cross-sectional areas. This study was also of interest to see if these regioisomeric compounds would undergo a "walk-on-the-sphere" rearrangement under the reductive conditions of – ve ion mode ESIMS.

The tethered bisadducts **(40)**, **(41)**, **(43)**, **(44)** and **(46)** were chemically prepared according to Nierengarten's report giving the desired products with satisfactory yields and purities. Transesterification of these tethered bisadducts with distilled and dry methanol generated the non-tethered bisadducts **(47)** – **(50)**.

The employment of IMMS in this study was to enable a comparison of the cross-sectional areas of the tethered and non-tethered [60]fullerenyl bisadducts, providing some structural information that might be useful for further studies of fullerenyl derivatives of complicated structures in the future. The size of the cross-sectional area of a fullerenyl derivative was directly reflected by the length of the drift time required to travel through the drift tube of the spectrometer, in both the + ve and – ve ion modes. In the case of this study, all of the four non-tethered bisadducts **(47)** – **(50)** may have experienced an incomplete "walk-on-the-sphere" rearrangement under the reductive conditions of their – ve ion IMMS studies. Further improvements of experimental conditions might be necessary in order to enhance the occurrence of such rearrangements in future studies.

Chapter 1: Introduction

1.1 Fullerene

By definition fullerene refers to a series of carbon atom clusters (such as C_{44}, C_{50}, C_{60}, C_{70}, C_{76}, C_{78}, C_{80}, C_{82}, C_{84}, C_{90}, C_{94}, C_{96}, C_{120}, C_{180}, C_{240}, C_{540}, etc.) consisting of non-planar pentagons and hexagons that form hollow and closed spherical, elliptical or tubular conjugated polyenes. In many cases the term fullerene specifically refers to C_{60} ([60]fullerene) which is the most intensely and widely studied member. Discovered in 1985,[1] the fullerene family has become the third allotrope of carbon following diamond and graphite.

1.1.1 Discovery

In 1985, an experiment was carried out by Kroto, Curl and Smalley with an assembled apparatus at Rice University. After being vaporised by a laser beam followed by the application of an ultrasonic wave produced by helium of 1Mpa, a sample of graphite was shattered into vaporised carbon atoms. These atoms, subsequently, passed through a nozzle into a vacuum environment where they expanded, cooled down rapidly and led to the formation of unknown new carbon molecules. Mass spectrometry showed that one new molecule was made up of 60 atoms (C_{60}).[1] Its true structure, however, puzzled Smalley at the time. Later, inspired by the shape of the round roof of Montreal's Biosphère designed by architect Richard Buckminster Fuller [Figure 1.1 (a)], Smalley cut 12 pentagons and 20 hexagons out of a piece of hardboard and put them together to form a spheroid with a total of 60 vertices [Figure 1.1 (b)].[1,2] The structure of this new carbon molecule C_{60} was thus determined and nominated Bucky ball in order to commend the architect for his contribution in its structural determination. Alternative names such as Buckminster fullerene, Buckminsterene, and fullerene are also found in a large number of references while fullerene is most frequently used. In addition, C_{60} is also sometimes referred to as footballene for its similarity to a football in shape [Figure 1.1 (c)]. Following C_{60}, higher order homologues of the fullerene family like C_{70}, C_{76},

C_{82}, C_{84}, etc. were found successively.[3] The great discovery of C_{60} led to the 1996 Nobel Prize for Chemistry shared by Harold W. Kroto, Richard E. Smalley and Robert F. Curl.

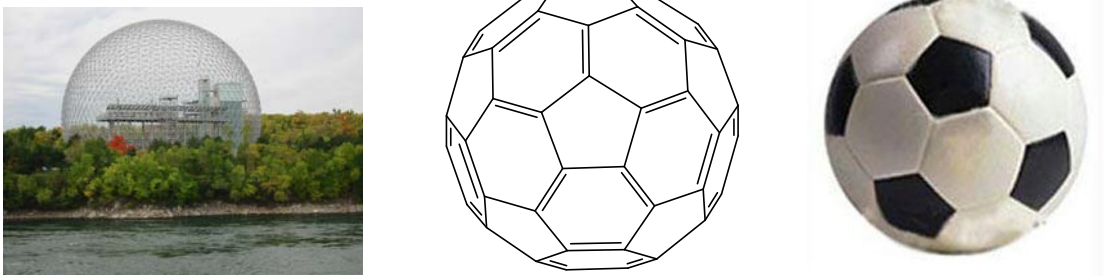

(a) (b) (c)

Figure 1.1: Structural similarities among (a) the Montreal Biosphère (designed by Richard Buckminster Fuller in 1967, http://unusual-architecture.com/montreal-biosphere-canada/); (b) C_{60} shape hypothesised by R. E. Smalley and (c) a common football.

1.1.2 Structure

At the time when C_{60} was discovered by Kroto, Curl and Smalley an efficient method for the milligram scaled synthesis of C_{60} was not available and further analysis on this newly discovered molecule was impossible without an adequate supply. Therefore structural studies were carried out through pure theoretical calculation and deduction until 1990 when Kratschmer and Huffman *et al*. successfully developed a scaled-up C_{60} synthesis method (the carbon arc light method), fulfilling further research activities on the carbon allotrope.[4,5] Systematically C_{60} is named [5,6]-fullerene-60-I_h,[6] which indicates some of its important structural and stereotypic characters: pentagons and hexagons partitioned by 60 carbon atoms and the icosahedral molecular symmetry. All the 60 carbon atoms as vertices form totally 32 planar faces, 12 of which are pentagons and the other 20 are hexagons. sp^2-Hybridised, each carbon atom forms 3 sigma bonds with its 3 adjacent carbon atoms through head-to-head overlap, with each bond angle being nearly 116 degrees due to non-coplanarity. There is, on each of the 60 carbon atoms, a remaining *p* electron forming a huge and delocalised π electron cloud covering both the inside and the outside of the spheroid molecule surface. The spherical C_{60} molecule has a diameter of 710 pm.

With each of its pentagons being surrounded by 5 hexagons, C_{60} is the smallest molecule that conforms to the isolated pentagon rule (IPR)[1,5] which does not allow adjacent pentagons. Bonds are alternating in length, 0.140 nm between two hexagons and 0.146 nm between one hexagon and one pentagon,[3] and therefore its energy level can be minimised by assigning double bonds to 6,6 junctions and single bonds to 5,6 junctions. In this sense, pentagons and hexagons in the C_{60} molecule can be regarded as cyclohexatriene and radiapentalene respectively. Therefore a total of 60 single bonds and 30 double bonds divide the spherical surface into its 12 pentagons and 20 hexagons. Some structural properties of C_{60} are illustrated in Figure 1.2.

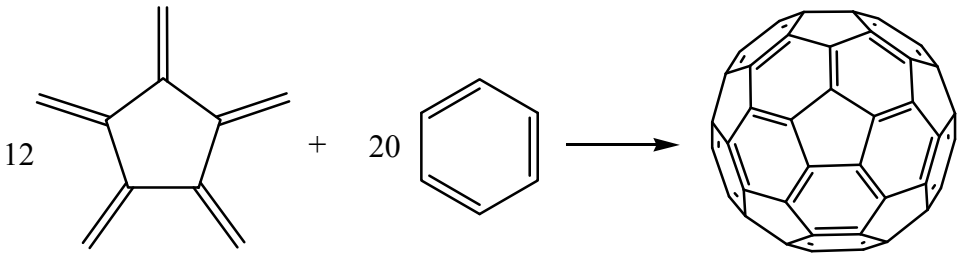

Figure 1.2: C_{60} structural characters presented in the Kekulé formulas. Actually all bonds in pentagons are of the same length (0.146 nm) and all bonds at junctions between hexagons are also of the same length (0.140 nm). The C_{60} surface is covered on both sides by a huge and delocalised electron cloud formed by a total of 60 π electrons. All bond angles are approximately 116 degrees.

Spectroscopically the C_{60} molecule is characterised by four strong absorption signals in the infrared (IR, 1429, 1183, 577 and 528 cm^{-1}),[7] and one signal in the ^{13}C-NMR spectrum (δ_c = 143.2 ppm).[8] Dissolved in hexane, C_{60} shows the strongest absorptions at 328 nm, 256 nm and 211 nm in its ultraviolet spectrum (Figure 1.3).[9]

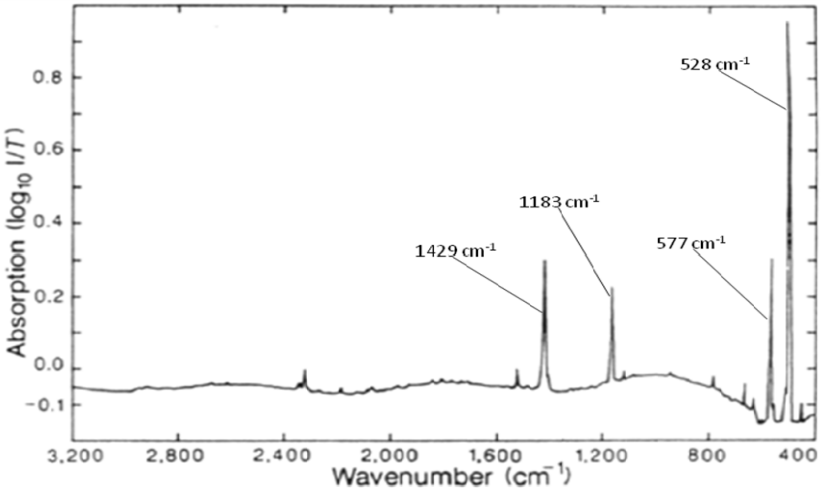

(a)

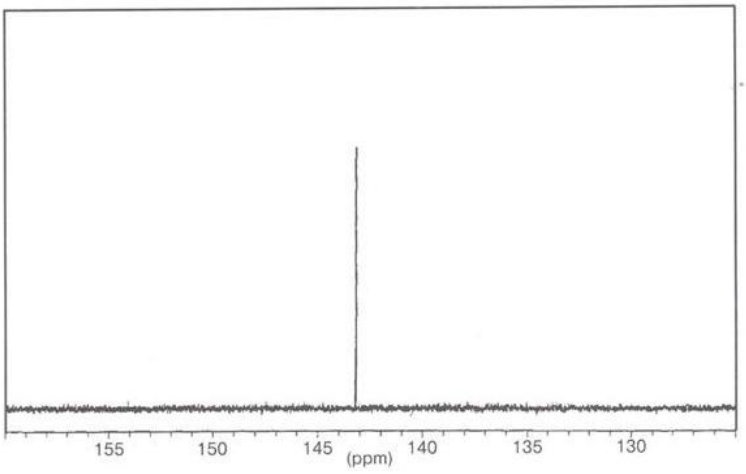

(b)

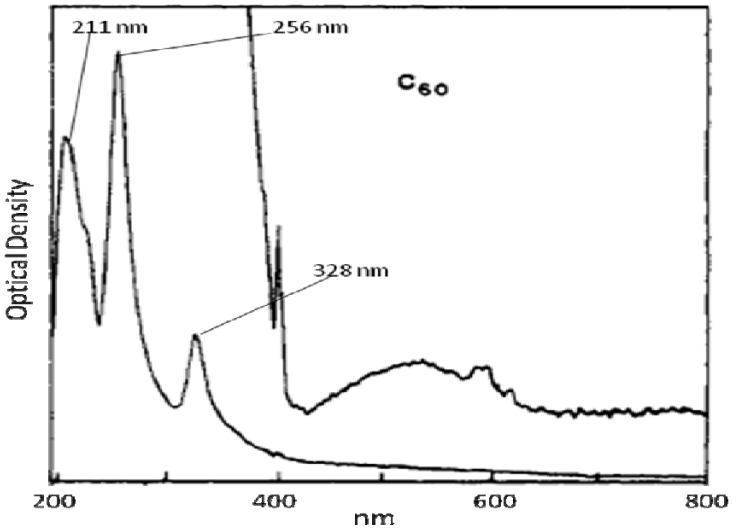

(c)

Figure 1.3: C_{60} Spectra. (a) IR (soot); (b) ^{13}C-NMR ($CDCl_3$); (c) UV-Vis (part of amplified spectrum above the normal spectrum also shown). (a) and (c) are derived from reference 2; (b) is adapted from reference 3.

1.1.3 Physical and Chemical Properties

Pure C_{60} appears as a brownish black solid, weighs 1.7 $g \cdot cm^{-3}$ and is insoluble in water. However, it possesses limited solubility in non-polar solvents such as hexane, benzene, toluene, carbon disulfide and carbon tetrachloride. C_{60} is more readily dissolved in aromatic solvents. It turns crimson when dissolved in benzene and purple in toluene.

The C_{60} cage is relatively stable and readily undergoes reactions such as hydrogenation, oxidation, electrophilic addition, nucleophilic addition, radical reactions as well as reactions with metals.[10] The C_{60} chemical reactivity will be briefly reviewed in the second part of this chapter.

1.1.4 Applications

Research activities following the discovery of fullerene led to a heavy disappointment for the fact that fullerene and its derivatives were not soon ready for the market as had been expected.[10] Nevertheless, more potential has been predicted, especially in the fields of biomedical and material sciences.[10,11] In most cases new derivatives retain the main properties of the original fullerene while their processibilities have been improved. For this reason researchers are still optimistic about realising applications of functionalised fullerene molecules in the future.

1.1.4.1 Prospective Biological Applications

Chemical functionalisations have improved the solubility in physiological media by attaching hydrophilic appendages to C_{60}.[12-15] Homogeneously dissolved fullerene or its derivatives exhibit their potential applications in photodynamic therapy, anti-HIV activity (through inhibition of HIV-1 protease), neuroprotection and anti-apoptosis.

C_{60} can be excited to the long-lived (lifetime = 50-100 μs) triplet state via the short-lived (lifetime = 1.3 ns) singlet intermediate. The former turns molecular oxygen into strongly oxidative singlet oxygen by efficient energy transfer.[16] By this mechanism C_{60} deactivates enveloped viruses such as Togaviridae and Rhabdoviridae that are sensitive to strong oxidants.[17] The cytotoxicity of the fullerene derivative **(1)** on irradiation has been demonstrated in terms of DNA cleavage (usually selective at guanosine sites) by the supposed mechanism of electron transfer rather than the existence of singlet oxygen.[18] An *in vitro* study on tumor infected mice showed **(1)** inhibited tumor cell growth with specific chemotropism of this fullerene derivative towards the tumoral tissue.[19]

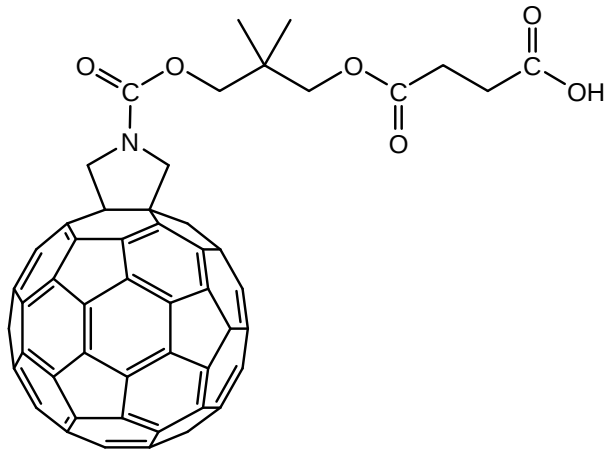

(1)

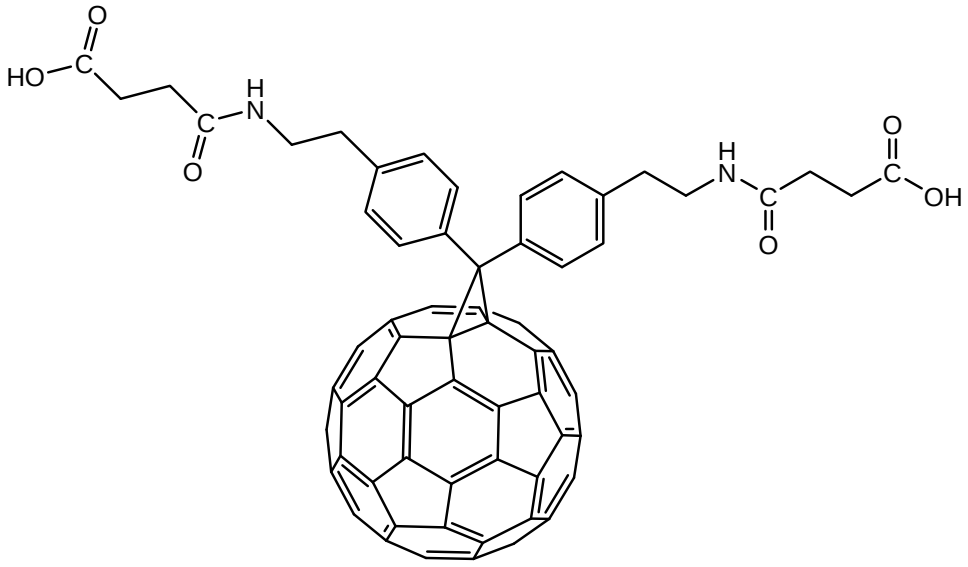

(2)

In another field scientists have demonstrated that HIV-1 protease (HIVP) is inhibited by

a water soluble fullerene derivative **(2)** having a suitable 3-D structure for accomodation into the HIVP active site.[20] The physiological effect was confirmed by a decrease in the number of peripheral blood mononuclear cells (PBMC) in hosts that were either acutely or chronically infected.[21] This result has stimulated more trials of functionalised fullerene candidates in anti-HIVP studies in the hope of an optimised therapy.[22-24]

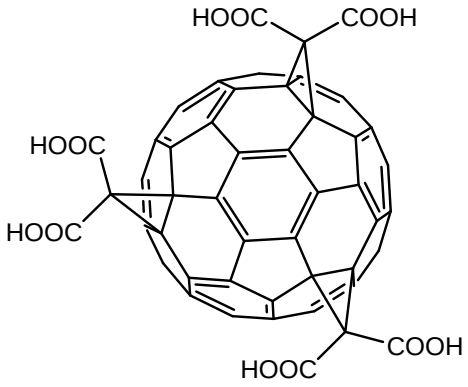

(3)

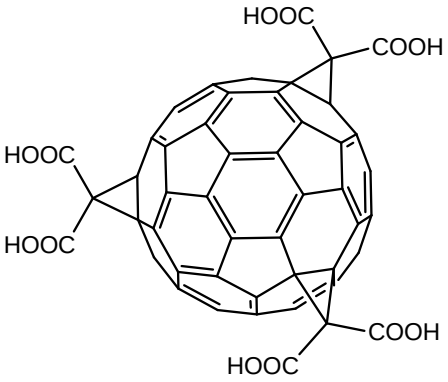

(4)

Neurodegenerative diseases are usually caused by excessive production of superoxide and nitric oxide radicals resulting from overexcitation of glutamic acid receptors. Due to their antioxidant properties and their high reactivity toward free radicals, functionalised trismalonic acid adducts of C_{60}, **(3)** and **(4)**, also reduced death of cultured neural cells as well as increased the lifetime of model mice with amyotrophic lateral sclerosis.[25]

The trisadducts **(3)** and **(4)** were also found to be apoptosis inhibitors due to their ability to scavenge radicals which are formed during apoptosis.[25-27]

It is impossible to address the biomedical potentials of fullerene and its derivatives exhaustively. Researchers will continue their extensive efforts in order to increase pharmaceutical effects and minimise toxicity at the same time.

1.1.4.2 Potential Applications in Material Science and Technology

Early studies of C_{60} disclosed some of its physical properties such as non-linear optical

properties[28,29] and superconductivity in the form of M_3C_{60} species (M = alkali metals) with high critical temperatures.[30,31] Its advantages over superconductors of oxides are their 3-dimensional superconductivities that provide high stabilities and current densities as well as ideal plasticities into linear materials. In addition, $[TDAE^+]C_{60}$ was defined as an organic soft ferromagnet.[32] Extensive studies on functionalised fullerene derivatives later found their potentials in mainly these four fields: polymers, thin films, electrooptical devices and liquid crystals.

Polymers containing fullerenes can be obtained by chemical linking of fullerene to a preformed polymer,[32-37] a polymer being formed[37-40] or by polymerisation of fullerene-containing monomers.[41,42] Dendrimers have also been formed based on a fullerene nucleus.[43,44] In addition, 3-D starburst polyurethane networks can also be generated from fullerenols.[45,46]

As to the formation of fullerene containing thin films, control of organised structures is regarded as a priority, and therefore self-assembled monolayers (SAM) and Langmuir films are increasingly used to deliver fullerene properties to bulk materials by simple surface coating.[47,48]

Due to the inherently electron deficient property of C_{60}, it is believed that the design of novel molecular electronic devices by attaching electron-rich moieties (such as the ferrocene structure)[49] or π-conjugated polymers[50,51] to C_{60} should open a new realm of electrooptical devices.

After experiences of fluctuating fortune, efforts to utilise fullerene's practical application as novel materials continue with optimism with updated efficient methodologies.[10]

1.2 Chemical Reactivity of C_{60}

Rather than a "super aromatic" molecule as initially hypothesised, C_{60} was later found to be of a polyenic structure.[52] Because of deviation of all its double bonds from planarity[30] and pyramidalisation of C atoms (all sp^2-hybridised), the C_{60} molecule sustains excess geometrical strain. The driving force for most of its chemical reactivities is actually the release of such strain from sp^2 to sp^3 hybridisation of the C atom on the reaction site.[53] In fact, the majority of reactants react only with 6,6 double bonds that possess higher electron density while insertions into 5,6 single bonds were only reported as rearrangements following initial attack at the 6,6 junction.[10]

The disappointment following fullerene's discovery was the fact that the fullerene family could not find immediate practical applications. This was mainly attributed to its poor solubility. However, this provoked extensive studies of C_{60} chemical modification (also known as fullerene functionalisation) for the purpose of improved manipulation in solvents. With chemically attached "handles", C_{60} not only obtains better solubility which facilitates easier processing, but also becomes synthons for further assembly.[10]

1.2.1 Reduction

According to the theoretical molecular orbital calculation of C_{60}, its lowest unoccupied molecular orbitals (LUMO) and LUMO + 1 are triply degenerated with comparatively low energy,[54-57] suggesting the electronegativity of the molecule and being reducible up to the hexaanion (Figure 1.4),[58] which was further supported by cyclic voltammetry studies (Figure 1.5)[59] on C_{60} in solution. The latter showed its facile and stepwise reduction: such a study detected di- and trianions first,[60,61] and shortly later tetra-,[62] penta-[63] and hexaanions[59,64,65] at increased expansion of the available potential window.

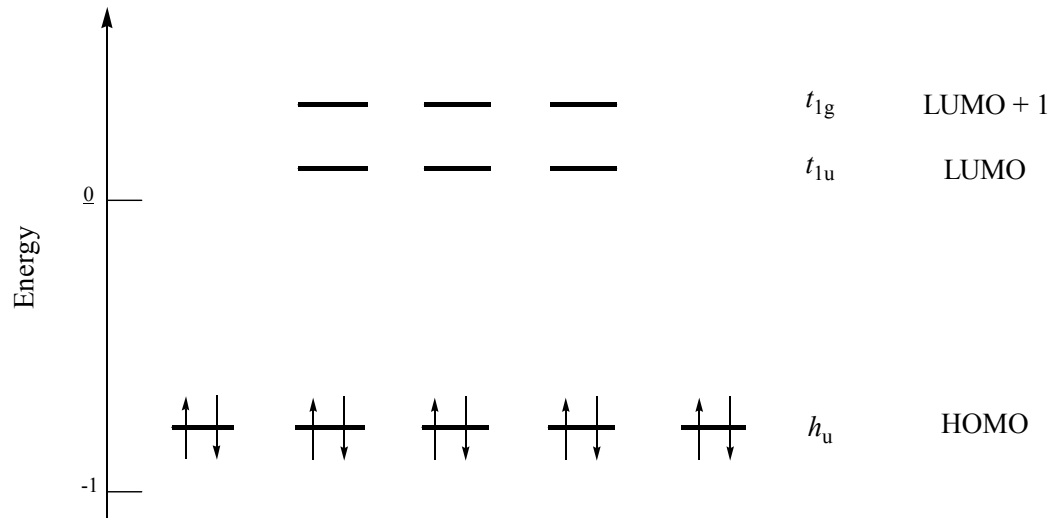

Figure 1.4: Partial Hückel molecular orbital diagram of C_{60} (only HOMO, LUMO and LUMO + 1 represented).[58]

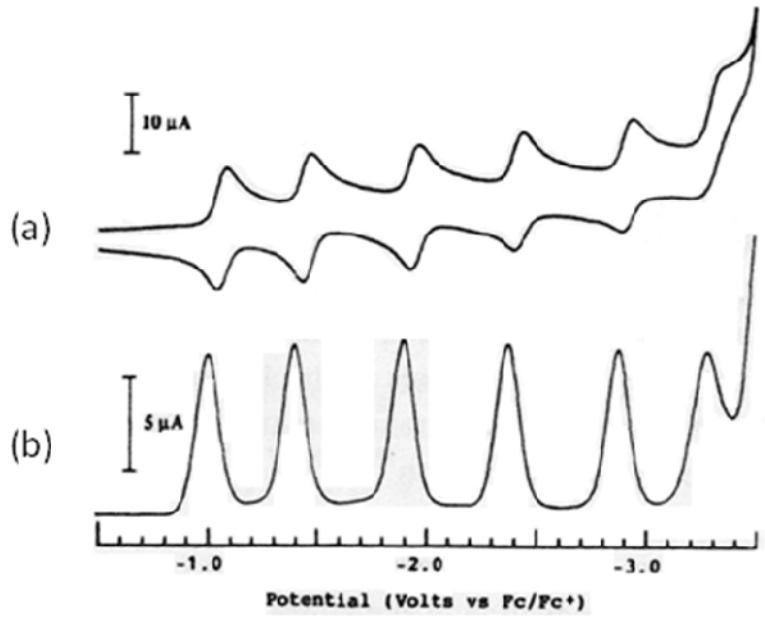

Figure 1.5: Reduction of C_{60} in CH_3CN/toluene at -10°C detected by (a) cyclic voltammetry; (b) differential pulse voltammetry.[59]

Following the discovery of reductivity of C_{60}, fulleride anions were generated either chemically or electrochemically.[3] In addition, some species containing C_{60} anions can be precipitated with a proper solvent, such as $C_{60}^{2-}(TBA^+)_2$ and $C_{60}^{-}(TBA^+)$ in acetonitrile (Scheme 1.6).[66]

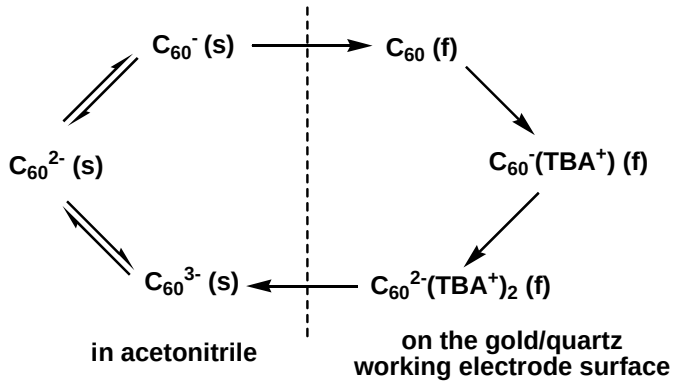

Figure 1.6: The circulatory stepwise reduction of C_{60} using tetra-*n*-butyl ammonium perchlorate ($TBAClO_4$) carried out in acetonitrile with a gold/quartz working electrode, on which reduced species $C_{60}^{2-}(TBA^+)_2$ and $C_{60}^{-}(TBA^+)$ are deposited as a film from acetonitrile dissolved C_{60}^{3-}, C_{60}^{2-} and C_{60}^{-}. "s" and "f" stand for "solution" and "film" respectively.[66]

Quenched by electrophiles, fulleride anions can undergo electrophilic additions to yield covalent organofullerene derivatives, which is illustrated by the synthesis of the simplest C_{60} dialkyl derivative, dimethyldihydro[60]fullerene (Scheme 1.1)[67] and a fullerenyl Pd-complex (Scheme 1.2).[68]

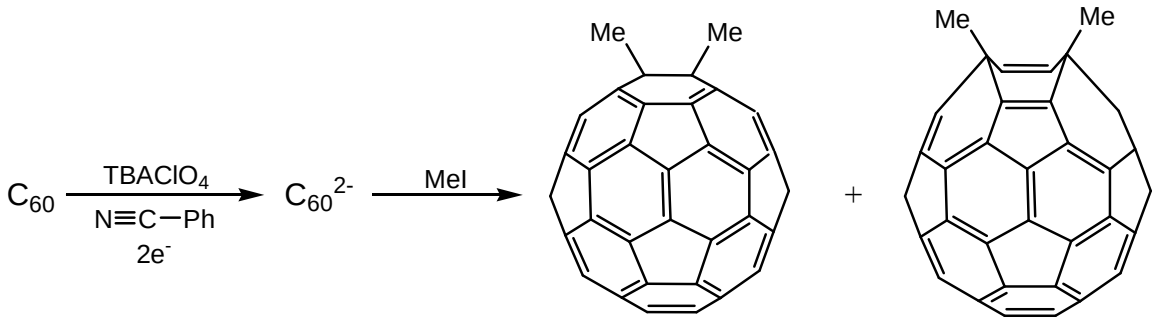

Scheme 1.1: Treatment of electrochemically generated C_{60}^{2-} with MeI gives rise to a mixture of 1,2- and 1,4-dimethyldihydro[60]fullerenes **(5)** and **(6)** in a ratio of 1.4:1. In this case the electrochemically generated C_{60}^{2-} readily undergoes alkylation with methyl iodide.[67]

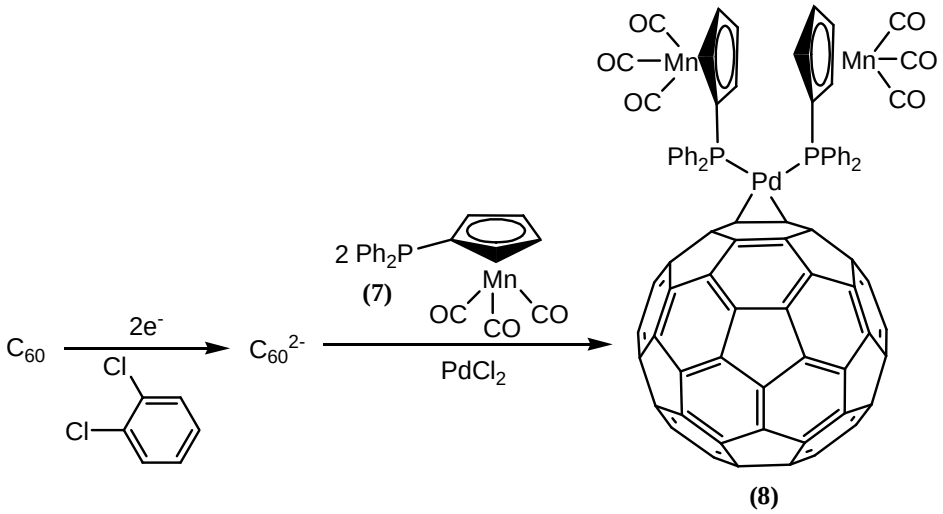

Scheme 1.2: Formation of the Pd-complex **(8)** through quenching the electrochemically generated C_{60}^{2-} by a phosphine ligand **(7)**.[68]

In addition to chemical precipitation and electrochemical ionisation, C_{60} can also be reduced directly by alkali metals (in suitable solvents),[69-77] alkaline earth metals (vapor) and mercury,[78] as well as organic or organometallic donor molecules such as tetrakis(dimethylamino)ethylene (TDAE) to form $[TDAE^{+}]C_{60}^{-}$ (Scheme 1.3).[79]

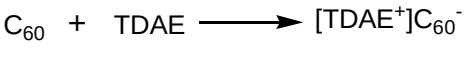

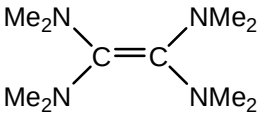

tetrakis(dimethylamino)ethylene (TDAE)

Scheme 1.3: Direct reduction of C_{60} by the electron-donor TDAE.[79]

1.2.2 Nucleophilic Addition

The alternating short (between any two hexagons) and long bonds (between a pentagon and a hexagon) distributed on the C_{60} sphere implies that its chemical behaviours are like those of an electron-deficient, conjugated polyolefin rather than a "superarene", therefore theoretically additions by nucleophiles (of carbon, nitrogen and oxygen types) can easily occur to C_{60}.[6]

Carbon nucleophiles include organolithium and Grignard compounds. Their alkyl, phenyl or alkynyl derivatives readily add to C_{60} to give the intermediate anion RC_{60}^-. These are converted to $RC_{60}H$ products upon the addition of water to the reaction mixture. As examples, *t*-BuC_{60}H (Langmuir-Blodgett Films) and C_{60} polymers were synthesised through *t*-BuLi and macromolecular carbon anions, respectively (Scheme 1.4).[80,81,82] The reactions of C_{60} with Grignard reagents have been recently reviewed.[83]

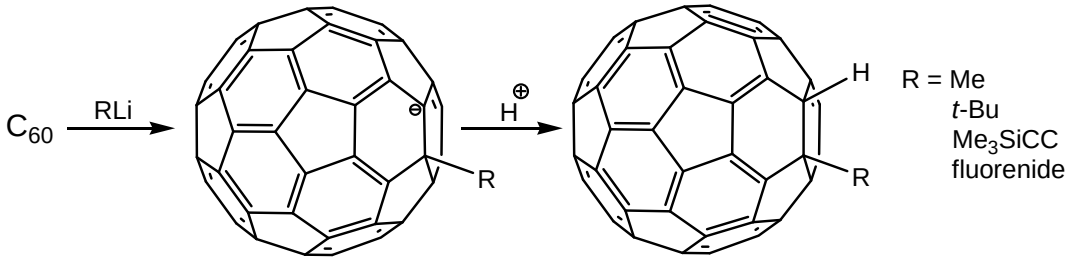

(a)

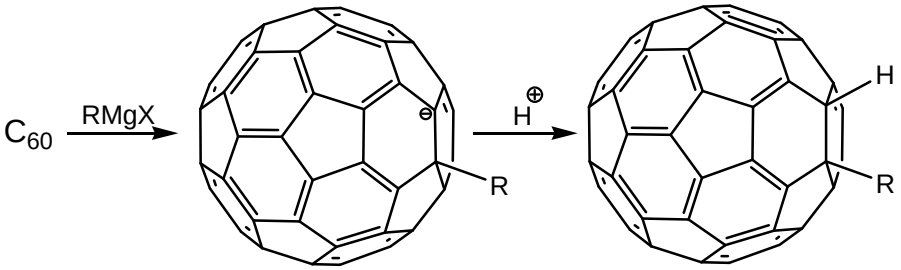

RMgX = EtMgBr
i-PrMgBr
CH_2=CH$(CH_2)_2$MgBr
$CH_3(CH_2)_7$MgBr
PhMgBr
$(CH_3)_3SiCH_2$MgCl

(b)

Scheme 1.4: Addition of C_{60} by various nucleophilic (a) organolithium and (b) Grignard compounds.

Beside these organometallic nucleophiles, carbon anions are also widely used to synthesise fullerenyl methanoadducts through cyclopropanation (known as the Bingel reaction).[84] Bingel reported the synthesis of diethyl methano[60]fullerenyl diester from the reaction of diethyl 2-bromomalonate with C_{60} under basic conditions (NaH) (Scheme 1.5).[84] The mechanism of the Bingel reaction is discussed in Section 1.4. Deprotonation of methyl 2-chloroacetylacetate, α-bromoacetophenone and

desylchloride with 1,8-diazabicyclo[5.4.0]undec-7-ene (DBU) produces the corresponding carbanions that undergo nucleophilic addition to C_{60} to give the methanofullerene derivatives **(9)**, **(10)** and **(11)** as shown in Scheme 1.6.[84]

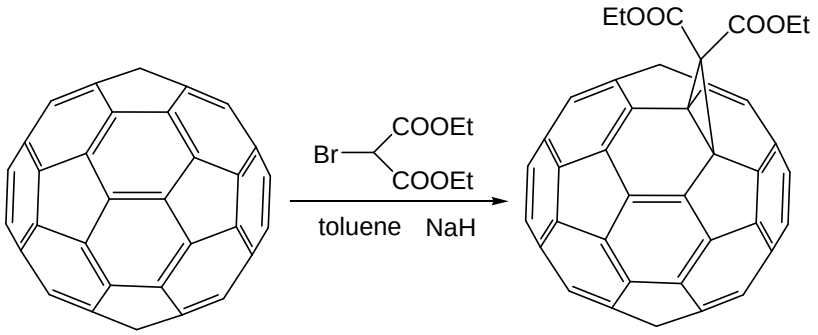

Scheme 1.5: Diethyl methano[60]fullerenyl diester synthesised through cyclopropanation by depronated diethyl bromomalonate, reported by Bingel.[84]

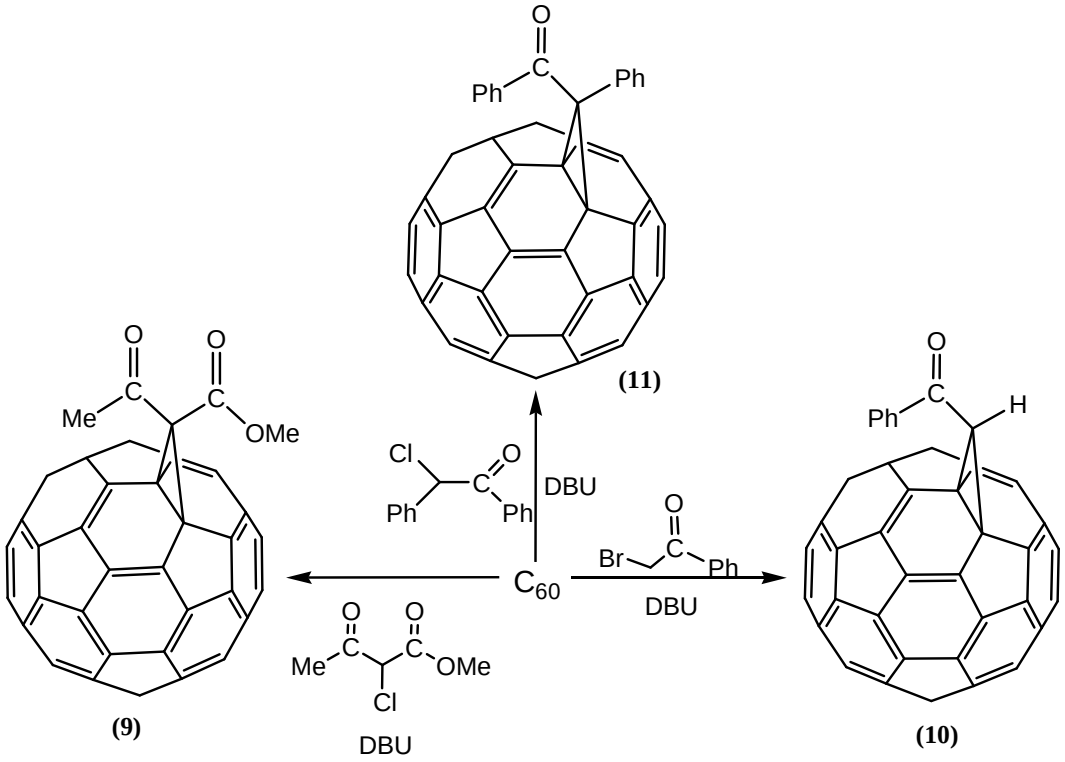

Scheme 1.6: Nucleophilic additions by methyl 2-chloroacetylacetate, α-bromoacetophenone and desylchloride under Bingel conditions.[84]

As polymer side chains, primary and secondary amines are utilised to react with C_{60} to generate polymer bound C_{60}.[85,86] Nitrogen atoms with various types of linkers have shown potential in the formation of 3-dimensional fullerene structures via

self-assembly.[87,88]

Additions to C_{60} by hydroxides, however, still remains ambiguous and need further investigations.[89]

1.2.3 Cycloadditions

Only the 6-6 double bonds on the C_{60} sphere can act as dienophiles in cycloaddition reactions.[10] The cycloaddition reactions that occur to C_{60} are categorised as [4+2], [3+2], [2+2], and [2+1] types. Some fullerenyl cycloadducts, due to high stability to heat, satisfactorily fulfill further side-chain chemistry allowing the preparation of new fullerenyl derivatives of biological or of materials importance.

A large number of 1,4-dienes can be added to the 6-6 double bonds in a [4+2] manner (Diels-Alder reaction).[90-97] As 1,3-dipoles, diazomethane,[98,99] diazoacetates [100,101] and diazoamides[102] are reactive to C_{60} via the [3+2] route, and subsequent extrusion of N_2 results in methano-bridged fullerenes (Scheme 1.7).

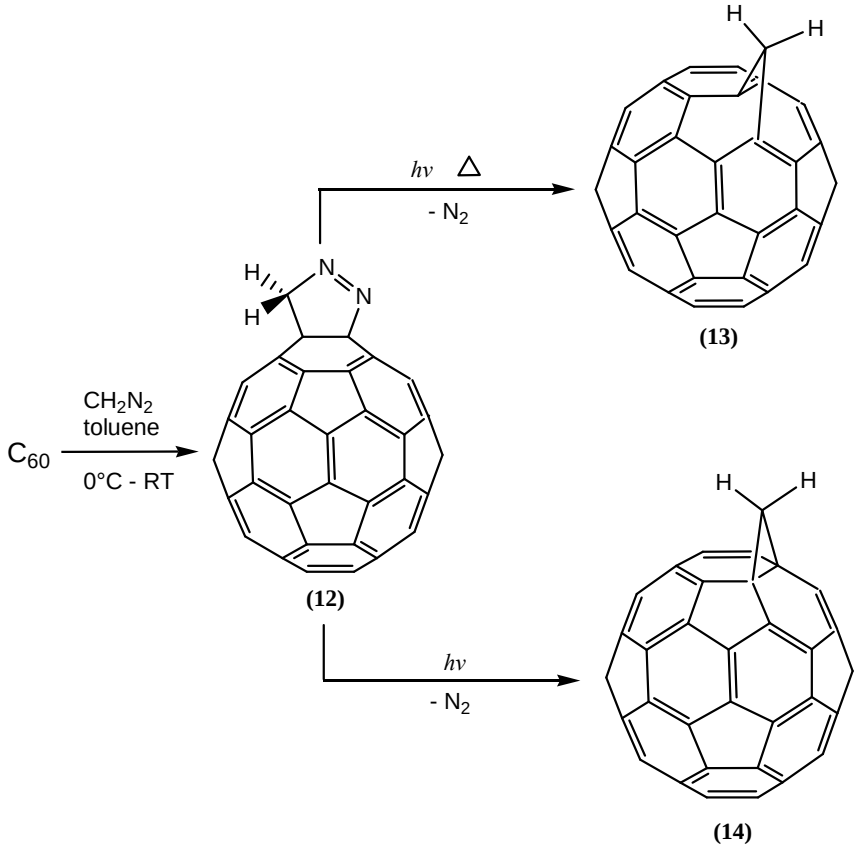

Scheme 1.7: Diazomethane, a typical 1,3-dipole as an example of [3+2] cycloaddition to C_{60}.

Induced by heat or irradiation, some intermediates also add to C_{60} in a [2+2] manner. These include benzyne,[103,104] enones,[105] quadricyclane[106] and electron-rich alkynes.[107]

1.2.4 Radical Addition

A broad range of free radicals have been added to C_{60}. The intermediates $R_nC_{60}^{\bullet}$ (n=1, 3, 5) have been investigated by electron spin resonance (ESR) spectroscopy, which have shown the ability of these intermediates to form fullerene dimers among other interesting phenomena.[6]

An organic radical species $R^{\bullet}$ is usually generated *in situ* from suitable precursors photochemically or thermally by an established free radical reaction. In the example illustrated in Scheme 1.8, the alkyl radical $R^{\bullet}$ is formed either directly from an alkyl compound or indirectly from di-*tert*-butylperoxide (via the *tert*-butoxy radical) initiated

by UV light.[108-111]

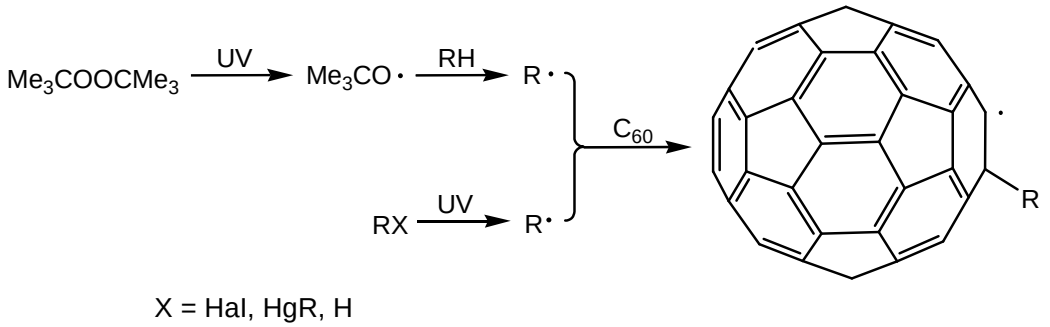

Scheme 1.8: Radical addition to C_{60}.

Many other types of radical additions to C_{60} have also been reported, including multiple radical additions, metalation by pentacarbonyl-rhenium radicals,[112] hydrostannylation,[113] and addition by bis(trifluoromethyl)nitroxide.[114]

1.2.5 Oxidation and Reactions with Electrophiles

C_{60} has been reported to be oxidised either electrochemically or chemically in the presence of oxidants such as O_2,[115,116] *m*-chloroperoxybenzoic acid (MCPBA),[117] and O_3,[118] to form mono-oxygenated C_{60}. The first C_{60} derivatives fully characterised in history was osmylated fullerene generated by addition of OsO_4, a strong and selective oxidative, to C_{60} in the solvent pyridine.[119-123] Other oxidants include Lewis acids,[124,125] aromatics[125] and chloroalkanes.[126-128] The versatility of C_{60} chemistry is also reflected by the reported halogenation, hydrogenation and the formation of C_{60}-transition metal complexes.[3]

1.3 Regioisomerism, Stereoisomerism and Chiral Functionalised Fullerenyl Bisadducts

There are thirty 6-6 double bonds on the surface of a C_{60} molecule and it is predictable that two [6,6] addition reactions that occur to any two of these bonds will probably result in isomeric products. Due to the configurational rigidity by which C_{60} molecules

are characterised, their bisadducts can be categorised into three isomeric forms: regioisomers, stereoisomers and enantiomers, based on the relative position of the second substituent, orientation of substituent groups and ring numbering orders, respectively. Below is a detailed discussion of these three forms of isomerism illustrated by the example of methanofulleryl bisadducts.

1.3.1 Regioisomerism

In the case of functionalised bismethanofulleryl derivatives, there are in total nine possible regioisomeric configurations.[3,129] They differ from one another by the relative positions of the double bonds on which the two functionalised additions have occured. Each of these nine isomeric bismethanoadducts is nominated: *cis-1*, *cis-2*, *cis-3*, *e-face*, *e-edge*, *trans-4*, *trans-3*, *trans-2*, *trans-1*. *Cis*-notations are given to those cases in which the two additions occur on the same hemisphere while *trans*- ones are used to nominate those with two addends on both hemispheres. In addition, *cis*-numbering increases as the second addend retreats from the bond where the first addend is located and *trans*-numbering decreases in the same direction. Figure 1.7 shows the diagrammatic description of the nine regioisomeric possibilities of bismethanofullerenyl adducts.[129]

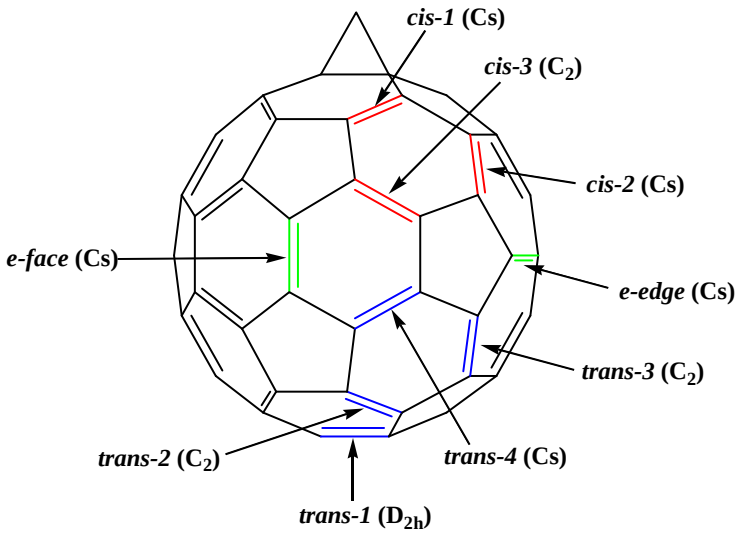

Figure 1.7: Positional notation for C_{60} bismethano-adducts. In brackets are their corresponding symmetry operations. Addition that occurs on *e-face* or *e-edge* gives rise to bisadducts of identical regioisomeric pattern.[3]

By the line model shown in Figure 1.7, each labelled bond has its counterpart on the same sphere, e.g., a methanofullerenyl bisadduct, provided not tethered, can be turned into the identical molecular configuration through a certain symmetry operation, which is either *Cs* (for *cis-1*, *cis-2*, *e*, *trans-4*) or *C2* (for *cis-3*, *trans-2*, *trans-3*). The bond labeled *trans-1* exceptionally corresponds to the *D2h* symmetry operation. Symmetry operation types *Cs* and *C2* are characterised by a symmetry plane and a symmetry axis, respectively, see Figure 1.8.[129]

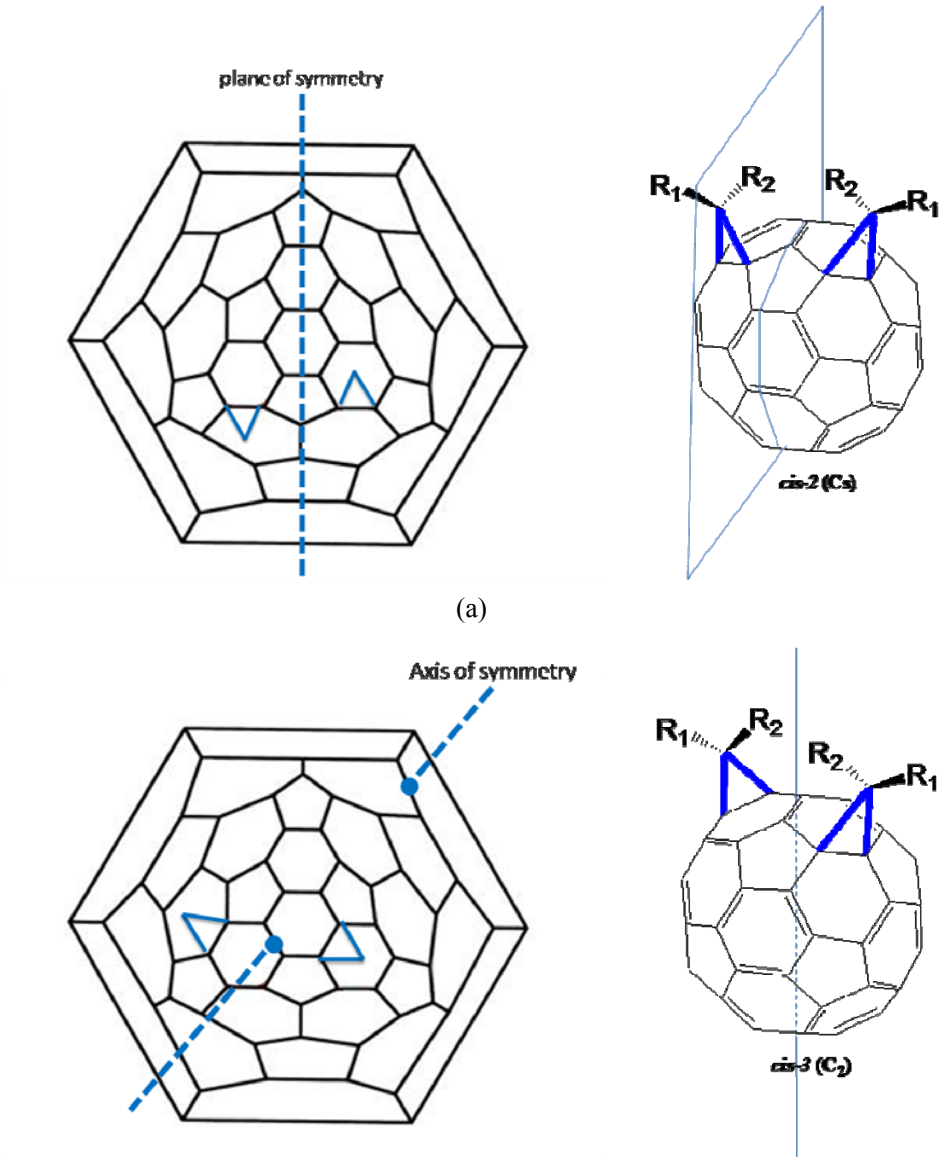

Figure 1.8: Schlegel and schematic diagrams of typical (a) the C_S-symmetrical methanofulleryl bisadducts, *cis*-2 as example here, containing a plane of symmetry, while (b) the C_2-symmetrical methanofulleryl bisadducts, for example *cis*-3 (one enantiomer shown), containing an axis of symmetry. Substituents R_1 and R_2 are supposedly identical in this case.

1.3.2 Stereoisomerism

Stereoisomerism is caused by the spatial positions of the two bridgehead substituents which are not identical to each other (either tethered or non-tethered) on either methano

C atom. In the example illustrated in Figure 1.8, any change in the orientation of R_1 and R_2 may lead to isomerism if R_1 and R_2 are not identical. This results in diastereoisomerisation for each regiomeric structure.[131] Table 1.1 contains the complete list:

Regioisomeric Pattern	Symmetry Operation	Possible Diastereoisomers and their Symmetry
cis-1	*Cs*	2 *Cs* (*in-in*, *out-out*), 1 *C1* (*in-out*)
cis-2	*Cs*	2 *Cs* (*in-in*, *out-out*), 1 *C1* (*in-out*)
cis-3	*C2*	2 *C2* (*in-in*, *out-out*), 1 *C1* (*in-out*)
e	*Cs*	2 *C1* (*out-out*, *in-out*)
trans-4	*Cs*	2 *Cs* (*in-in*, *out-out*), 1 *C1* (*in-out*)
trans-3	*C2*	2 *C2* (*in-in*, *out-out*), 1 *C1* (*in-out*)
trans-2	*C2*	2 *C2* (*in-in*, *out-out*), 1 *C1* (*in-out*)
trans-1	*D2h*	1 *C2v* (*out-out*), 1 *C2* (*in-out*)

Table 1.1: Summary of symmetry operations and stereoisomerism corresponding to regioisomeric assignments for fullerenyl bisadducts.[131]

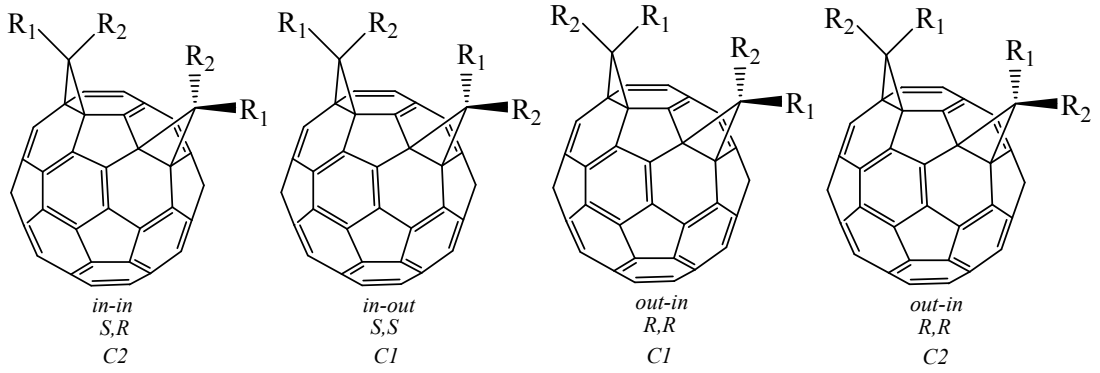

(a) *cis-2*

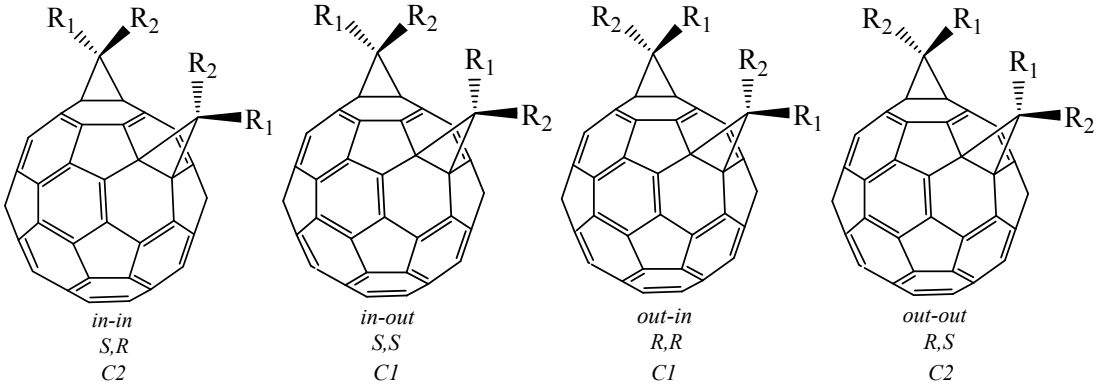

(b) *cis-3*

Figure 1.9: Stereoisomerism illustrated by (a) the *cis-2* and (b) the *cis-3* methanofullerenyl bisadducts. Isomerism is determined by the spatial positioning of R_1 and R_2 which are not identical. *In-out* and *out-in* structures are identical in each case.[131]

1.3.3 Chirality

The pristine C_{60} molecule is inherently an achiral molecule, e.g., there exists an axis around which either a clockwise or anticlockwise C-atom numbering scheme leads to geometrically equivalent results. The two numbering schemes are defined '^{f}C' and '^{f}A' respectively, where letters 'C' and 'A' refer to clockwise and anti-clockwise and the superscript 'f' stands for fullerene.[130] In cases of functionalised fullerenyl bisadducts, ^{f}A and ^{f}C naturally result in two enantiomers for any *C2*-symmetrical regioisomeric type, e.g., *cis-3*, *trans-2* and *trans-3*, in which structures there exists an axis of symmetry. Such chirality, nevertheless, has nothing to do with the bridgehead groups that are linked to the methano-carbon atoms (Figure 1.10).

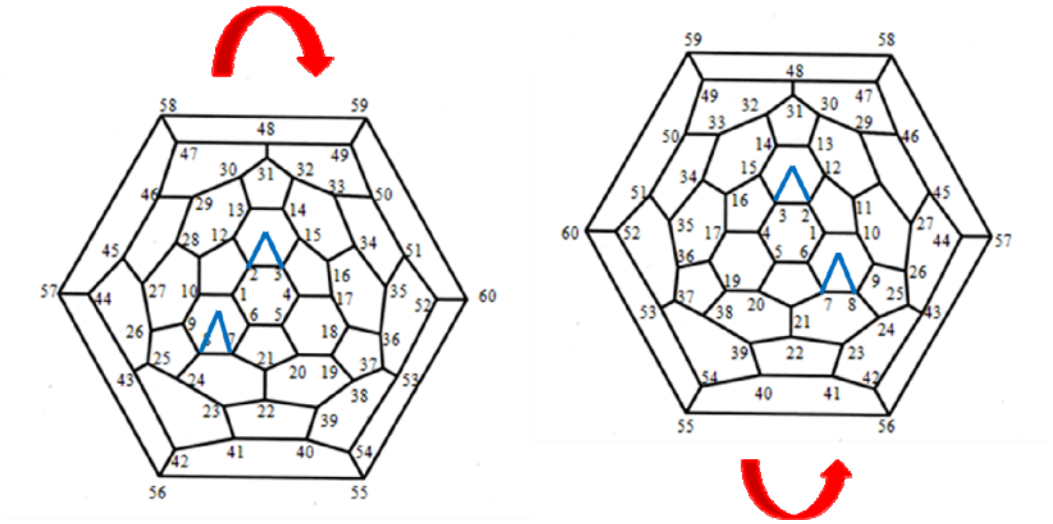

(a) (b)

Figure 1.10: The (a) ^{f}C and (b) ^{f}A numberings schemes lead to a pair of enantiomers of the *cis-3* methanofullerenyl bisadduct. [131]

1.4 Bingel Reaction

Bingel reactions are one of the most broadly utilised reactions with C_{60}, characterised by the nucleophilic attack of stabilised α-halocarbanions to the C_{60} molecule at room temperature. The fused methano structure is then generated from the intramolecular displacement of the halide by the anionic centre on the C_{60} as the result of the previous nucleophilic attack. This mechanism can be regarded as addition/substitution (addition by an α-halocarbanion followed by substitution of the halogen).[84]

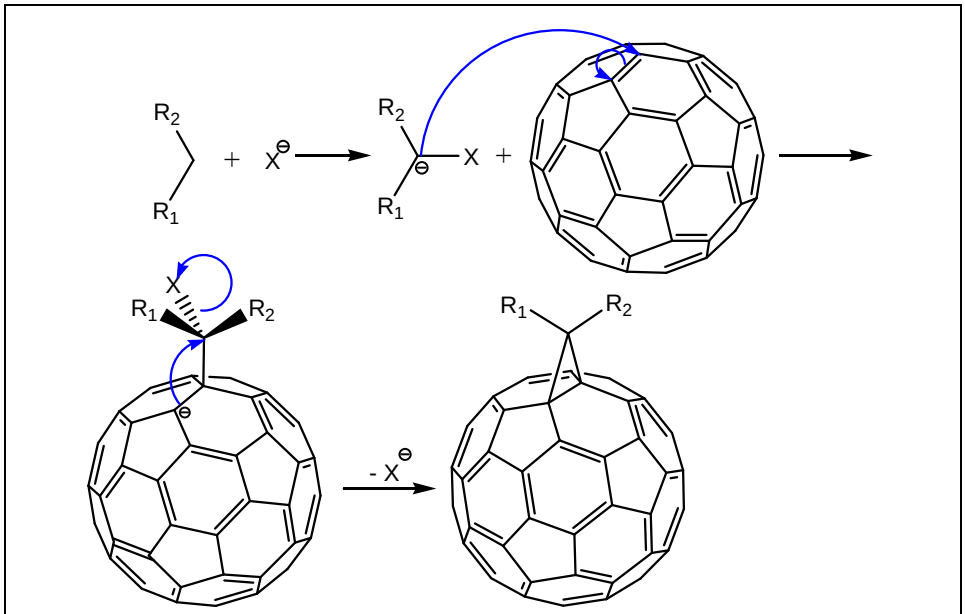

Compound	R_1	R_2	X	Yield (%)
(15)	COOEt	COOEt	Br	45
(16)	COMe	COOMe	Cl	27
(17)	COPh	H	Br	21
(18)	COPh	Ph	Cl	25
(19)	C≡CTMS	C≡CTMS	Br	55

Table 1.2: Methanofullerenes formed under Bingel reaction conditions by addition/substitution mechanism.[15]

A refined version of the Bingel reaction is the use of malonic esters in which the electron density on the α-C is greatly reduced by the neighbouring two carbonyl groups. With the presence of an auxiliary base such as DBU, as well as a halogenation reagent, (for example, CBr_4, or I_2) iodo- or bromo-malonate is generated *in situ* to facilitate the Bingel reaction with efficiency, reliability and acceptable yields (Table 1.3).[130,132]

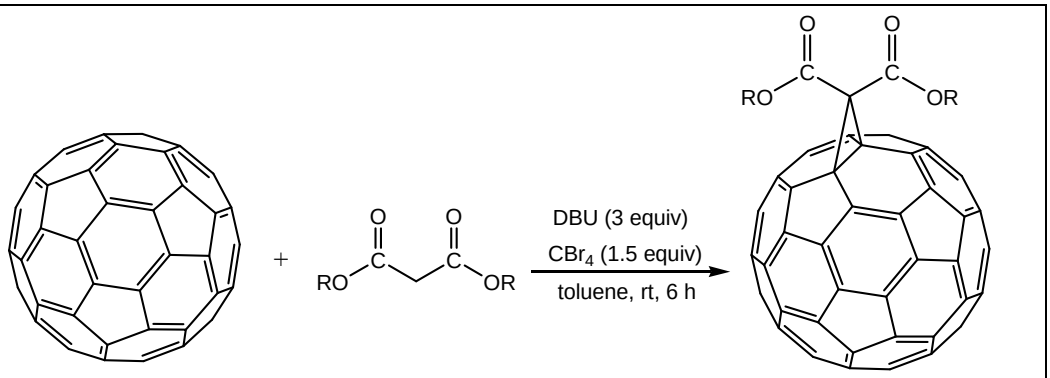

Compound	R	Yield (%)
(20)	Ethyl	57
(21)	Octadecyl	65
(22)	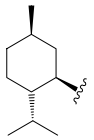	55
(23)	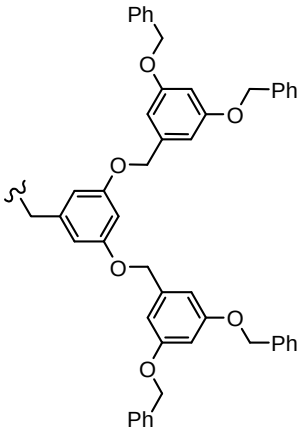	29

Table 1.3: Bingel reaction of C_{60} with malonic esters.

In fact, any reactant containing an active methylene component CH_2WW', where W and W' are electron withdrawing groups, can essentially undergo an addition/substitution reaction to C_{60} under Bingel reaction conditions. One example is *N*-(diphenylmethylene)glycinate esters shown in Table 1.4.[15,84] This reaction does not give a methanofullerene product but a pyrrolidine derivative.[133]

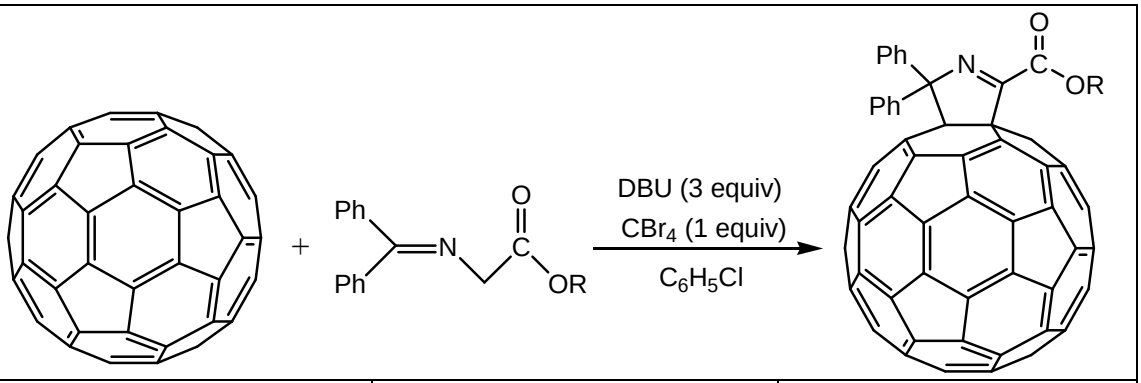

Compound	R	Yield (%)
(24)	*t*-Bu	46
(25)	Et	76
(26)	*I*-menthyl	31
(27)	$EtCOOCH_2$	46

Table 1.4: Addition reactions of *N*-(diphenylmethylene)glycinate esters to C_{60}. The compounds generated are [60]fullerenyldihydropyrroles[133] rather than methano[60]fullerenyl iminoesters as initially reported.[15,84]

1.5 Chemical Realisation of Methanofullerenyl Bisadducts of Desired Regioselectivity

The Bingel reaction provides a satisfactory method of fullerene monofunctionalisation. In order to avoid the tedious chromatographic separation required to isolate the mixed products of different regioisomeric patterns resulting from a sequential second functionalisation, the use of rigid tethers is a good strategy for the achievement of the regioselective formation of fullerene bisadducts.[134,135] Examples include the regioselective synthesis of fullerenyl bisdihydropyrroles (Scheme 1.9)[136,137] and the double Diels-Alder cycloadditions with α,ω-dioxamethylene tethers.[138-140]

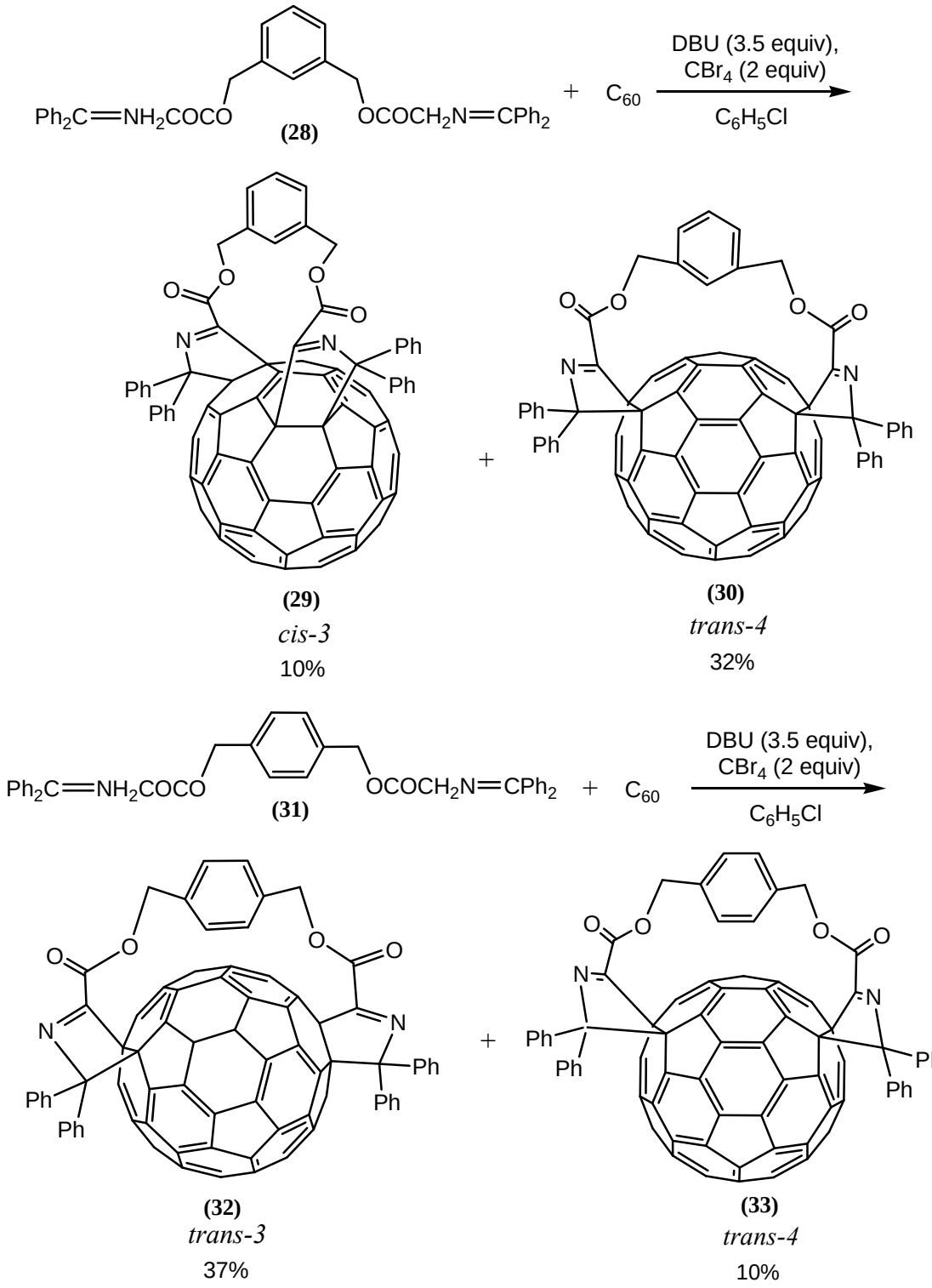

Scheme 1.9: Regioselective double dihydropyrrolidation with *m*- and *p*-benzenedimethanol derived tethered bis-*N*-(diphenylmethylene)glycinate esters under Bingel reaction conditions.[137]

In the cases of bismethano[60]fullerene derivatives, tethered bismalonates have been

employed to provide those compounds in a regioselective manner (Scheme 1.10). The

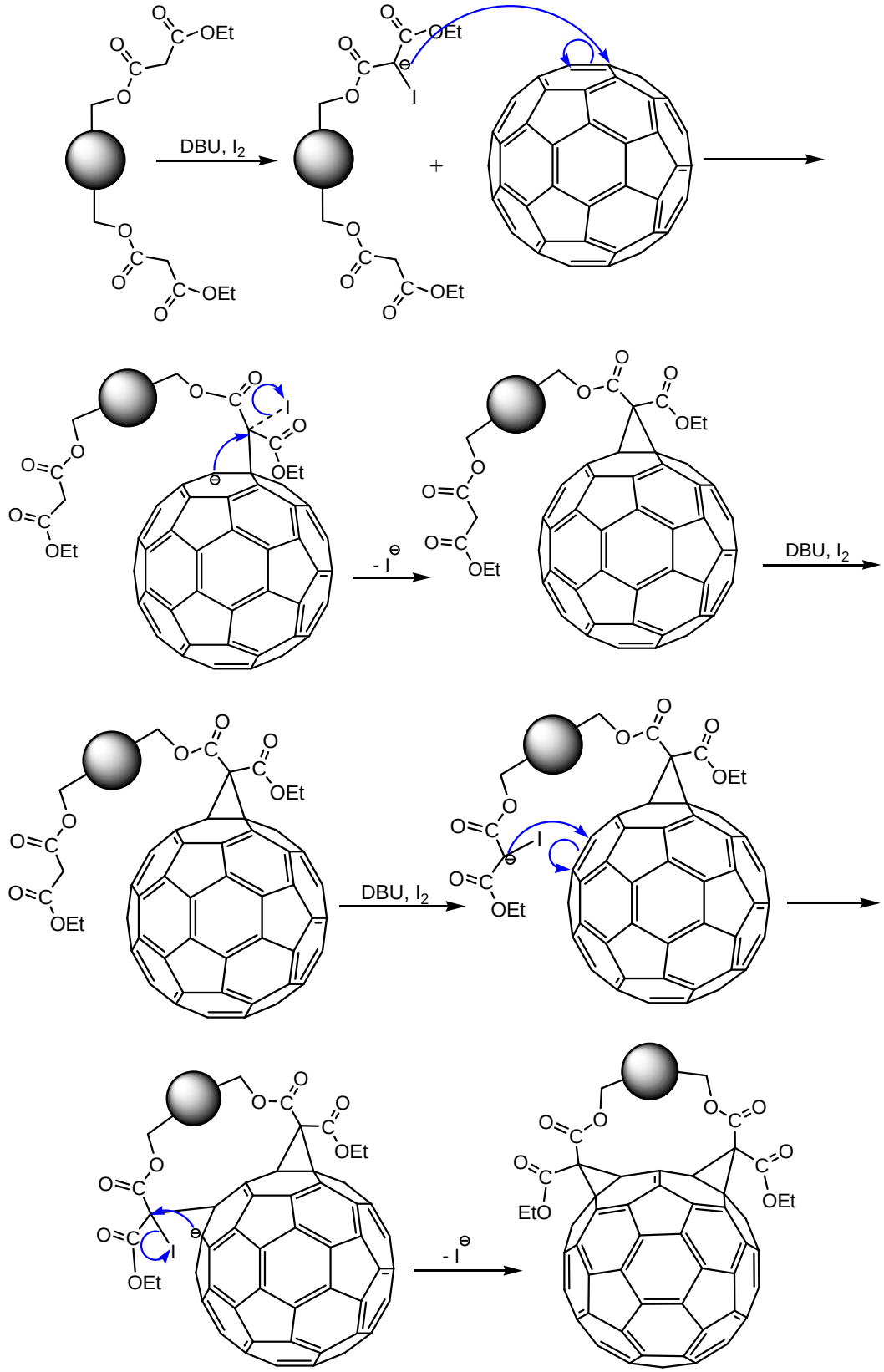

Scheme 1.10: The two-step mechanism of bisfunctionalisation of C_{60} by a tethered malonate ester. In this case a *cis-2* isomer of the tethered bismethano[60]fullerenyl adduct resulted.

regioselectivity was confirmed by Nierengarten et al.,[129, 161] on the basis of molecular symmetry deduced from ^{1}H- and ^{13}C-NMR spectra as well as of UV/Vis spectral comparisons. The tethered double functionalisation of the C_{60} molecule occurs in two steps. The initial attachment of one reactive group to C_{60} provides an anchored reactive group (RG) conjugate first, followed by the addition of the second reactive group to a kinetically or thermodynamically favourable site on the carbon sphere (Figure 1.11).[131] However, the dynamic mechanism underlying the regioselective patterns obtained from a certain tether still remains ambiguous and needs further investigations.

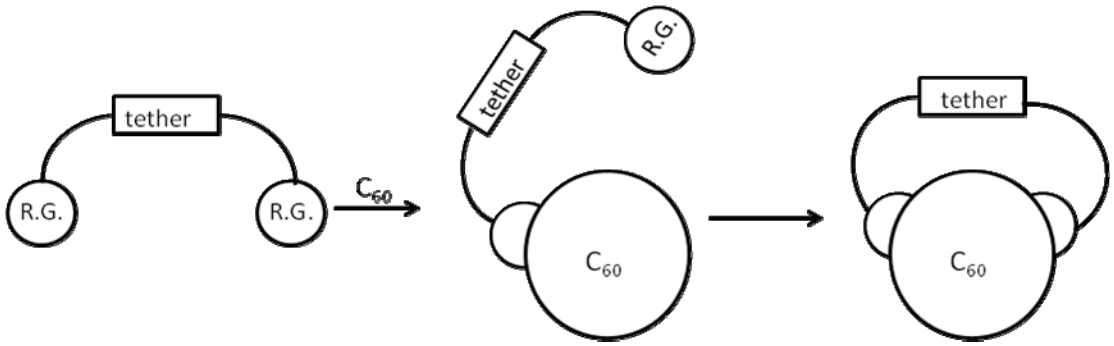

Figure 1.11: A general scheme of tethered double functionalision of C_{60}. R.G.= reactive group.

1.6 Electrochemically Induced Isomerisation of Tetraethyl Bismethano[60]fullerenyl Malonates

Chemical functionalisation of C_{60} with diethyl bromomalonate under Bingel reaction condition results in the monoaddition product diethyl 1,2-methano[60]fullerene-61,61-dicarboxylate, and subsequent cyclopropanation with the same malonic ester leads to a mixture of seven regioisomeric bisadducts, all possible regioselective patterns are formed except *cis-1* in which the ethyl ester substituents would be sterically hindered (Scheme 1.11).[136]

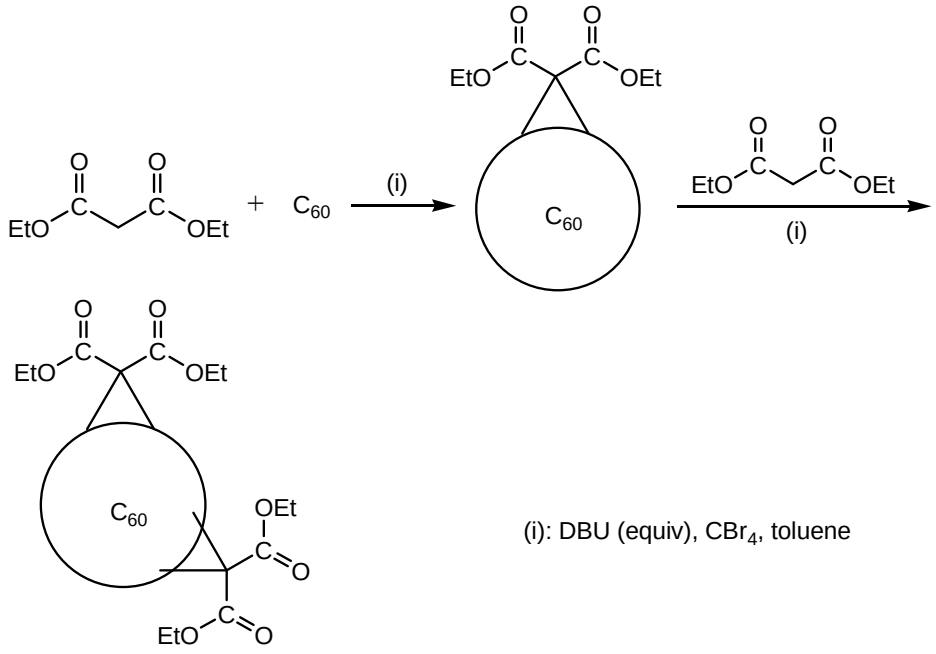

trans-1, trans-2, trans-3, trans-4, e, cis-3, cis-2, cis-1

Scheme 1.11: Mixed regioisomers of tetraethyl bismethano[60]fullerenyl malonates resulted from double cycloaddition to C_{60} with diethyl malonate. The yield of each regioisomer varies from 2% to 37%, after chromatographic column separation. [136]

The more amazing findings were brought by further electrochemical studies on these bisadducts: two-electron coulometrically controlled potential electrolysis (CPE) of any isomer, except *trans-1*, which was not reported, leads to a walk-on-the-sphere rearrangement of addends.[141] For instance, CPE of the *cis-3* isomer which was stopped at the second reduction potential (2 electrons per molecule have been transferred), then reoxidised to 0 V, yielded the monoadduct (28%) and a mixture of bisadducts (53%). The mixture of bisadducts consisted of the *e* (22%), *trans-4* (6%), *trans-3* (10%), *trans-2* (51%) and *trans-1* (11%) isomers. *Cis-2* underwent one electron CPE to its monoanionic state, reoxidation resulted in a walk-on-the-sphere rearrangement of its addends, though such isomerisation was not observed from other regioisomers under one-electron CPE.

The absence of *cis* isomers in the resulting bisadduct mixtures may be a result of the inherent intramolecular strain from two cyclopropanes in close proximity. There is a

competition between isomerisation and retro-Bingel reaction under two-electron CPE, which was evident by the formation of the monoadduct no matter what the starting isomer was. In fact, exhaustive CPE, which turns a bisadduct to its hexaanionic state, finally yielded 75% of C_{60} after reoxidation, indicating that the retro-Bingel reaction dominates.

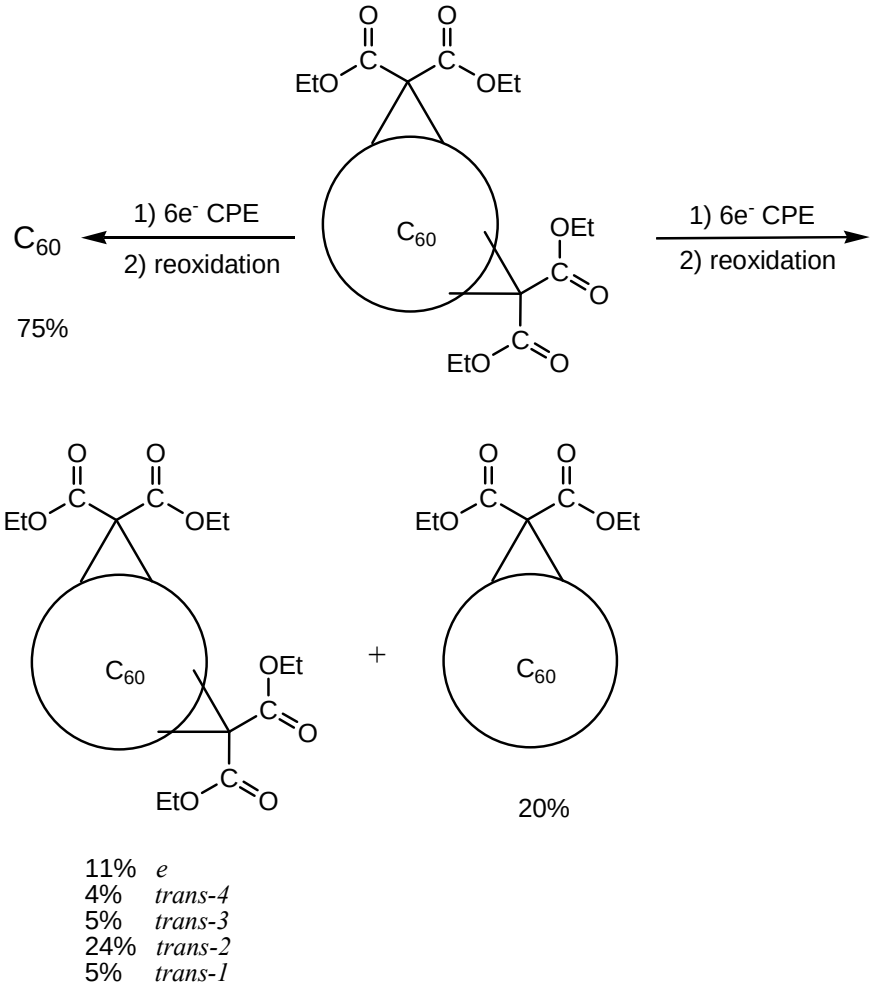

Scheme 1.12: Electrochemically induced "walk-on-the-sphere" rearrangement of two addends to give mixtures of regioisomers with the approximate distributions in percentages. The starting material can be any one of *cis-2* (one-electron CPE), or *cis-3*, *e*, *trans-4*, *trans-3* and *trans-2* (two-electron CPE).[141]

Another noteworthy point is that the relative distribution of regioisomers in the mixture generated from any starting isomer is essentially the same, e.g., HPLC analysis showed approximately 11%, 4%, 5%, 24% and 5% for *e*, *trans-4*, *trans-3*, *trans-2* and *trans-1*, respectively, as yields regardless of the regioisomer on which two-electron CPE had

been applied.

1.7 Ion Mobility Mass Spectrometry (IMMS)

1.7.1 Introduction of IMMS

As indicated by its name, ion mobility mass spectrometry (IMMS) is an analytical measurement composed of ion mobility spectroscopy (IMS) and mass spectrometry (MS) that complement each other and fuse into one methodology. With IMMS, ions are separated on the basis of their unique drift times that they have in the drift region of the IMMS instrument. The drift time depends on the average cross-sectional area of these ions when they collide with the neutral drift-gas molecules that counter-flow in the same drift region. Today, after 30 years of development, IMMS can be integrated into various types of ion sources (e.g., ^{63}Ni, electrospray ionisation (ESI), laser and matrix-assisted laser absorption) and mass analyzers (e.g., quadrupole, time-of-flight and Fourier-transform ion cyclotron resonnance mass spectrometries).[142] Up to now, IMMS has found broad applications in the analysis and/or detection of biomolecules, explosives, chemical warfare degradation products, illicit drugs, combinational chemistry samples and chlorinated or brominated byproducts in drinking water disinfectors.[142] In addition, it has shown its unique advantages in differentiating isomeric structures of protein and polypeptide complexes.[143]

1.7.2 Development of IMMS

In spite of advantages of Faraday plate detection, which most commercial IMS instruments employ, such as simplicity, inexpensiveness, suitability for both anions and cations, this method is often replaced by mass spectrometry that can afford mass information to the separated ions. However, it required around 30 years before researchers finally reached a rationalized understanding of IMS and started its wide

usage together with MS.

As early as 1971, the first coupled IMS-MS instrument, Alpha II PC/MS was brought by Franklin GNO Corporation into applications such as detection of compounds in trace amounts, understanding of ion formation in the reaction region of IMS as well as establishing refined correlationships between mass and mobility (*m/z* vs V_d).[144] However, interest in IMS, after booming since 1970, declined after 1976 mainly due to low resolution and lack of mass information.[145] PCP (West Palm Beach, FL, USA) continued this early technology and supplied commercial IMMS for limited applications in medical fields and in explosives.[142] Later in the 1980s with the understanding of IMS refined and it being treated as a spectrometric rather than a chromatographic method, and few essential improvements were made until the 1990s when a time-of-flight mass spectrometer (TOFMS) was interfaced with an IMS instrument supplied by PCP. This was actually a modification in which the original Finnigan quadrupole mass spectrometer was replaced by the TOFMS, which enabled complete mass spectra for individual peaks.[146]

From 1997-2001 a large amount of work was performed by Clemmer and coworkers on biomolecules with IMS incorporated to quadrupole and TOFMS. The latter enabled flight time – drift time plots to be generated.[147-159]

1.7.3 Principle of Ion Mobility Spectroscopy (IMS)

A schematic of the IMMS instrument is illustrated in Figure 1.12. Its various components include (1) an electrospray ionisation source, (2) an ESI-IMS interface, (3) a desolvation chamber in which the electrospray solvent is evaporated, (4) the ion gate, (5) the drift region, where ions are separated on the basis of mobility, (6) a pinhole interface to vacuum, (7) transfer and focusing ion lenses that move ions from high pressure to low pressure and (8), a reflection TOF mass spectrometer that separates ions

on the basis of *m/z*. Ions are separated in the drift region (Region (5), Figure 1.12) on the basis of their velocities under an applied constant electric field (E, V/cm) against the counter-flow of neutral gas molecules within this region. During this process, ions are accelerated by the electric field while they are losing their velocities to collisions with molecules of the netural buffer gas. The kinetic energy that these ions lose after collisions is converted to their internal energy resulting in increased temperatures and reduced velocities, and subsequent collisions then confer part of their internal energy to drift gas molecules, resulting in lowered ion temperatures. Therefore neither the temperature nor the velocity of each ion remains constant within the drift region and consequently, it is only possible to describe the movement of ions by the time they need to pass through the drift region (drift time, t_d, ms) as well as by their average velocity (V_d, $cm \cdot s^{-1}$):

$$V_d = K \cdot E$$

E --- applied electric field strength ($V \cdot cm^{-1}$); K --- ion mobility constant ($cm^2 \cdot V^{-1} \cdot s^{-1}$).

The above equation is valid only when $E < 1000\ V \cdot cm^{-1}$. The ion mobility constant (K), which is dependent on properties of both the ion of interest and the drift gas molecule, becomes no longer directly proportional to E as the field strength increases. Under low-field conditions, the ion mobility constant K is related to the ions collision cross section by the Mason-Schamp equation shown below:

$$K = (3q/16N) \cdot (2\pi/KT)^{1/2} [(m+M)/m \cdot M]^{1/2} (1/\Omega)$$

q --- ion charge (C); N --- number density of the drift gas ($molecules \cdot cm^{-1}$); T --- absolute temperature (K); m --- mass of buffer gas; M --- mass of ion; Ω --- average collision cross-section area between ion and drift gas molecule.

Practically, K can be converted to a reduced mobility value (K_0) under the operating temperature T (K) and the operating pressure P (Torr, 1 Torr = 133.322 Pa):

$$K_0 = K \cdot (P/760) \cdot (273/T)$$

Concluded from above, V_d, which is decided by K, takes the size and shape of an ion into account. This constitutes one advantage of IMS over mass spectrometry, which is

incapable of separating isomers or complexes of the same mass. With IMS interfaced with MS, the mass-to-charge ratio (*m/z*) of each component of a mixture of ions, after being separated by IMS, can be decided and a 2-D or 3-D orthogonal spectrum can be constructed on *m/z* vs t_d (ms).

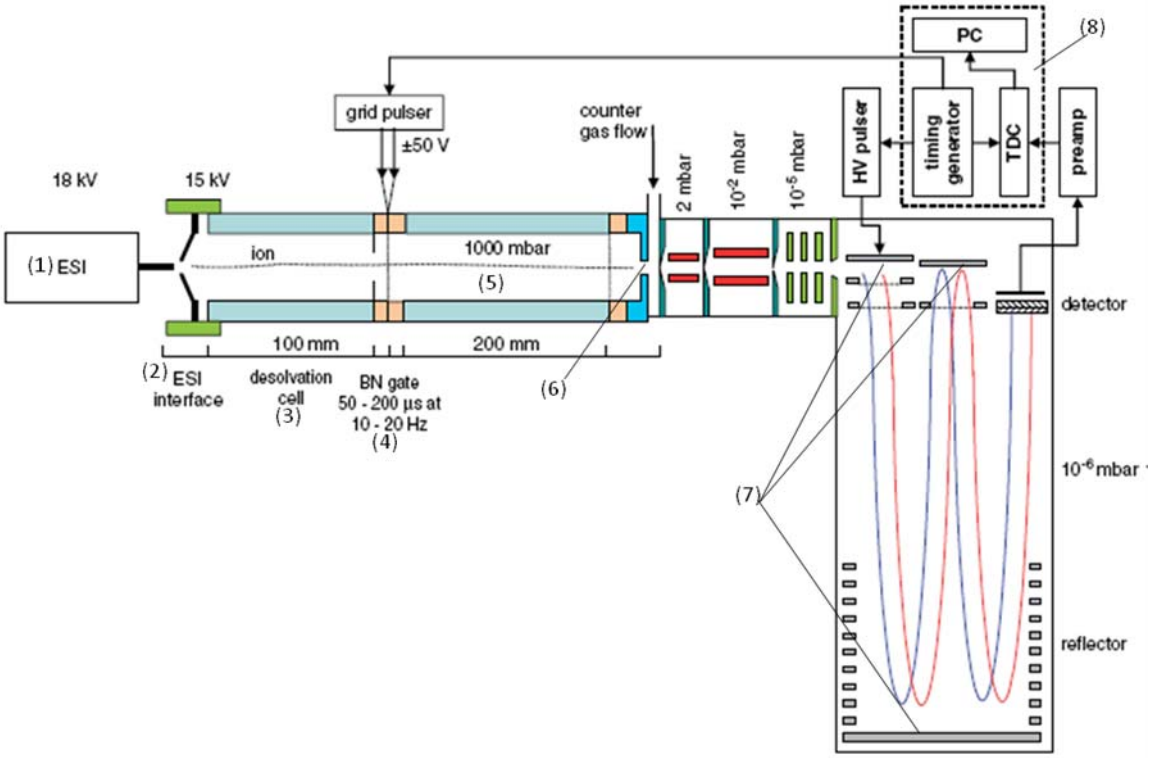

Figure 1.12: A schematic ambient-pressure IMMS.[160] (1) ESI source, (2) the ESI interface to the IMS, (3) a desolvation cell in which the electrospray solvent is evaporated, (4) ion gate to the drift region, (5) the drift region, (6) a pinhole interface to vacuum, (7) transfer and focusing ion lenses (8) a reflectron time-of-flight mass spectrometer.

1.8 Project Aims

This project aims to examine the potential of IMMS in distinguishing the different regisomeric tetraethyl bismethano[60]fullerenyl malonates of the same mass on the basis of their different drift times due to their different collision cross section areas because of their different sizes and shapes. Molecules for this study will be prepared chemically through tethered bisfunctionalisation of C_{60} under Bingel reaction conditions followed by transesterification. This method will provide four regioisomers of bisadduct

$C_{62}(COOEt)_4$ that are the *e*, *cis-2*, *cis-3* and *trans-4* regioisomers. Differences in their substituent orientation and relative fused cyclopropanyl positioning is expected to be reflected by their different drift times in the IMMS analysis. Further, IMMS studies in the negative ion ESI mode will be undertaken to see possible "walk-on-the-sphere" type rearrangement of these compounds. AM1 calculation will also be performed for all possible tethered and transesterified bisadducts to help rationalise the IMMS results.

Chapter 2: Results and Discussion

In order to study the relationship between the structures of regioisomeric bismethanol[60]fullerenyl adducts and their drift time using ion mobility mass spectrometry (IMMS), three selected tethered bismalonates, with an active methylene group between the two electron withdrawing carbonyl groups, were synthesised for the bisfunctionalisation of [60]fullerene. The Bingel reactions of these tethered compounds resulted in the corresponding bismethano[60]fullerenyl adducts of specific regioisomerism. Subsequent transesterification of these bismethano[60]fullerenyl adducts led to tetraethyl bismethano[60]fullerenyl tetracarboxylates that retained the regioisomerism of their starting bismethano[60]fullerenyl adducts.

The 1,3-benzenedimethanol and 1,4-benzenedimethanol tethered bismalonates, 1,4-bis{[(ethoxycarbonyl)acetoxy]methyl}benzene **(34)** and 1,3-bis{[(ethoxycarbonyl) acetoxy]methyl}benzene **(35)** respectively, as well as the tartaric acid derived tethered bismalonate, (+)-(4*R*,5*R*)-bis{[(ethoxycarbonyl)acetoxy]methyl-2,2-dimethyl-1,3-dioxolane **(36)**, were prepared for Bingel addition reactions to [60]fullerene to generate regioisomeric bisadducts. Their structures are illustrated in Figure 2.1.

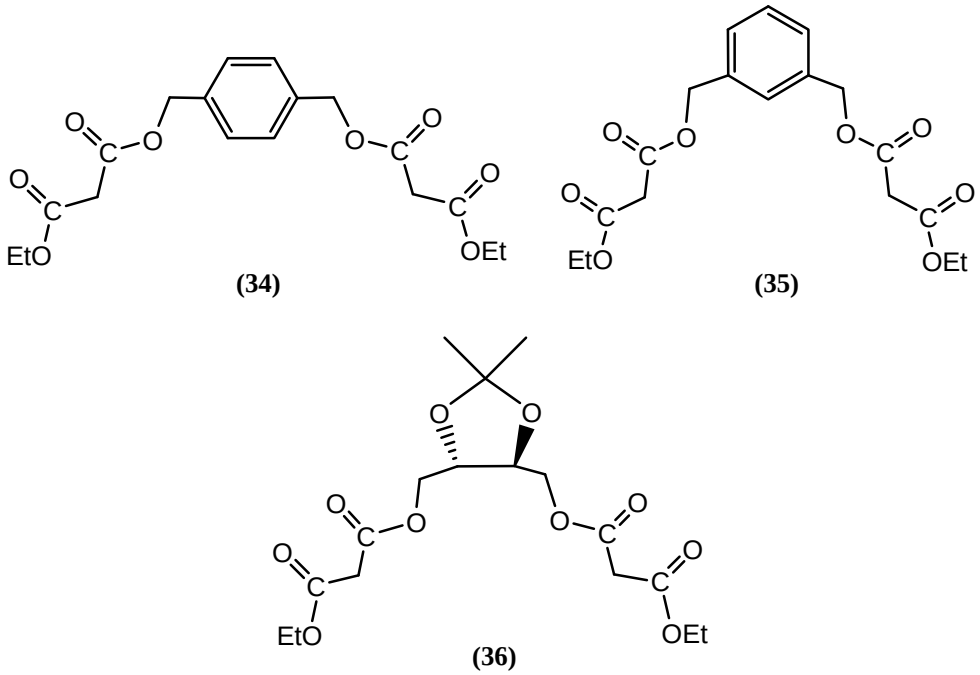

Figure 2.1: The structures of the target bismalonates, 1,4-bis{[(ethoxycarbonyl)acetoxyl]methyl} benzene **(34)**, 1,3-bis{[(ethoxycarbonyl)acetoxy]methyl}benzene **(35)** and (+)-(4*R*,5*R*) -bis{[(ethoxycarbonyl)acetoxy]methyl}-2,2-dimethyl-1,3-dioxolane **(36)** to be synthesised.

These tethered bismalonates were synthesised via diesterification reactions of the corresponding dimethanols.

2.1 Tartaric Acid Derived Tethered Bismethano[60]fullerenyl Adducts

2.1.1 Reduction of Dimethyl 2,2-dimethyl-1,3-dioxolane-4,5-dicarboxylate (37)

Due to its unavailability, dimethanol **(38)** had to be prepared from the commercially available diester **(37)**. Reduction of **(37)** with lithium aluminium hydride in THF solution at reflux for 1.7 h followed by treatment with water (Scheme 2.1) gave the diol **(38)** in 87% yield as an orange oil. This compound was spectroscopically similar to that previously reported.[162]

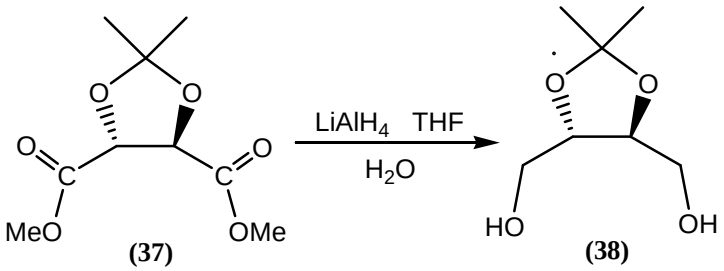

(37) **(38)**

Scheme 2.1: Reduction of dimethyl 2,2-dimethyl-1,3-dioxolane-4,5-dicarboxylate **(37)** by lithium aluminium hydride to generate the diol **(38)**.

The ^{1}H-NMR spectrum of **(38)** showed two doublet signals at 3.71 ppm (d, J = 9.3 Hz, 2H) and 3.82 ppm (d, J = 11.7 Hz, 2H), and a triplet signal at 4.02 ppm (t, J = 10.3 Hz, 2H) which were assigned to the diastereotopic methylene and the methine groups, respectively. The broad singlet peak at 2.08 ppm was assigned to the hydroxyl groups. In the ^{1}H-NMR spectrum of **(38)** reported by E. A. Mash *et al.*,[162] there was only one multiplet peak at 3.73 ppm (m, 6H) apart from the other two peaks at 1.42 ppm (s, 6H) and 3.94 ppm (m, 2H) assigned to the geminal methyl groups and the methine groups, respectively. The multiplet peak in Mash's spectrum undoubtedly belongs to the diastereotopic methylene (4H) and the hydroxyl (2H) protons. The difference in temperature and/or concentration between our sample and that of Mash's might have resulted in this overlap. Meanwhile, our ^{13}C-NMR spectrum of **(38)** was the same as Mash's (see Appendix II).[162]

The reductant lithium aluminium hydride initiates the reaction through nucleophilic addition of a hydride ion to the ester carbonyl group, and the tetrahedral intermediate then loses methoxide to generate an aldehyde which is subsequently reduced to the alcohol. This mechanism is illustrated in Scheme 2.2.

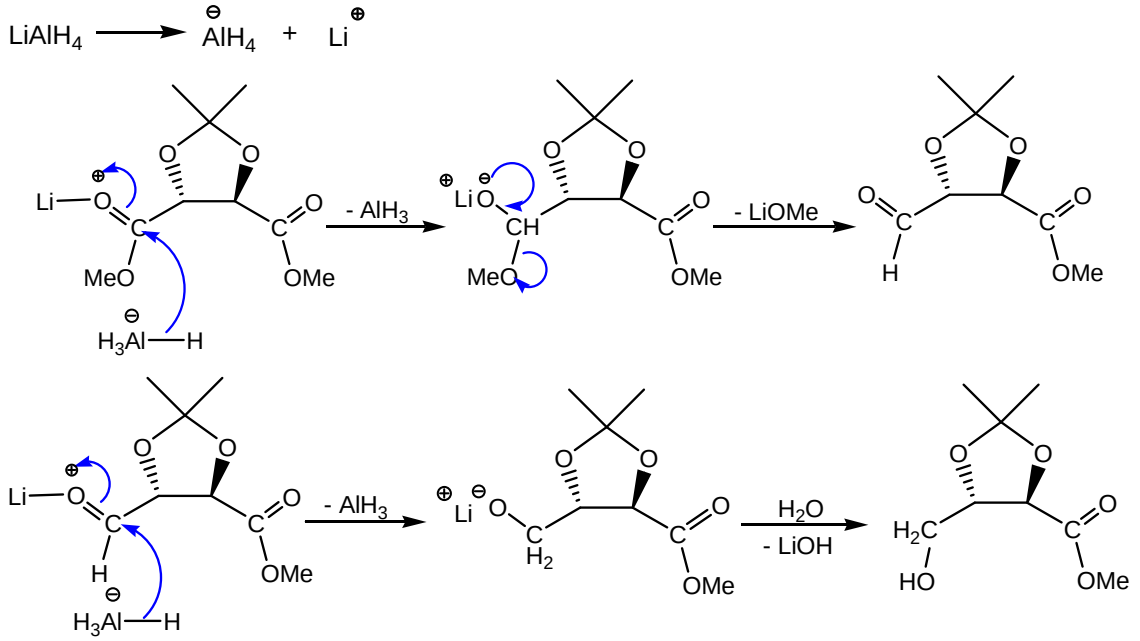

Scheme 2.2: Mechanism of reduction of the diester **(37)** by $LiAlH_4$ to form the diol **(38)**. For clarity the reduction of only one methyl ester group is depicted here though actually both methyl ester groups were reduced to hydroxymethyl groups.

2.1.2 Formation of the Tartaric Bismalonate Tether (+)-(4*R*,5*R*)-Bis {[(ethoxycarbonyl)acetoxy]methyl}-2,2-dimethyl-1,3-dioxolane (36)

As illustrated in Scheme 2.3, diesterification of the diol **(38)** by treatment with ethyl 3-chlorooxopropanoate **(39)** (2.57 mol. equiv.) in CH_2Cl_2/pyridine medium with stirring at rt for 5 h resulted in the tethered bismalonate **(36)** in 75% yield as a yellow oil. This product was nearly spectroscopically identical to that previously reported by Nierengarten *et al.* with the only discrepancy being the peak at 4.09 ppm where this signal assigned to the methine groups appeared as a broad singlet instead of the triplet (J = 2.5 Hz) reported in the literature.[161] This difference may be due to the poorer resolution of our sample.

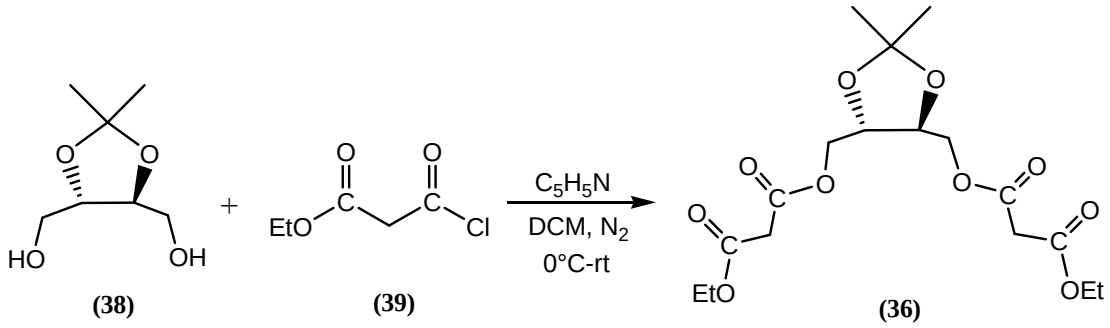

Scheme 2.3: Synthesis of the tartaric bismalonate tether **(36)**.

This reaction was carried out under anhydrous condition otherwise **(39)** could be readily hydrolysed in the presence of water. Scheme 2.4 shows the mechanism.

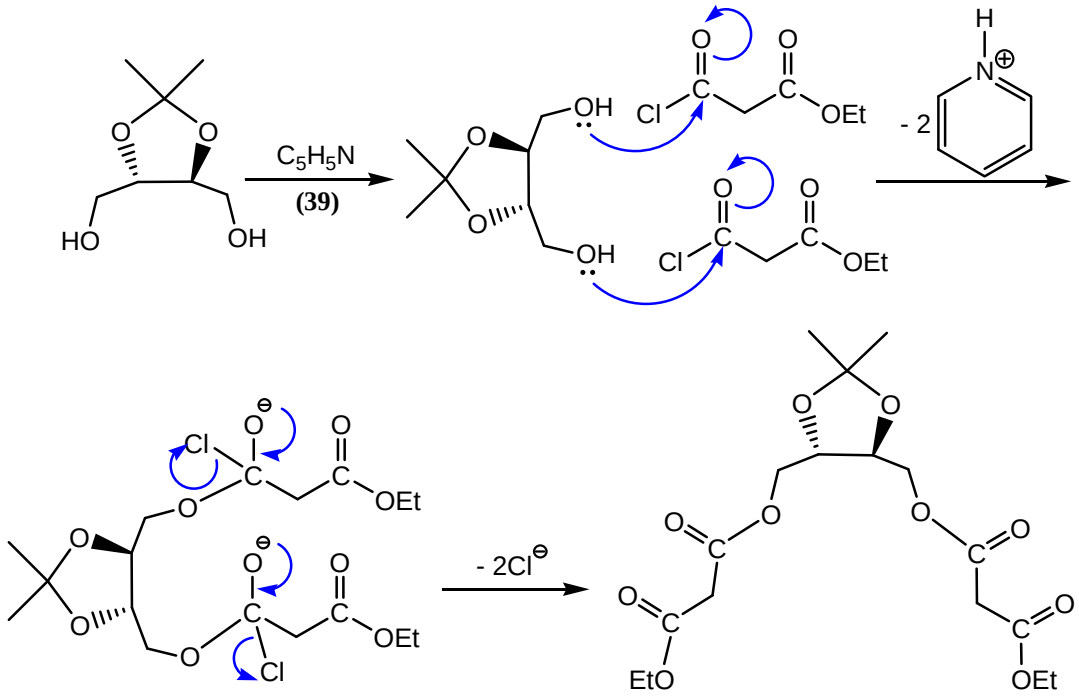

Scheme 2.4: Mechanism of diesterification of the diol **(38)** by **(39)** to form the tartaric bismalonate tether **(36)**.

2.1.3 Tethered Functionalisation of [60]Fullerene by (36) to Form Bismethano[60]fullerenyl Adducts under Bingel Reaction Condition

Under Bingel reaction conditions the tartaric acid derived tethered bismalonate **(36)** underwent double nucleophilic additions to [60]fullerene in the presence of DBU, and iodine in toluene solution with stirring for 8 h at rt. This led to the formation of two

regioisomeric fullerene adducts that were separated by column chromatography.

The *cis-2* adduct **(40)** was obtained in 10% yield as a dark-red solid and the *cis-3* regioisomer **(41)** in 6% yield as a brown solid (Scheme 2.5). The mechanism of the Bingel conditioned bisfunctionalisation reaction is outlined in the scheme of Table 1.2.

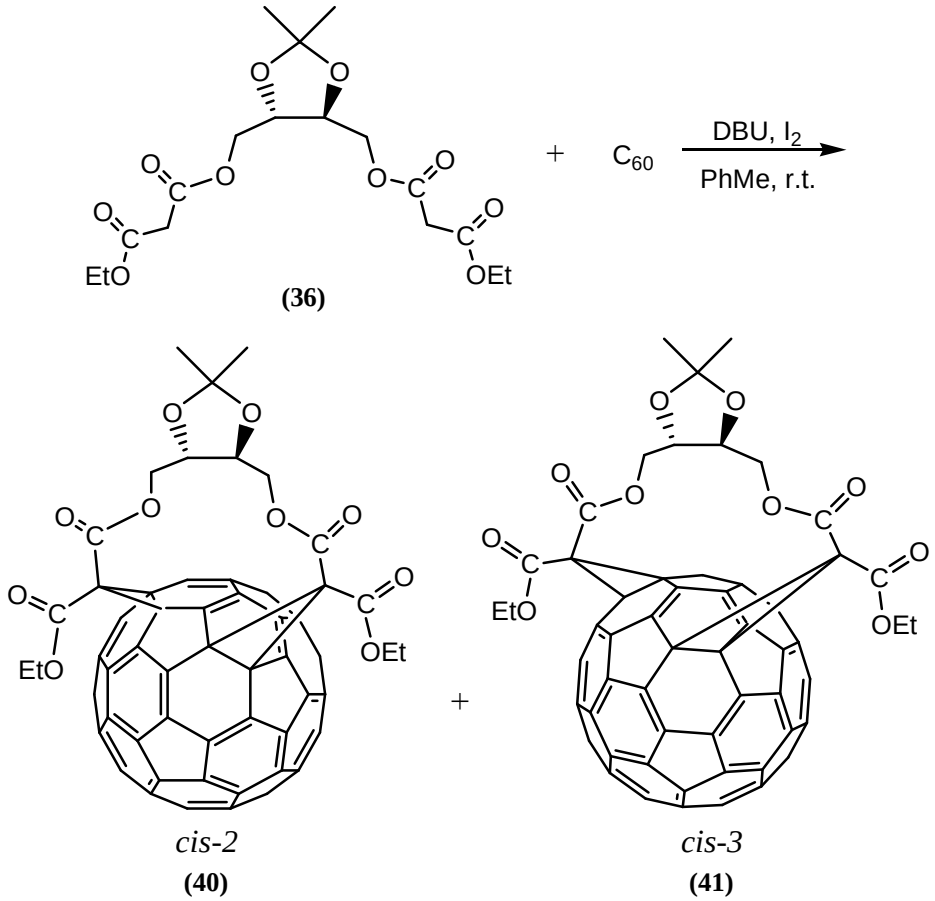

Scheme 2.5: Synthesis of tartaric acid derived tethered bismethano[60]fullerenyl adducts **(40)** and **(41)** under bingel reaction condition.

In the ^{1}H-NMR spectrum of **(40)** the signals at 4.17 ppm (d, J = 10.1 Hz, 1H) and 5.00 ppm (d, J = 8.0 Hz, 1H) appeared as broad doublets instead of doublet of doublets (J = 10.5, 2.6 Hz), and the signals at 4.24 ppm (d, J = 11.0 Hz, 1H) and 4.61 ppm (d, J = 10.7 Hz, 1H) also appeared as doublets instead of doublet of triplets (J = 10.5, 2.6 Hz) as reported by Nierengarten *et al.*[161] These four signals were assigned to the two diastereotopic methylene groups indicating the non-existence of a plane of symmetry within the molecule.

The ^{1}H-NMR spectrum of **(41)** was nearly identical to that reported by Nierengarten *et al.*[161] The two multiplet diastereotopic methylene signals were consistent with the lack of symmetry in the molecule. In the ^{13}C-NMR spectra of both **(40)** and **(41)** there were several fullerene carbon signals missing compared to those reported by Nierengarten *et al.*[161] (see Appendix II for details). These discrepancies may have been caused by the low concentration of our NMR sample and/or signal acquisition time that were not long enough. However, apart from these discrepancies, the ^{13}C-NMR signals observed matched well with reported by Nierengarten *et al.*[161]

2.2 1,4-Benzenedimethanol Tethered Bismethano[60]fullerenyl Adducts

2.2.1 Formation of the 1,4-Benzenedimethanol Tethered Bismalonate, 1,4-Bis{[(ethoxycarbonyl)acetoxy]methyl}benzene (34)

As illustrated in Scheme 2.6, diesterification of 1,4-benzenedimethanol **(42)** by ethyl 3-chloro-oxopropanoate **(39)** (2.52 mol. equiv.) in CH_2Cl_2/pyridine medium with stirring at rt for 3 h resulted in the 1,4-benzenedimethanol tethered bismalonate **(34)** in 68% yield as a yellow oil which spectroscopically closely matched that reported by Nierengarten *et al.*[161] (Appendix II).

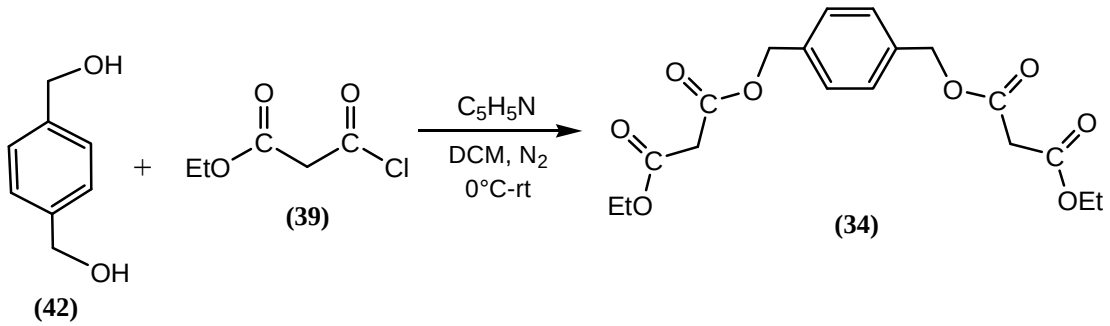

Scheme 2.6: Synthesis of the 1,4-benzenedimethanol tethered bismalonate **(34)**.

2.2.2 Tethered Functionalisation of [60]Fullerene by (36) to Form Bismethano[60]fullerenyl Adducts under Bingel Reaction Conditions

Under Bingel reaction conditions the tethered bismalonate **(34)** underwent double nucleophilic addition to [60]fullerene in the presence of DBU and iodine in toluene solution with stirring for 5 h at rt. This reaction led to the formation of two regioisomeric bismethanofullerenyl adducts. The mixture was separated by column chromatography to give the *e*-regioisomer **(44)** in 10% yield as a dark-red solid and the *trans-4* regioisomer **(43)** in 30% yield as a brown solid (Scheme 2.7).

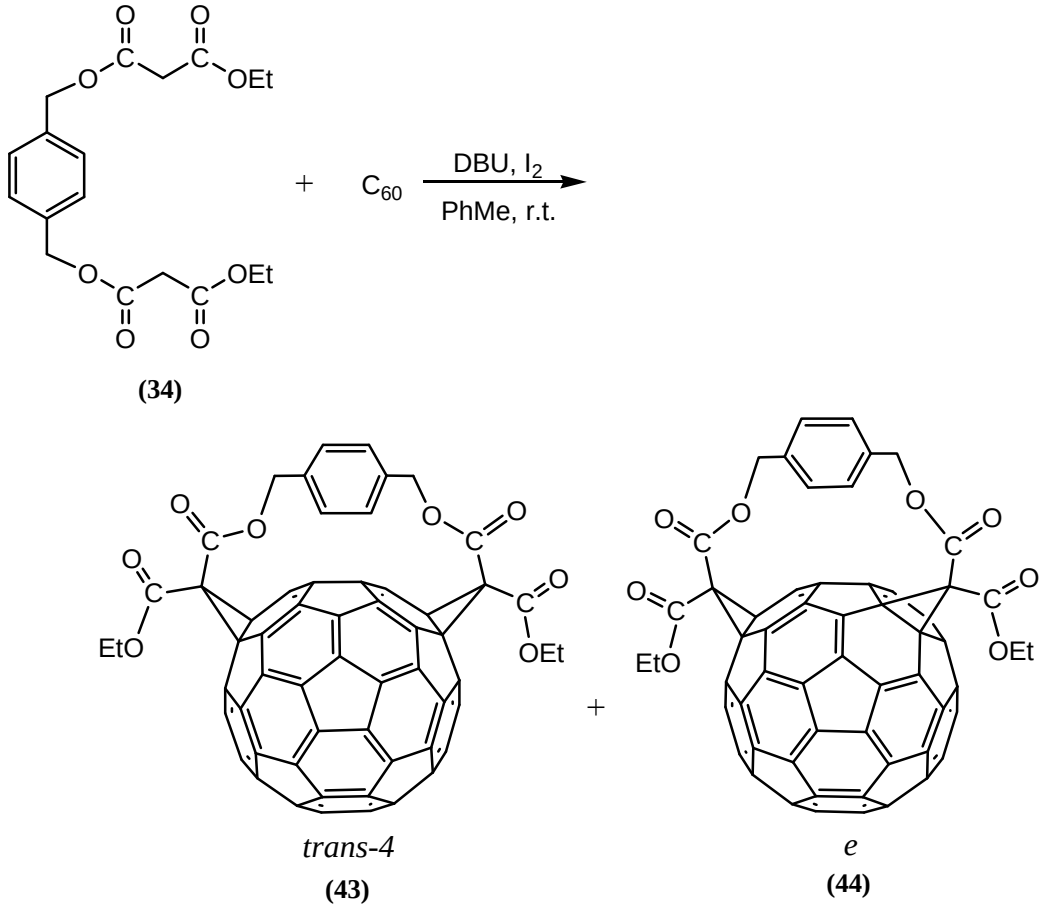

(34)

trans-4
(43)

e
(44)

Scheme 2.7: Synthesis of 1,4-benzenedimethanol tethered bismethano[60]fullerenyl adducts **(43)** and **(44)** under Bingel reaction condition.

^{1}H-NMR signals assigned to the aromatic protons of **(43)** at 7.17 ppm (s, 2H) and 7.34 (s, 2H) ppm appeared as singlets in contrast to the doublets (J = 1.8 Hz) reported by Nierengarten *et al*.,[161] and those of **(44)** at 6.91 ppm (d, J = 7.7 Hz, 1H), 7.00 ppm (d, J = 7.7 Hz, 1H), 7.64 ppm (d, J = 7.8 Hz, 1H) and 7.66 ppm (d, J = 8.0 Hz, 1H) appeared as doublets instead of doublet of doublets (J = 7.5, 1.5 Hz and J = 8.0, 1.5 Hz) as reported. Apart from these discrepancies the ^{1}H-NMR spectra of both **(43)** and **(44)**

were identical to those reported by Nierengarten *et al*.[161] In the ^{1}H-NMR spectrum of **(43)**, there were two singlet signals each integrating for 2H assigned to the aromatic protons and only two benzylic ether proton doublet signals each integrating for 2H which were consistent with the *Cs* symmetry of the molecule. In contrast, in the ^{1}H-NMR spectrum of **(44)**, four different aromatic proton doublet signals (J = 7.7 – 8.0 Hz) were observed and four benzylic ether proton doublet signals were observed consistent with the symmetry in the molecule. Again, dilute solutions and/or too short signal acquisition times resulted in some of the ^{13}C-NMR signals not to be observed (see Appendix II for details).

2.3 1,3-Benzenedimethanol Tethered Bismethano[60]fullerenyl Adducts

2.3.1 Formation of the 1,3-Benzenedimethanol Tethered Bismalonate 1,3-Bis{[(ethoxycarbonyl) acetoxy]methyl}benzene (35)

As illustrated in Scheme 2.8, diesterification of 1,3-benzenedimethanol **(45)** by ethyl 3-chloro-oxopropanoate **(39)** (2.52 mol. equiv.) in CH_2Cl_2/pyridine medium with stirring at rt for 3 h resulted in the 1,3-benzenedimethanol tethered bismalonate **(35)** in 72% yield as a pale yellow oil which spectroscopically closely matched that reported by Nierengarten *et al.*[161] (Appendix II).

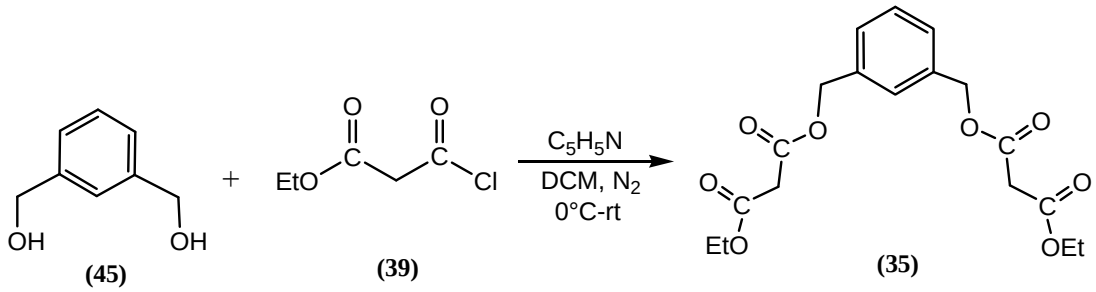

Scheme 2.8: Synthesis of the 1,3-benzenedimethanol tethered bismalonate **(35)**.

2.3.2 Tethered Functionalisation of [60]Fullerene by (35) to Form Bismethano[60]fullerenyl adducts under Bingel Reaction Conditions

Under Bingel reaction conditions the 1,3-benzenedimethanol tethered bismalonate **(35)** underwent double nucleophilic additions to [60]fullerene in the presence of DBU and iodine in toluene solution with stirring for 5 h at rt. This led to the formation of a single regioisomeric bismethanofullerenyl adduct **(46)** in 31% yield as a dark-red solid (Scheme 2.9).

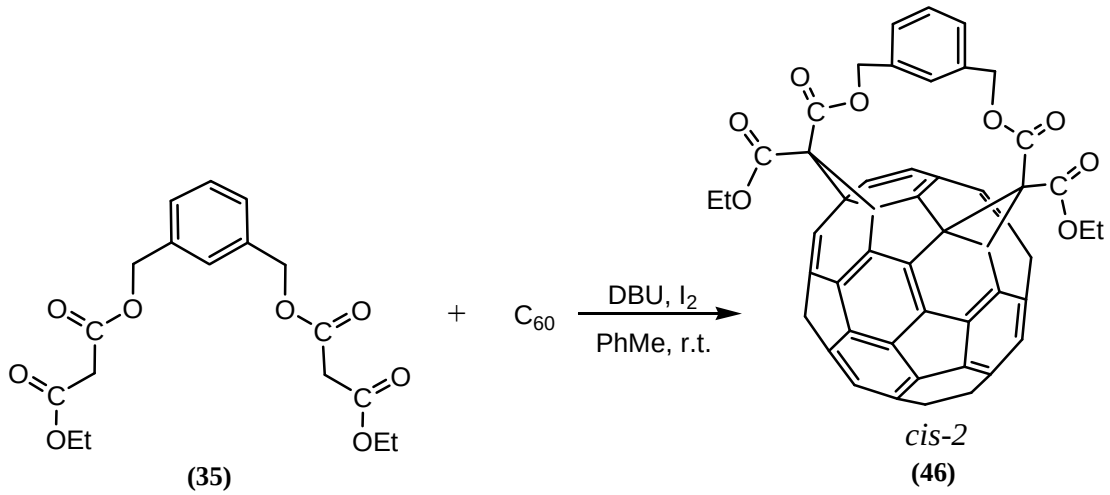

(35) **(46)**

Scheme 2.9: Synthesis of 1,3-benzenedimethanol tethered bismethano[60]fullerenyl adduct **(46)**.

There were two discrepancies between our ^{1}H-NMR spectrum of **(46)** and that of the literature.[161] In our ^{1}H-NMR spectrum of **(46)**, the signal at 7.28 ppm was observed as a doublet (d, J = 7.5 Hz, 2H) instead of a doublet of doublets (J = 7.5, 1.5 Hz), the one at 7.38 ppm was observed as a doublet (d, J = 7.5 Hz, 1H) instead of a triplet (J = 7.5 Hz) and the one at 7.52 ppm (s, 1H) was observed as a singlet instead of a triplet (J = 1.5 Hz) as reported by Nierengarten *et al*., perhaps due to the low resolution of our NMR experiment. The signals assigned to the diastereotopic methylenes of **(46)** appeared as two doublets at 5.16 ppm (d, J = 12.9 Hz, 2H) and at 5.86 (d, J = 12.9 Hz, 2H), due to the plane of symmetry in the molecule. In the ^{13}C-NMR spectrum of **(46)** one fullerene carbon signal was missing at 145.26 ppm compared to the ^{13}C-NMR spectrum of Nierengarten.[161]

2.4 Generation of Tetraethyl Bismethano[60]fullerenyl Tetracarboxylate

Regioisomeric tetraethyl bismethano[60]fullerenyltetracarboxylates were generated from the tethered bismethano[60]fullerene bisadducts **(40)**, **(41)**, **(43)**, **(44)** and **(46)** through transesterification by ethanol under basic conditions (Scheme 2.4). In a typical reaction the bisadducts were dissolved in a 1:1 mixture of THF/ethanol and solid K_2CO_3 (80 mol. equiv.) was added. The mixture was stirred at rt for 1.5 h and the transesterified products were isolated by column chromatography. The yields varied from 31–53% (Scheme 2.10). The transesterified products had the same regioisomerism as their tethered starting materials and the retention of regiochemistry was confirmed by Nierengarten et al.,[129] by UV/Vis spectra and molecular symmetry deduced from ^{1}H- and ^{13}C-NMR spectra.

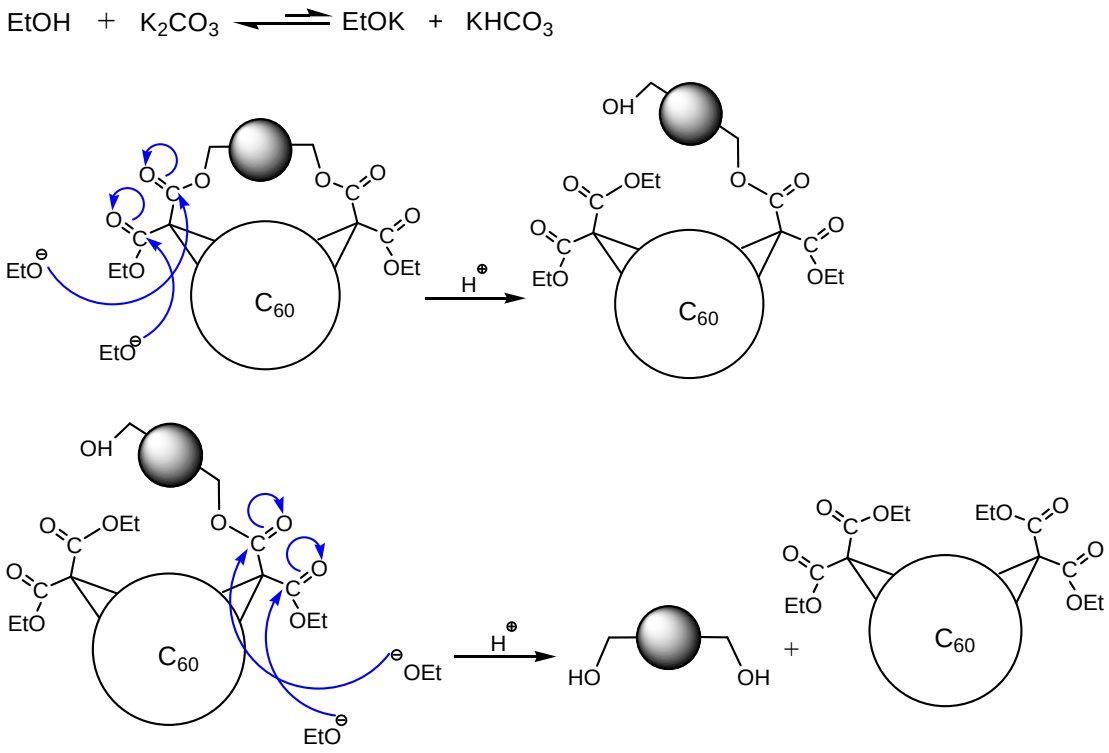

(a)

Scheme 2.10: continued next page

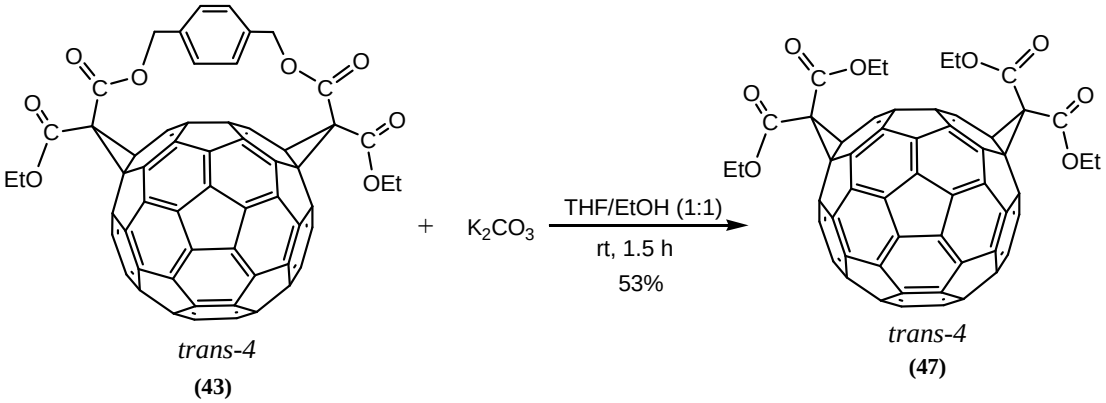

trans-4
(43)

trans-4
(47)

(b)

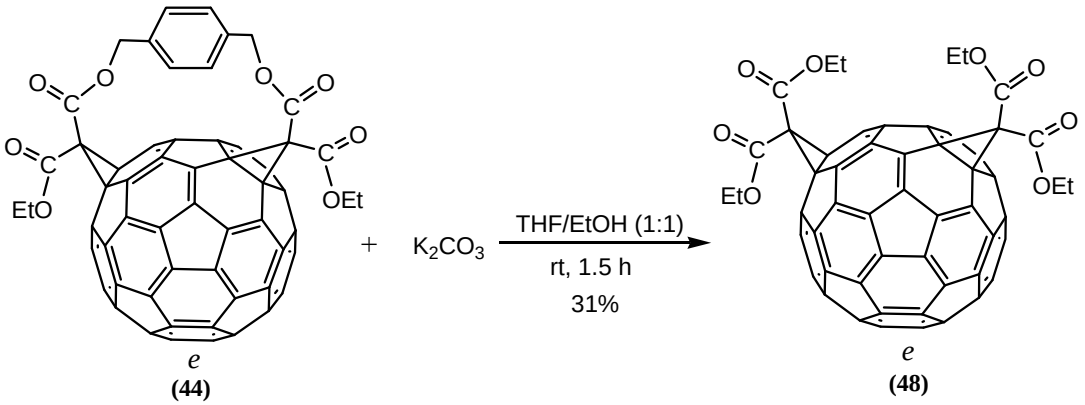

e
(44)

e
(48)

(c)

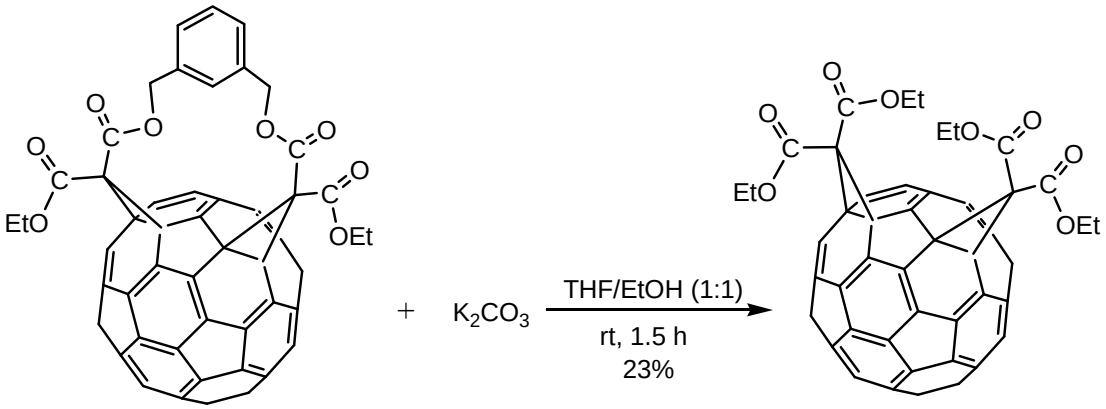

cis-2
(46)

cis-2
(49)

(d)

Scheme 2.10: continued next page

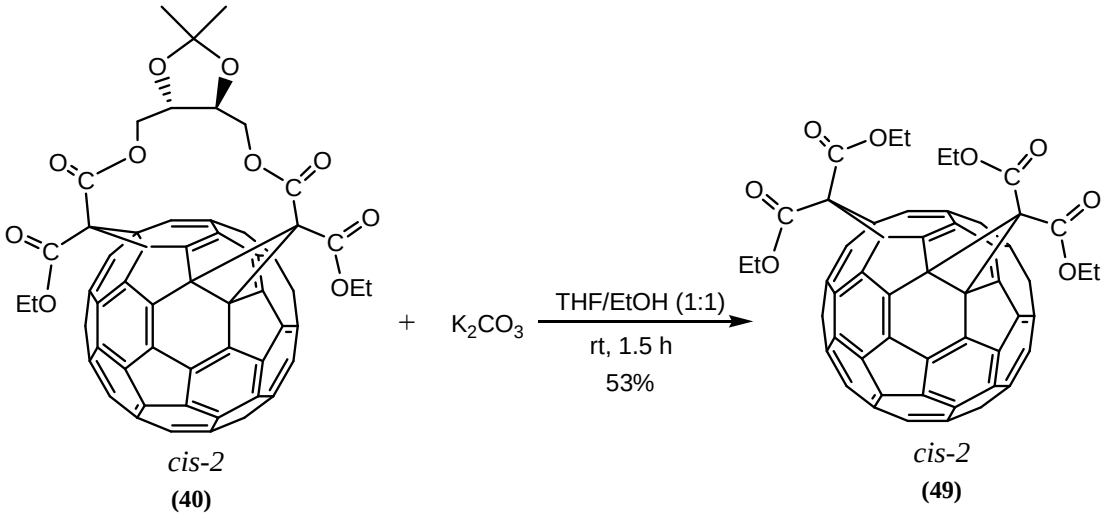

cis-2
(40)

cis-2
(49)

(e)

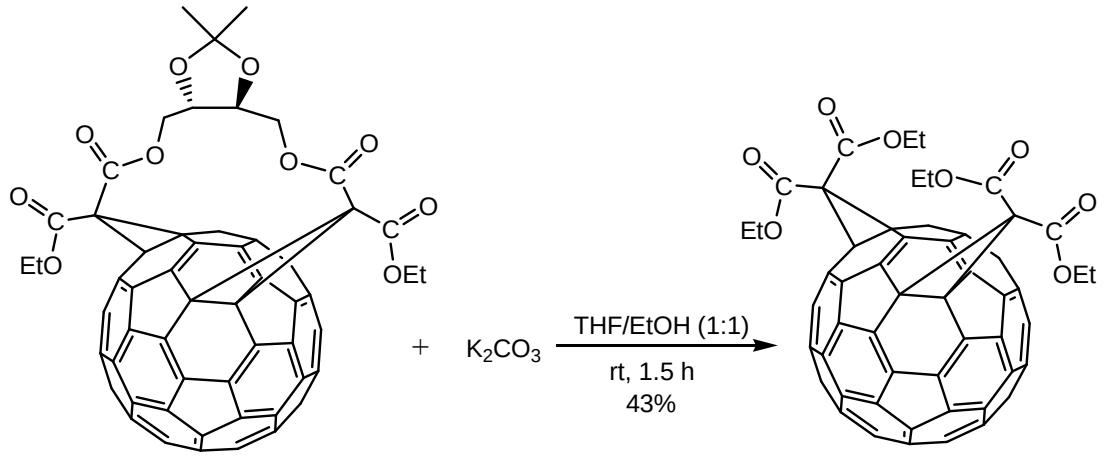

cis-3
(41)

cis-3
(50)

(f)

Scheme 2.10: Transesterification of bisadducts by ethanol. In each case the regioisomerism was unchanged. (a): Mechanism of transesterification. (b)-(f): Transesterification of bisadducts **(40)**, **(41)**, **(43)**, **(44)** and **(46)** and the resulted tetraethylcarboxylates **(47)**-**(50)**.

Transesterification of bisadducts **(40)**, **(41)**, **(43)**, **(44)** and **(46)** by ethanol must be carried out under absolute anhydrous conditions. Hydroxy anions generated from water molecules would attack the carbonyl groups of these bisadducts prior to ethoxy anions leading to tetradimethano[60]fullerenylcarboxylic acids instead of **(47)** - **(50)**. Due to low amounts of **(47)** - **(50)** available, ^{13}C-NMR spectra were not performed. The ^{1}H-NMR spectra of these transesterified products showed 1 or 2 triplet methyl signals

and 1 or 2 multiplet or quartet signals for the ester methylene groups (Appendix II)

2.5 Semi-empirical Calculations of Heat of Formation of Regioisomeric Bisadducts

If the regioisomeric tetraethyl ester bisadducts undergo a "walk-on-the-sphere" rearrangement in the mass spectrometer then the major regioisomeric product formed should be the thermodynamically more stable. To determine the most stable regioisomers, molecular modelling studies (Spartan AM1) were performed and the results are shown in Table 2.4. To demonstrate the rationality of their formation via Bingel reactions, the heats of formation of all possible regioisomers of tethered bismethano[60]fullerene bisadducts were also calculated for comparison (Table 2.1 - 2.3).

Table 2.1: 1,4-Benzenedimethanol tethered bisadducts.

Entry	Structure	Regioisomerism	Heat of Formation (kJ/mol)
1	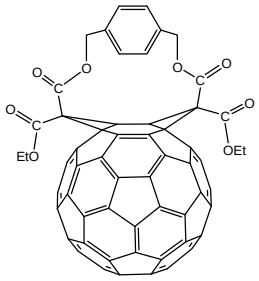	*cis-1*	3190
2	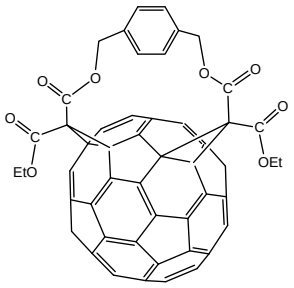	*cis-2*	3040

3	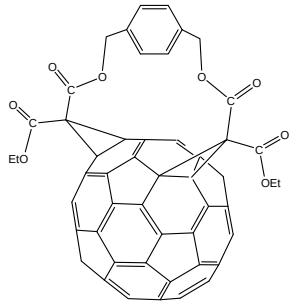	*cis-3*	2992
4	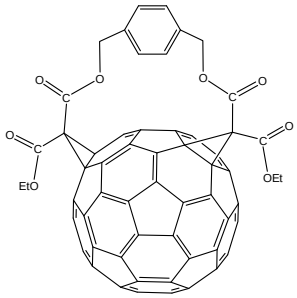 **(44)**	*e*	3004
5	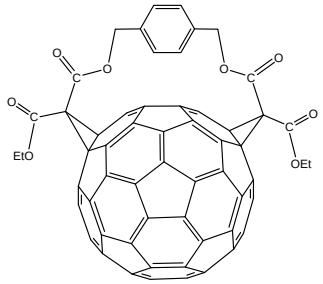 **(43)**	*trans-4*	3044
6	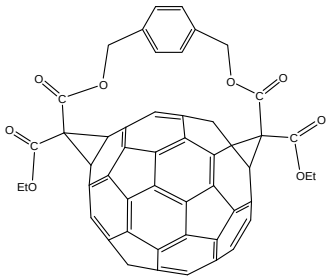	*trans-3*	3266
7	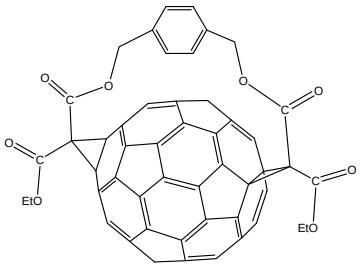	*trans-2*	3427

8	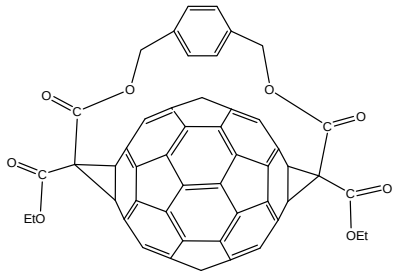	*trans-1*	N/A

Table 2.2: 1,3-Benzenedimethanol tethered bisadducts.

Entry	Structure	Regioisomerism	Heat of Formation (kJ/mol)
1	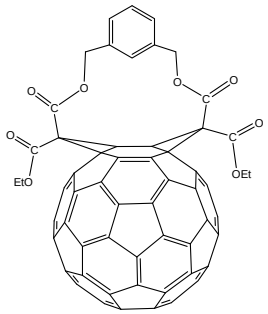	*cis-1*	3132
2	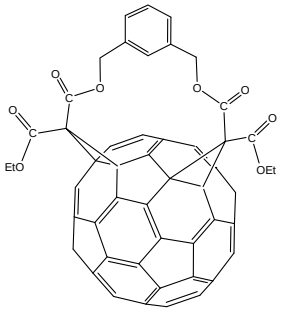 **(46)**	*cis-2*	3009
3	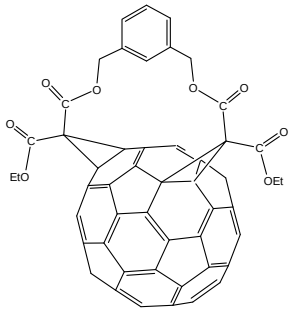	*cis-3*	2975

4	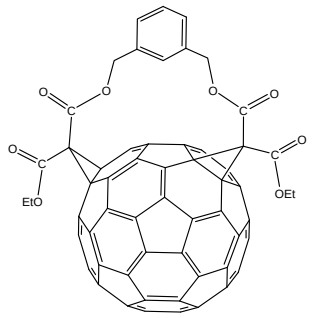	*e*	3006
5	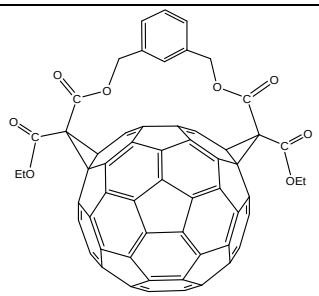	*trans-4*	3011
6	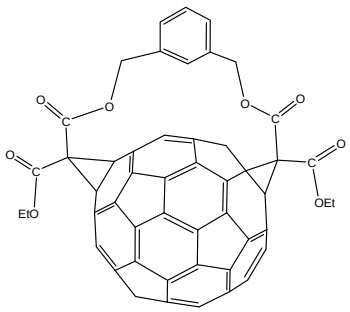	*trans-3*	3389
7	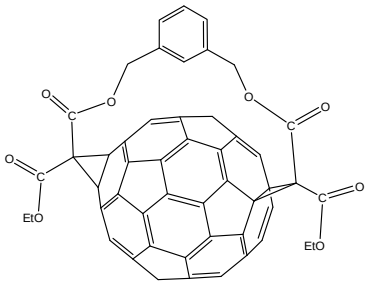	*trans-2*	3578
8	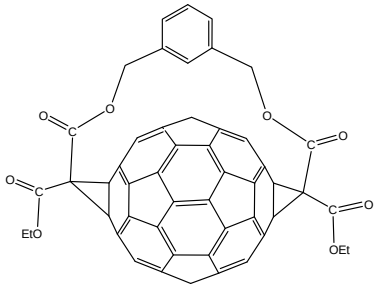	*trans-1*	N/A

Table 2.3: Tartaric acid derived bismethano[60]fullerenyl tethered bisadducts.

Entry	Structure	Regioisomerism	Heat of Formation (kJ/mol)
1	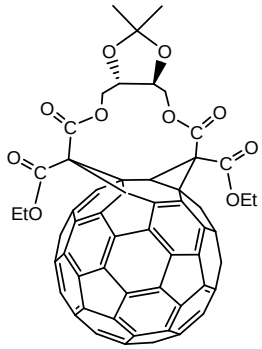	*cis-1*	2546
2	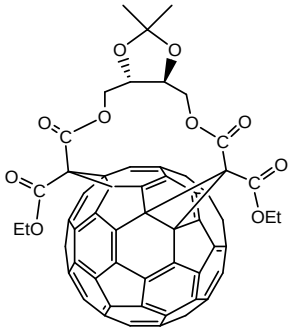 **(40)**	*cis-2*	2486
3	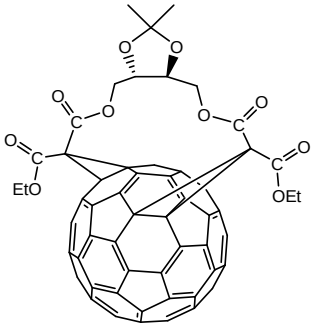 **(41)**	*cis-3*	2507
4	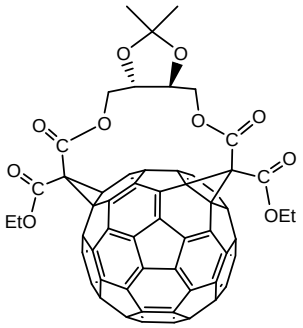	*e*	2540

5	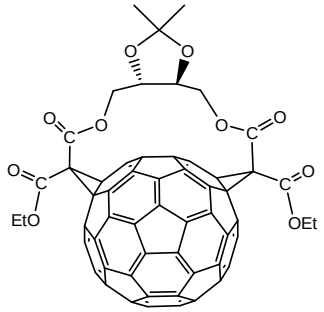	*trans-4*	2603
6	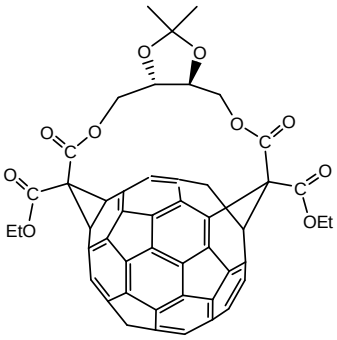	*trans-3*	2621
7	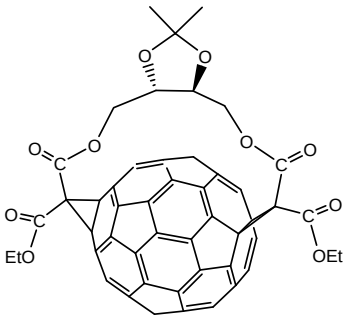	*trans-2*	3399
8	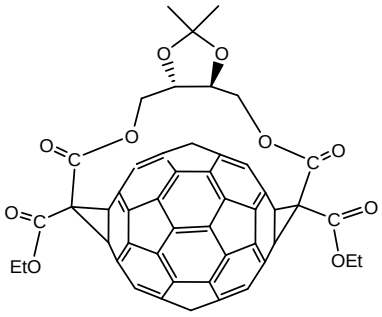	*trans-1*	N/A

Table 2.4: Tetraethyl bismethano[60]fullerenyl tetracarboxylates.

Entry	Structure	Regioisomerism	Heat of Formation (kJ/mol)
1	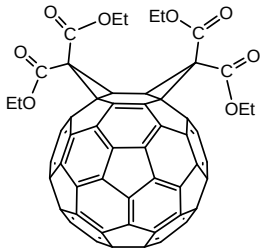	*cis-1*	2845
2	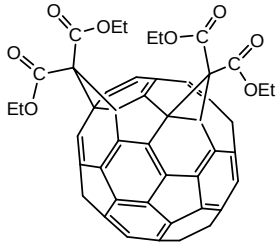 **(49)**	*cis-2*	2786
3	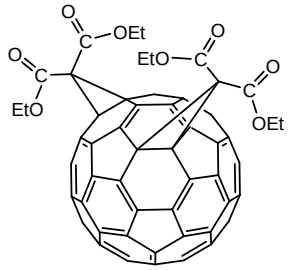 **(50)**	*cis-3*	2792
4	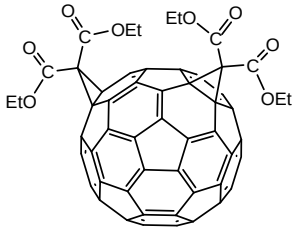 **(48)**	*e*	2788
5	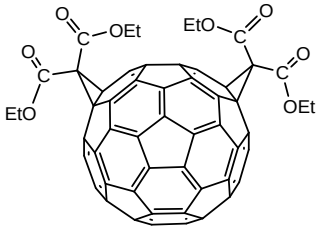 **(47)**	*trans-4*	2779

6	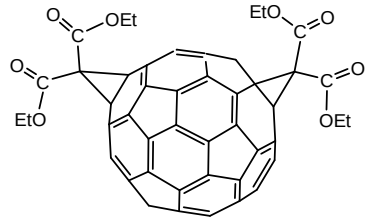	*trans-3*	2766
7	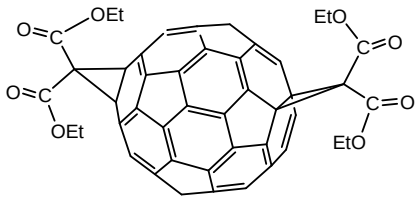	*trans-2*	2789
8	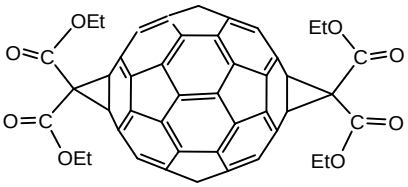	*trans-1*	2784

The Spartan program did not allow the heat of formation of the *trans-1* regioisomers of tethered bisadducts to be calculated due to their structural impossibility because of the extended distance between the two cyclopropane groups. The lowest value of the heat of formation did not coincide with the observed products **(43)** or **(44)** among the regioisomeric bisadducts formed from **(34)** (Table 2.1). The same was true for **(46)** among those formed from **(35)** (Table 2.2). Therefore the heat of formation is not the only element that accounts for which regioisomer is favoured in the Bingel reaction. As mentioned in section 1.5, a tethered bisfunctionalisation of [60]fullerene under Bingel reaction conditions is a two-step process and the orientation for the S_N2 ring closing reaction contributes to the product distribution. Therefore the regioselectivity of [60]fullerene Bingel bisfunctionalisation must be considered dynamically rather than statically, and entropy factors must also be considered.

2.6 The Study of Tethered and Non-tethered Methano[60]fullerenyl Bisadducts

Of the 1,4-benzenedimethanol tethered bisadducts, the extended *trans*-regioisomers had higher calculated heats of formation than the *cis*- and *e*-regioisomers. Of the *cis*-regioisomers, the *cis-3* regioisomer had the lowest heat of formation (Table 2.1,

Entry 3) and would thus be predicted to be the most thermodynamically stable regioisomer. The observed regioisomers, **(43)** and **(44)**, however, had the second and third lowest calculated heats of formation (Table 2.1, Entry 5 and 4, respectively). Of the 1,3-benzenedimethanol tethered bisadducts, the observed *cis-2* **(46)**, together with the *e* and *trans-4* regioisomers (Table 2.2, Entry 2, 4 and 5) had similarly low calculated heats of formation although the lowest was found with the *cis-3* regioisomer (Table 2.2, Entry 3). The observed regioisomers of the tartaric acid derived bismethano [60]fullerenyl tethered bisadducts **(40)** and **(41)** had the lowest and second lowest calculated heats of formation (Table 2.3, Entry 2 and 3).

These Bingel reaction products are most likely formed under kinetically controlled conditions and entropy factors also play an important role in the rates of bisadduct formation. Thus we can only use the calculated heats of formation as a guide to which regioisomer may be preferentially formed.

2.7 Mass Spectrometry (MS) and Ion Mobility Mass Spectrometric (IMMS) Studies

2.7.1 ESIMS Studies

With tethered bisadducts **(43)**, **(44)**, **(46)**, **(40)** and **(41)** as well as non-tethered bisadducts **(47)** - **(50)** available, mass spectrometry and ion mobility mass spectrometry studies were undertaken in an attempt to determine their molecular weights and to examine the possibility of resolving the different regioisomers that have the same mass by IMMS. The results of the electrospray ionisation mass spectrometric (ESIMS) studies are shown in Table 2.5. The ESI MS of the tethered bisadducts showed a $[M + Na]^+$ molecular ion in the positive ion mode while in the negative ion mode a $[M + H]^-$ ion was observed (Table 2.5). $[M + Na]^+$ and $[M + H]^-$ molecular ions were also observed in the ESI (+ve) and ESI (-ve) MS of the non-tethered, tetraethyl ester

bisadducts, respectively (Table 2.5). The $[M + H]^-$ ions presumably arises from protonation of the radical anion ($M^{\bullet-}$) by methanol to give $MH^\bullet$ followed by capture of an additional electron. An alternative mechanism would be formation of M^{2-} from the addition of 2 electrons to M followed by protonation.

Table 2.5: Mass spectrometry studies on tethered and non-tethered bisadducts.

Tethered bisadducts		Tethered bisadducts		Non-tethered bisadducts		Non-tethered bisadducts	
ESI +, $[M + Na]^+$		ESI –, $[M + H]^-$		ESI +, $[M + Na]^+$		ESI –, $[M + H]^-$	
	m/z		*m/z*		*m/z*		*m/z*
trans-4 **(43)**	1105	*trans-4* **(43)**	1083	*trans-4* **(47)**	1059	*trans-4* **(47)**	1037
e **(44)**	1105	*e* **(44)**	1083	*e* **(48)**	1059	*e* **(48)**	1037
cis-2 **(46)**	1105	*cis-2* **(46)**	1083	*cis-2* **(49)**	1059	*cis-2* **(49)**	1037
cis-2 **(40)**	1129	*cis-2* **(40)**	1107	*cis-2* **(49)**	1059	*cis-2* **(49)**	1037
cis-3 **(41)**	1129	*cis-3* **(41)**	1107	*cis-3* **(50)**	1059	*cis-3* **(50)**	1037

The ESI (-ve) MS of the tethered bisadducts **(40)**, **(41)**, **(43)**, **(44)** and **(46)** also showed ions for a methanol adduct (Table 2.6). These ions presumably arose from the methanol that was used as the solvent for these MS studies, a possible general structure for these methanol adducts is shown in Scheme 2.11. Methanol adducts were not seen in the ESI (-ve) MS of the non-tethered bisadducts **(47)** – **(50)**. We assume that these were less reactive towards methanol because of their less strained nature.

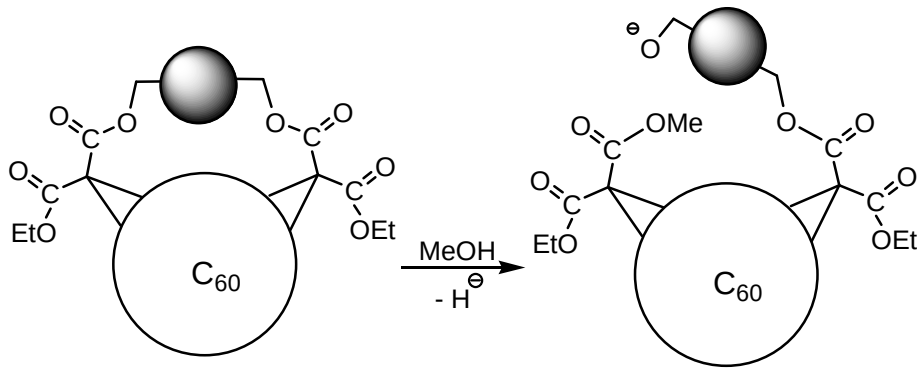

Scheme 2.11: Methanol adduct of a tethered bisadduct in methanol solvent.

Table 2.6: ESI (-ve) results of methanol adducted tethered bisadducts.

	m/z of $[M + H]^-$	*m/z* of $[M + MeO]^-$
trans-4 **(43)**	1083	1113
e **(44)**	1083	1113
cis-2 **(46)**	1083	1113
cis-2 **(40)**	1107	1137
cis-3 **(41)**	1107	1137

2.7.2 IMMS Studies

The drift times from the IMMS studies of the tethered and non-tethered bisadducts (**(40)**, **(41)**, **(43)**, **(44)**, **(46)** and **(47)**, **(48)**, **(49)**, **(50)**) are shown in Table 2.7 and Figures 2.2 to 2.5.

Table 2.7: Drift times from the ion mobility mass spectrometry studies on tethered and non-tethered bisadducts. The *cis-2* structure **(46)** contains the *m*-benzene based tether and *cis-2* **(40)** contains the chiral tether.

Tethered bisadducts		Tethered bisadducts		Non-tethered bisadducts		Non-tethered bisadducts	
ESI + $[M + Na]^+$		ESI – $[M + H]^-$		ESI + $[M + Na]^+$		ESI – $[M + H]^-$	
	Drift time (μs)		Drift time (μs)		Drift time (μs)		Drift time (μs)
trans-4 **(43)**	3.60	*trans-4* **(43)**	3.15	*trans-4* **(47)**	3.66	*trans-4* **(47)**	3.15
e **(44)**	3.47	*e* **(44)**	3.08	*e* **(48)**	3.47	*e* **(48)**	3.08
cis-2 **(46)**	3.21	*cis-2* **(46)**	3.21	*cis-2* **(49)**	3.21	*cis-2* **(49)**	3.02
cis-2 **(40)**	3.41	*cis-2* **(40)**	3.47	*cis-2* **(49)**	3.21	*cis-2* **(49)**	3.08
cis-3 **(41)**	3.66	*cis-3* **(41)**	3.41	*cis-3* **(50)**	3.41	*cis-3* **(50)**	3.08

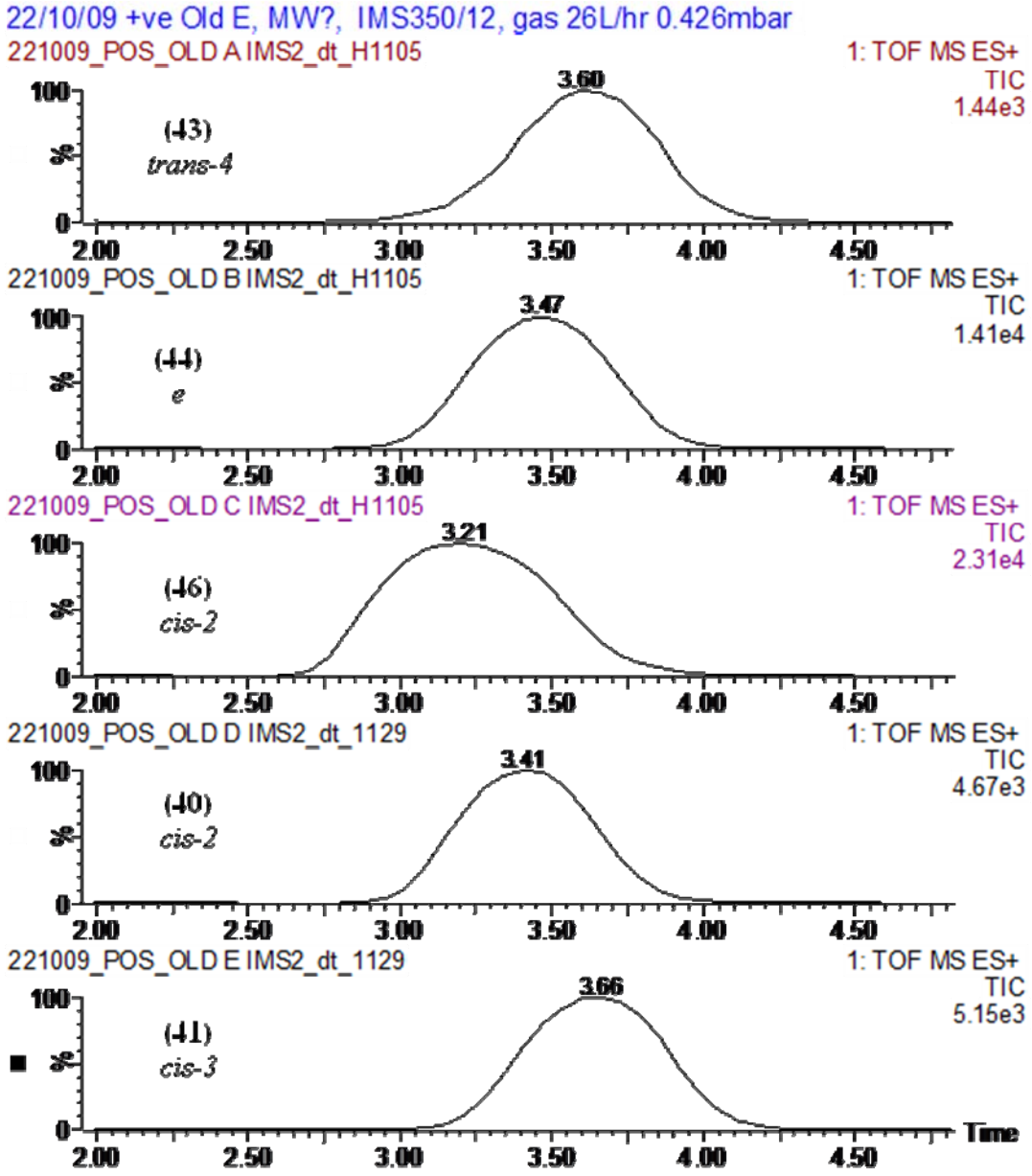

Figure 2.2: IMMS spectra of tethered bisadducts, +ve ion mode. The drift times on the x-axis are in µs.

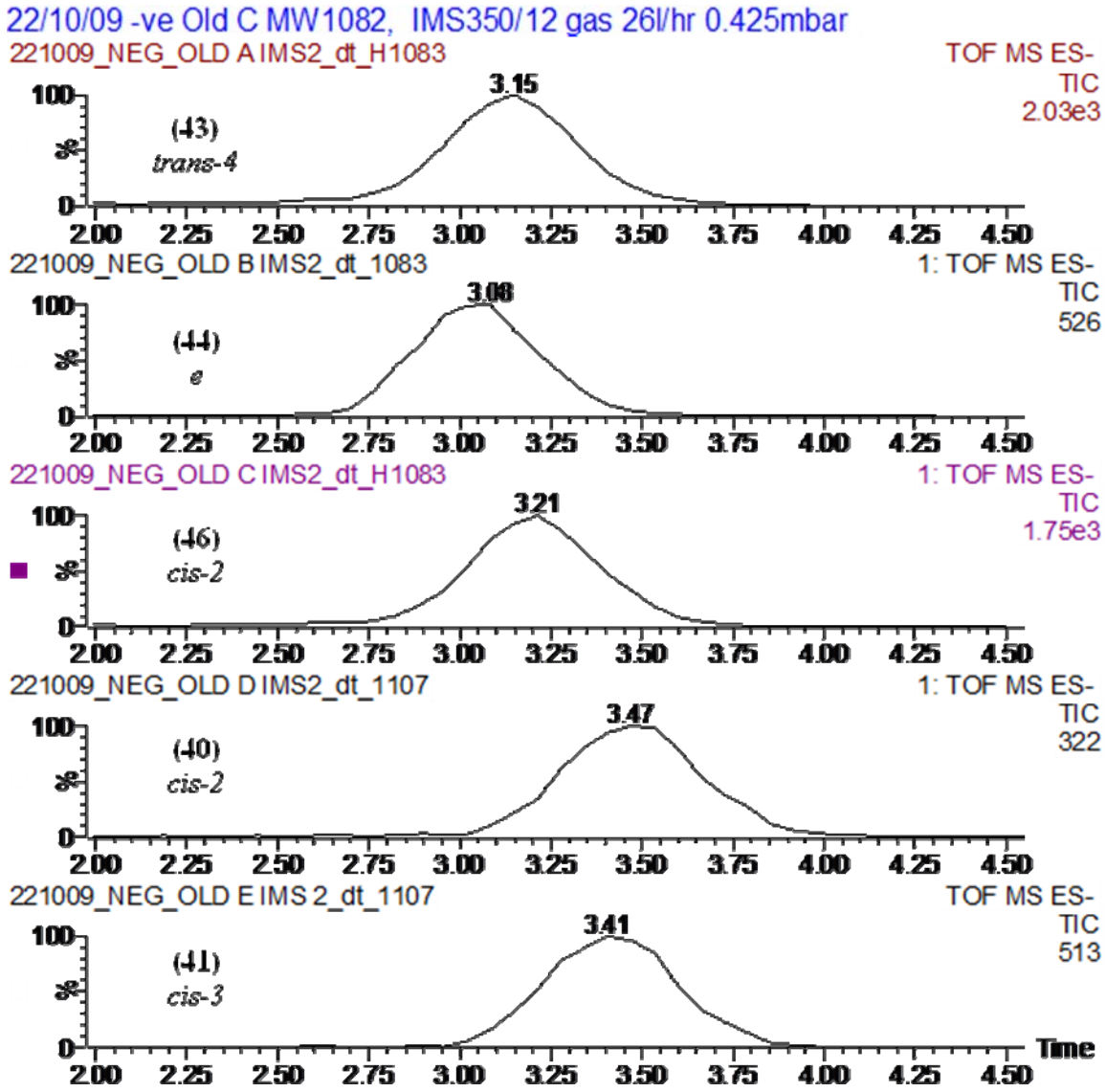

Figure 2.3: IMMS spectra of tethered bisadducts, -ve ion mode. The drift times on the x-axis are in μs.

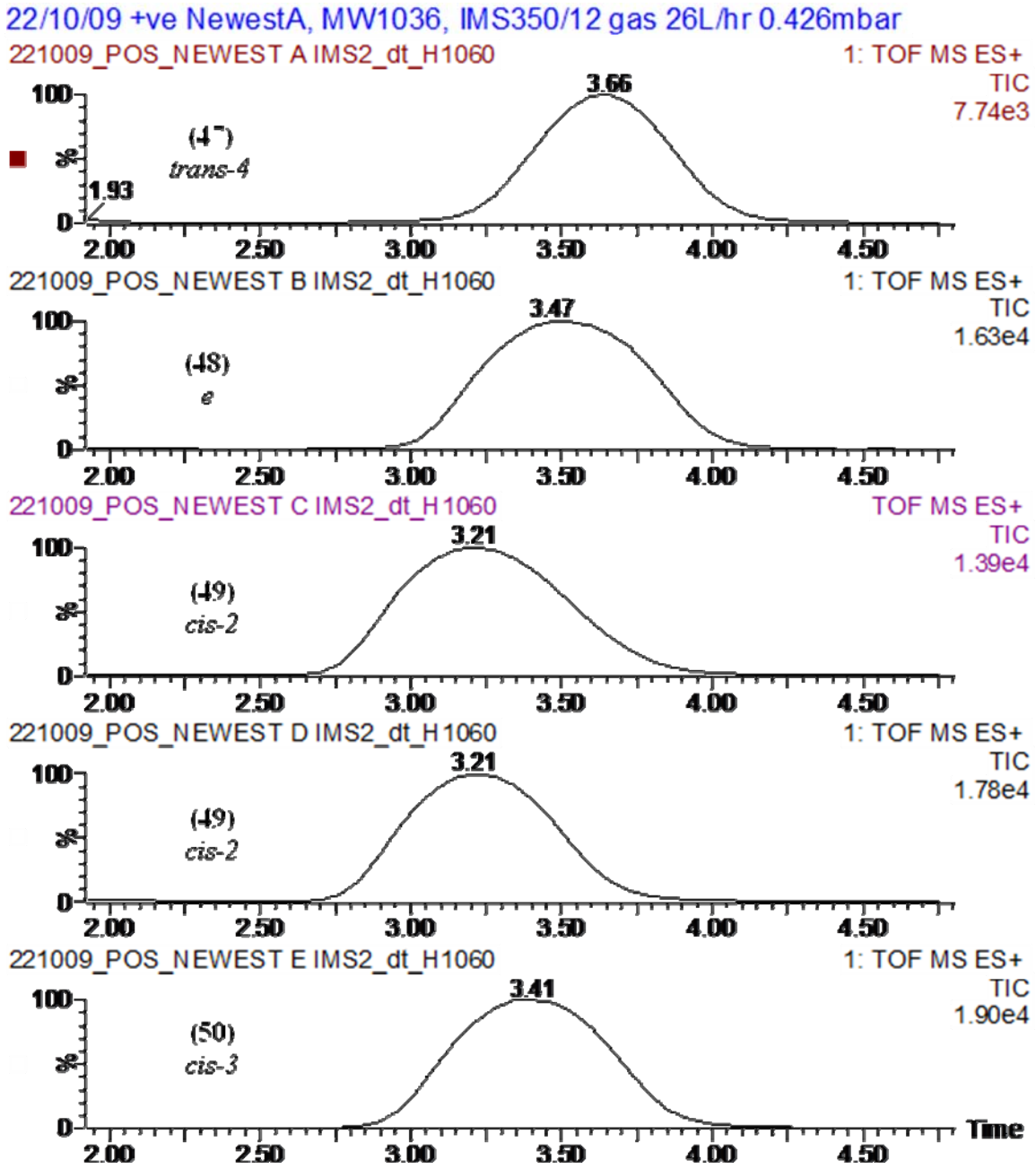

Figure 2.4: IMMS spectra of non-tethered bisadducts, +ve ion mode. The drift times on the x-axis are in μs.

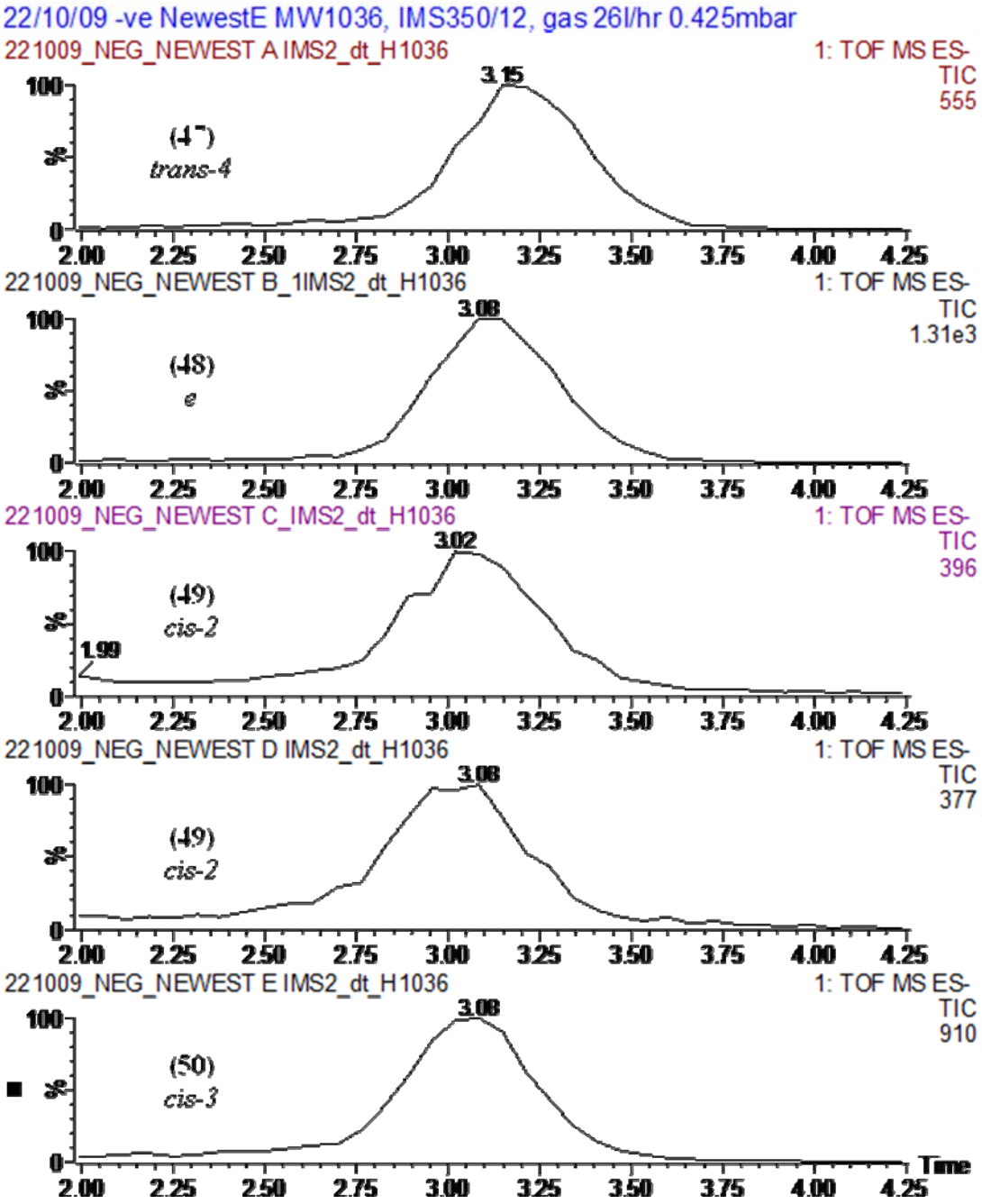

Figure 2.5: IMMS spectra of non-tethered bisadducts, -ve ion mode. The drift times on the x-axis are in μs.

Each of tethered bisadducts showed one broad peak on the drift time (μs) axis in their IMMS spectra, in the positive and negative ion modes. The different regioisomeric pairs of compounds showed different drift times. For example the *e* compound **(44)** had a

shorter drift time (3.47 μs) than its *trans-4* regioisomer **(43)** which had a drift time of 3.60 μs in the + ve ion mode (Figure 2.2). These differences in drift times are consistent with the larger cross-sectional area of the *trans-4* isomer when compared with that of the *e*. This difference is expected based on the relative distances between two cyclopropane units in **(43)** and **(44)**. Of the +ve ion mode IMMS, the 1,3-benzenedimethanol tethered bisadduct **(46)** showed the shortest TOF while in the -ve mode the 1,4-benzenedimethanol tethered bisadduct **(44)** showed the shortest TOF (Figure 2.2). Therefore we can conclude that **(46)** has the smallest molecular cross-sectional area among the $[M + Na]^+$ ions and **(44)** has the smallest molecular cross-sectional area among the $[M + H]^-$ ions. For the same reason, the tartaric acid derived tethered bisadducts **(41)** and **(40)** have the largest molecular cross-sectional areas among the $[M + Na]^+$ positive ions and the $[M + H]^-$ negative ions, respectively (Figure 2.2).

Among the non-tethered bisadducts (tetraethyl bismethano[60]fullerenyl tetracarboxylates), in accordance with the +ve ion mode IMMS results, the order of molecular cross-sectional areas was *trans-4* > *e* > *cis-3* > *cis-2* (Figure 2.4). This result was reasonable because the closer the sites of cycloadditions are, the smaller the molecule should be. Under the reductive conditions of the -ve mode IMMS experiments, however, "walk-on-the-sphere" rearrangements may have occurred to all of these non-tethered bisadducts, reflected by shoulders in the peaks which may indicate the formation of the resulting isomers (Figure 2.3 and Figure 2.5). This was particularly noticeable in the –ve ion mode IMMS spectrum of **(49)** (Figure 2.5). Because of these shoulders, we can tentatively conclude that such "walk-on-the-sphere" rearrangements were partial ones. The same structures **(49)** that were generated from different starting compounds **(40)** and **(46)** produced slightly different drift times (Table 2.7).

Thus we can conclude that IMMS can be used to separate regioisomeric fullerene bisadducts based upon their different cross-sectional areas. These preliminary

experiments may suggest that “walk-on-the-sphere” mode rearrangements might be occuring in the – ve ion mode mass spectrometric experiments.

Chapter 3: Conclusions

In this study the synthesis of the regioisomeric tetraethyl bismethano[60]fullerenyl tetracarboxylates **(47)** – **(50)** was repeated on the basis of Nierengarten's report[161] with essentially satisfactory yields and purities. The yields of the tartaric acid derived tethered bisadducts **(40)** and **(41)** were approximately half of what were reported, probably due to the column separation procedure that could still be further optimized. In addition, proper concentrations as well as signal acquisition times might need more trials to reach for the improvement of the ^{13}C-NMR spectra of the tethered bisadducts **(40)** and **(44)**.

Transesterification of the tethered bisadducts **(40)**, **(41)**, **(43)**, **(44)** and **(46)** to generate the non-tethered bisadducts **(47)** – **(50)** experienced several repeated failures. This problem was solved by using distilled and dry methanol as the reaction solvent. Therefore such failures could probably be attributed to the methanol-containing-water-generated hydroxy ions that reacted with these tethered bisadducts giving rise to tetramethano[60]fullerenyl carboxylic acids instead of the desired non-tethered bisadducts **(47)** – **(50)**.

The chemically generated bisadducts **(43)**, **(44)** and **(46)** were not exactly the ones that showed the lowest values of the heats of formation calculated by Spartan AM1 in their respective tethered categories, which indicated that elements other than heat of formation should also be considered for the dynamic mechanism of the formation of regioisomeric tethered bisadducts. The key point most likely lies in the second addition of the anchored and conjugated reactive group to a kinetically and/or thermodynamically favourable 6,6-double bond on the C_{60} sphere.

The employment of IMMS in this study enabled the comparison of the cross-sectional areas of the tethered and non-tethered [60]fullerenyl bisadducts, providing some structural information that might be useful for further studies of fullerenyl derivatives of complicated structures in the future. The size of the cross-sectional area of a fullerenyl derivative was directly reflected by the length of the drift time it travelled through the drift tube of the IMMS spectrometer, in both the +ve and –ve modes. In the case of this study, all of the four non-tethered bisadducts **(47)** – **(50)** may have experienced an incomplete "walk-on-the-sphere" rearrangement under the reductive conditions of their –ve ion mode IMMS studies.

Further improvements of experimental conditions might be necessary in order to enhance the occurrence of such rearrangements in future studies.

Chapter 4: Experimental

Experimental General Methods

[60]Fullerene was purchased from MER Corporation, Tucson, Arizona AZ85706, USA. Other reagents and solvents were purchased reagent-grade and used without further purification except MeOH which was distilled from magnesium and iodine. All reactions were performed in standard glasswares and the synthesis of tethered bismalonates **(34)**, **(35)** and **(36)** was carried out under an inert atmosphere of nitrogen. Flash column chromatography was performed using silica 60 (230 – 400 mesh, 0.040 – 0.063 mm) purchased from Merck. Petroleum spirit refers to a hydrocarbon fraction with a boiling point of 40 – 60 °C.

Electrospray ionisation and ion mobility mass spectroscopies were obtained with a Waters Synapt HDMS™. The instrument parameters during experiments were as follows:

For ESI +, ESI – and IMMS	
Capillary	2.3 kV
Sampling Cone	50.0
Extraction Cone	4.0
Source Temperature	50 °C
Desolvation Temperature	120 °C
Desolvation Gas Flow	300.0 L/h
Trap Collision Energy	6.0 eV
Transfer Collision Energy	2.0 eV
For IMMS only	
IMS Cell Pressure	0.426 mbar
IMS Wave Velocity	350 m/s
IMS Wave Height	12 V

Tethered bismalonates were dissolved in CH_3CN (50%) and formic acid (0.2%), tethered and non-tethered bismechano[60]fullerene bisadducts were dissolved in MeOH for MS studies.

^{1}H-NMR and ^{13}C-NMR spectra were acquired on a VARIAN PREMIUM SHIELD 500

MHz NMR spectrometer or a VARIAN INOVA 500 MHz 3-channel NMR spectrometer at 499.9 MHz and 125.0 MHz, respectively. The deuterated solvent $CDCl_3$ was purchased from Sigma-Aldrich. All chemical shifts were reported relative to that of TMS (δ = 0.00 ppm).

2,3-*O*-Isopropylidene-l-threitol (38)

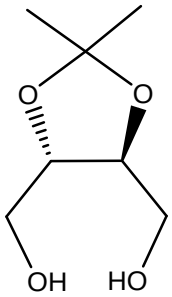

(38)

A solution of $LiAlH_4$ in THF (1 M, 15 ml) was added to (4*R*,5*R*)-dimethyl-2,2-dimethyl-1,3-dioxolane-4,5-dicarboxylate (1.50 g, 6.87 mmol) **(37)** at 0 °C. The mixture was allowed to warm to rt before being heated at reflux for 1.7 h. The solution was cooled and water (10 ml) was then added slowly. The mixture was extracted with EtOAc (4 × 8 ml) and the combined organic layers were dried ($MgSO_4$). The concentrated residue was subjected to silica gel column chromatography and elution with EtOAc provided **(38)** (0.98 g, 87%) as an orange oil. ^{1}H-NMR ($CDCl_3$, 500 MHz): δ 1.43 (s, 6H, 2 × CH_3), 2.08 (s, 2H, 2 × OH), 3.71 (d, *J* = 9.3 Hz, 2H, CH_2), 3.82 (d, *J* = 11.7 Hz, 2H, CH_2), 4.02 (t, *J* = 10.3 Hz, 2H, 2 × CH). ^{13}C-NMR ($CDCl_3$, 125 MHz): δ 26.9 (CH_3), 62.1 (CH_2), 78.2 (CH), 109.2 (CMe_2).

1,4-Bis{[(ethoxycarbonyl)acetoxy]methyl}benzene (34)

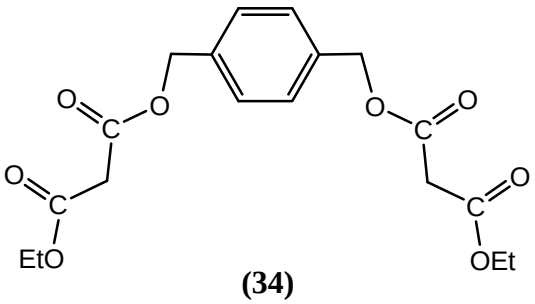

(34)

Ethyl 3-chloro-3-oxopropanoate **(39)** (2.3 ml, 18.27 mmol) was added to a stirred solution of 1,4-benzenedimethanol **(42)** (1.00 g, 7.24 mmol) and pyridine (1.5 ml, 18.58 mmol) in CH_2Cl_2 (100 ml) at 0 °C. The solution was allowed to warm to rt over 1 h before stirring for 3 h. The resulting mixture was washed with saturated aqueous NH_4Cl solution (2 × 100 ml), dried ($MgSO_4$), and the solvent was removed *in vacuo*. The concentrated

residue was subjected to silica gel column chromatography and elution with CH_2Cl_2/MeOH (97:3) provided **(34)** (1.82 g, 68%) as a yellow oil. IR: 2986 (C(sp^3)-H), 1731 (C=O), 1147 (C-O) cm^{-1}. ^{1}H-NMR ($CDCl_3$, 500 MHz): δ 1.24 (t, *J* = 7.1 Hz, 6H, 2 × CH_3), 3.41 (s, 4H, 2 × $COCH_2CO$), 4.19 (q, *J* = 7.0 Hz, 4H, 2 × $C\underline{H}_2CH_3$), 5.17 (s, 4H, 2 × $ArCH_2O$), 7.36 (s, 4H, 4 × ArH). ^{13}C-NMR ($CDCl_3$, 125 MHz): δ 13.4 (CH_3), 40.9 ($\underline{C}H_2CH_3$), 60.9 ($ArCH_2O$), 66.0 ($CO\underline{C}H_2CO$), 127.9 (ArCH), 135.2 (ArC), 165.9 (C=O). MS (ESI +) *m/z* 367 $[M + H]^+$ 25%, 389 $[M + Na]^+$ 80%, 405 $[M + K]^+$ 40%.

1,3-Bis{[(ethoxycarbonyl)acetoxy]methyl}benzene (35)

Ethyl 3-chloro-3-oxopropanoate **(39)** (1.15 ml, 9.14 mmol) was added to a stirred solution of 1,3-benzenedimethanol **(45)** (0.5 g, 3.62 mmol) and pyridine (0.75 ml, 9.29 mmol) in CH_2Cl_2 (50 ml) at 0 °C. The solution was allowed to warm to rt over 1 h before stirring for 3 h. The resulting mixture was washed with saturated aqueous NH_4Cl solution (2 × 50 ml), dried ($MgSO_4$), and the solvent was removed *in vacuo*. The concentrated residue was subjected to silica gel column chromatography and elution with CH_2Cl_2/MeOH (97:3) provided **(35)** (0.96 g, 72%) as a pale yellow oil. IR: 2986 (C(sp^3)-H), 1731 (C=O), 1146 (C-O) cm^{-1}. ^{1}H-NMR ($CDCl_3$, 500 MHz): δ 1.23 (t, *J* = 7.1 Hz, 6H, 2 × CH_3), 3.42 (s, 4H, 2 × $COCH_2CO$), 4.18 (q, *J* = 7.1 Hz, 4H, 2 × $C\underline{H}_2CH_3$), 5.17 (s, 4H, 2 × $ArCH_2O$), 7.34 (m, 4H, 4 × ArH). ^{13}C-NMR ($CDCl_3$, 125 MHz): δ 13.6 (CH_3), 41.1 ($\underline{C}H_2CH_3$), 61.1 ($ArCH_2O$), 66.3 ($CO\underline{C}H_2CO$), 127.5 (ArCH), 127.8 (ArCH), 128.4 (ArCH), 135.5 (ArC), 165.95 (C=O), 165.97 (C=O). MS (ESI +) *m/z* 367 $[M + H]^+$ 100%, 384 $[M + NH_4]^+$ 25%.

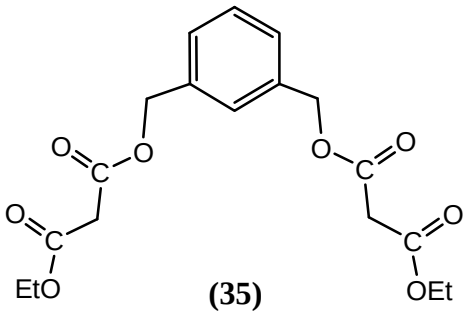

(35)

(+)-(4*R*,5*R*)-Bis{[(ethoxycarbonyl)acetoxy]methyl}-2,2-dimethyl-1,3-dioxolane (36)

Ethyl 3-chloro-3-oxopropanoate **(39)** (1.2 ml, 9.53 mmol) was added to a stirred solution of 2,3-*O*-isopropylidene-l-threitol **(38)** (600 mg, 3.70 mmol) and pyridine (0.72 ml, 8.92 mmol) in CH_2Cl_2 (60 ml) at 0 °C. The solution was allowed to warm to rt over 1 h before stirring for 5 h. The resulting mixture was washed with saturated aqueous NH_4Cl solution (2 × 60 ml), dried ($MgSO_4$), and the solvent was removed *in vacuo*. The concentrated residue was subjected to silica gel column chromatography and elution with CH_2Cl_2/MeOH (98:2) provided **(36)** (1.08 g, 75%) as a yellow oil. IR: 2986 ($C(sp^3)$-H), 1734 (C=O), 1151 (C-O) cm^{-1}. ^{1}H-NMR ($CDCl_3$, 500 MHz): δ 1.28 (t, *J* = 7.0 Hz, 6H, 2 × $CH_2C\underline{H}_3$), 1.42 (s, 6H, $O_2C(CH_3)_2$), 3.43 (s, 4H, 2 × $COCH_2CO$), 4.09 (s, 2H, 2 × CH), 4.21 (q, *J* = 2.7 Hz, 4H, 2 × $C\underline{H}_2CH_3$), 4.25-4.40 (m, 4H, 2 × $CHC\underline{H}_2O$). ^{13}C-NMR ($CDCl_3$, 125 MHz): δ 14.1 ($CH_2\underline{C}H_3$), 26.9 ($O_2C(\underline{C}H_3)_2$), 41.3 ($\underline{C}H_2CH_3$), 61.7 ($CH\underline{C}H_2O$), 64.5 ($CO\underline{C}H_2CO$), 75.6 (CH), 110.4 (CMe_2), 166.35 (C=O), 166.37 (C=O). MS (ESI +) *m/z* 391 $[M + H]^+$ 45% 408 $[M + NH_4]^+$ 100%.

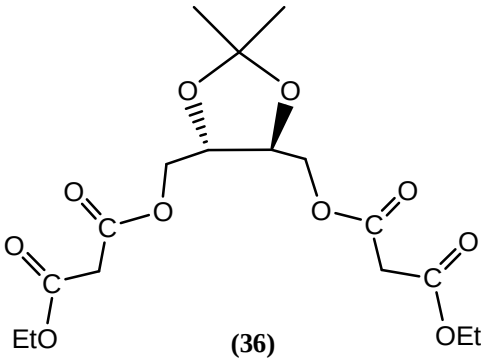

(36)

Diethyl endo-endo-[(4*R*,5*R*)-(2,2-dimethyl-1,3-dioxolane-4,5-diyl)dimethyl]-1,2:7,21-bis(methano)[60]-fullerene-61,61,62,62-tetracarboxylate (40) and diethyl endo-endo-[(4*R*,5*R*)-(2,2-dimethyl-1,3-dioxolane-4,5-diyl)dimethyl]-1,2:16,17-bis (methano)[60]-fullerene-61,61,62,62-tetracarboxylate (41)

A solution of C_{60} (350 mg, 0.49 mmol) in toluene (700 ml) was prepared by stirring at rt for 12 h. Then **(36)** (208 mg, 0.53 mmol), DBU (0.47 ml, 2.91 mmol) and I_2 (271 mg, 1.07 mmol) were added and the mixture was stirred at rt for 8 h. The solution was filtered through a short-plug of silica gel (15 cm), eluted with toluene (to remove unreacted C_{60}) and CH_2Cl_2/MeOH (97:3) successively before being applied onto a chromatographic column (SiO_2). Elution with CH_2Cl_2/petroleum spirit (9:1) followed

by recrystallisation from petroleum spirit/CH_2Cl_2 provided **(40)** (55.9 mg, 10%).

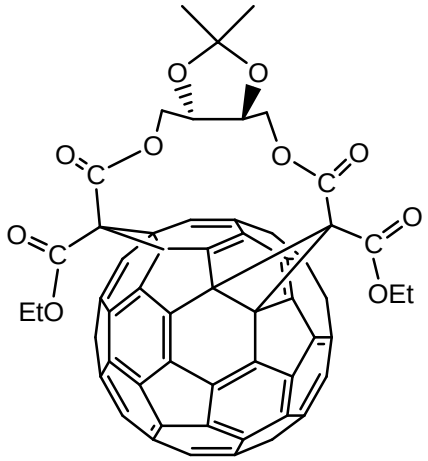

cis-2
(40)

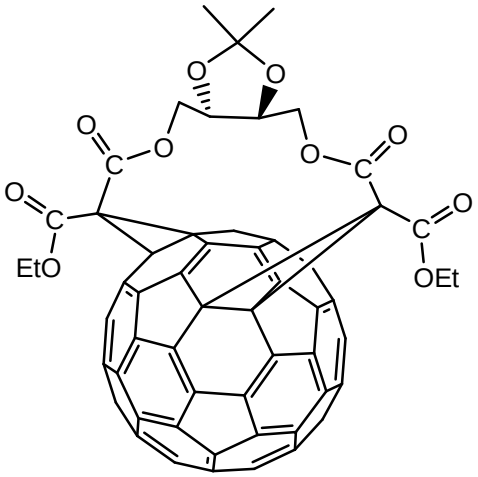

cis-3
(41)

Dark-red solid. IR: 2923 (C(sp^3)-H), 1748 (C=O), 1233 (C-O) cm^{-1}. ^{1}H-NMR ($CDCl_3$, 500 MHz): δ 1.38 (t, *J* = 6.7 Hz, 3H, $CH_2C\underline{H}_3$), 1.39 (t, *J* = 6.6 Hz, 3H, $CH_2C\underline{H}_3$), 1.48 (s, 3H, $O_2C\underline{Me}_AMe_B$), 1.49 (s, 3H, $O_2CMe_A\underline{Me}_B$), 4.07 (t, *J* = 10.5 Hz, 1H, CH), 4.17 (d, *J* = 10.1 Hz, 1H, $CHC\underline{H}_AH_BO$), 4.24 (d, *J* = 11.0 Hz, 1H, $CHCH_A\underline{H}_BO$), 4.34-4.48 (m, 4H, 2 × $C\underline{H}_2CH_3$), 4.61 (d, *J* = 10.7 Hz, 1H, $CHCH_C\underline{H}_DO$), 4.86 (t, *J* = 10.1 Hz, 1H, CH), 5.00 (d, *J* = 8.0 Hz, 1H, $CHC\underline{H}_CH_DO$). ^{13}C-NMR ($CDCl_3$, 125 MHz): δ 14.1 ($CH_2\underline{C}H_3$), 28.5 ($O_2C\underline{Me}_AMe_B$), 28.6 ($O_2CMe_A\underline{Me}_B$), 63.5, 66.9, 67.1, 111.4, 133.6, 137.7, 138.5, 138.6, 141.0, 141.3, 141.9, 142.4, 143.6, 143.9, 144.3, 144.4, 144.6, 144.7, 144.9, 145.2, 145.3, 145.7, 146.0, 147.4, 147.5, 149.5, 162.7 (C=O), 162.9 (C=O). MS (ESI +) *m/z* 1129 [M + Na^+]. Further elution with CH_2Cl_2/MeOH (199:1) followed by recrystallisation from petroleum spirit/CH_2Cl_2 provided **(41)** (36.5 mg, 6%). Brown solid. IR: 2925 (C(sp^3)-H), 1749 (C=O), 1230 (C-O) cm^{-1}. ^{1}H-NMR ($CDCl_3$, 500 MHz): δ 1.43 (t, *J* = 7.1 Hz, 6H, 2 × $CH_2C\underline{H}_3$), 1.50 (s, 6H, $O_2C(CH_3)_2$), 4.31-4.36 (m, 2H, $CHC\underline{H}_2O$), 4.39-4.44 (m, 2H, $CHC\underline{H}_2O$), 4.44-4.57 (m, 4H, 2 × $C\underline{H}_2CH_3$), 4.70-4.75 (m, 2H, 2 × CH). ^{13}C-NMR ($CDCl_3$, 125 MHz): δ 14.2 ($CH_2\underline{C}H_3$), 27.7 ($O_2C(\underline{C}H_3)_2$), 48.8, 63.6, 64.8, 68.9, 75.8, 109.8, 129.9, 136.1, 139.2, 139.4, 141.0, 141.1, 141.7, 141.8, 142.2, 142.4, 143.6, 144.5, 144.7, 144.9, 145.0, 145.2, 145.3, 145.6, 145.6, 146.4, 146.7, 163.3 (C=O), 163.4 (C=O). MS (ESI +) *m/z* 1129 [M + Na^+]. The spectroscopic data of **(40)** and **(41)** match with that in the literature.[161]

Diethyl endo,endo-(*p*-phenylenedimethyl)-1,2:34,35-bis(methano)[60]fullerene-61,61,62,62-tetracarboxylate (43) and diethyl endo,endo-(*p*-phenylenedimethyl)-1,2:18,36-bis(methano)[60]fullerene-61,61,62,62-tetracarboxylate (44)

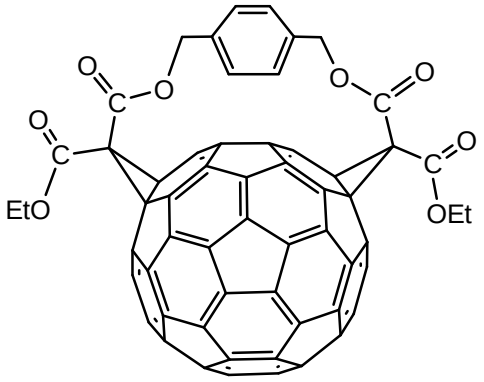

trans-4

(43)

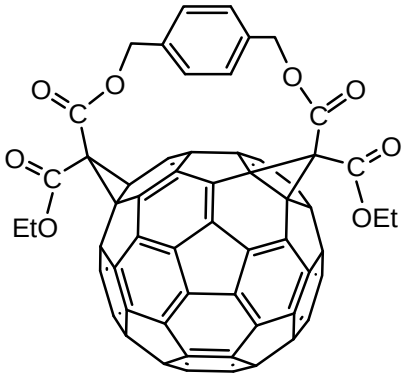

e

(44)

A solution of C_{60} (300 mg, 0.42 mmol) in toluene (600 ml) was prepared by stirring at rt for 12 h. Then 1,4-bis{[(ethoxycarbonyl)acetoxy]methyl}benzene **(34)** (152 mg, 0.42 mmol), DBU (0.4 ml, 2.68 mmol) and I_2 (211 mg, 0.83 mmol) were added and the mixture was stirred at rt for 5 h. The solution was filtered through a short-plug of silica gel (15 cm), eluted with toluene (to remove unreacted C_{60}) and CH_2Cl_2 successively before being applied onto a chromatographic column (SiO_2). Elution with CH_2Cl_2/petroleum spirit (1:1) followed by recrystallisation from petroleum spirit/CH_2Cl_2 provided **(44)** (48.8 mg, 10%). Dark-red solid. IR: 2919 (C(sp^3)-H), 1749 (C=O), 1231 (C-O) cm^{-1}. ^{1}H-NMR ($CDCl_3$, 500 MHz): δ 1.45 (t, *J* = 7.1 Hz, 6H, 2 × CH_3), 4.46-4.55 (m, 4H, 2 × C$\underline{H}_2$CH$_3$), 4.88 (d, *J* = 11.0 Hz, 1H, ArC$\underline{H}_A$H$_B$O), 5.07 (d, *J* = 11.7 Hz, 1H, ArC$\underline{H}_C$H$_D$O), 5.72 (d, *J* = 11.6 Hz, 1H, ArCH$_C\underline{H}_D$O), 5.86 (d, *J* = 11.0 Hz, 1H, ArCH$_A\underline{H}_B$O), 6.91 (d, *J* = 7.7 Hz, 1H, ArH), 7.00 (d, *J* = 7.7 Hz, 1H, ArH), 7.64 (d, *J* = 7.8 Hz, 1H, ArH), 7.66 (d, *J* = 8.0 Hz, 1H, ArH). ^{13}C-NMR ($CDCl_3$, 125 MHz): δ 14.20 (CH_3), 14.24 (CH_3), 52.1, 63.3, 63.4, 68.2, 68.9, 70.5, 71.0, 128.5, 129.9, 130.2, 132.7, 135.3, 137.4, 138.2, 138.4, 139.0, 141.1, 141,4, 141.5, 141.7, 142.1, 142.8, 142.9, 143.07, 143.12, 143.2, 143.3, 143.4, 143.5, 143.60, 143.64, 143.7, 143.9, 144.0, 144.1, 144.4, 144.46, 144.50, 144.6, 144.7, 144.79, 144.84, 144.9, 145.5, 145.6, 145.9, 146.0, 146.1, 146.2, 146.4, 146.5, 146.6, 146.8, 147.18, 147.23, 162.6 (C=O), 162.7 (C=O),

163.0, 163.7. MS (ESI +) *m/z* 1105 [M + Na^+]. Elution with CH_2Cl_2/petroleum spirit (2:1) followed by recrystallisation from petroleum spirit/CH_2Cl_2 provided **(43)** (135.8 mg, 30%). Brown solid. IR: 2919 (C(sp^3)-H), 1744 (C=O), 1242 (C-O) cm^{-1}. ^{1}H-NMR ($CDCl_3$, 500 MHz): δ 1.50 (t, *J* = 7.1 Hz, 6H, 2 × CH_3), 4.52-4.58 (m, 4H, 2 × C$\underline{H_2}$$CH_3$), 5.00 (d, *J* = 11.0 Hz, 2H, ArCH_2O), 6.02 (d, *J* = 11.2 Hz, 2H, ArCH_2O), 7.17 (s, 2H, 2 × ArH), 7.34 (s, 2H, 2 × ArH). ^{13}C-NMR ($CDCl_3$, 125 MHz): δ 14.3 (CH_3), 49.0, 63.5, 68.2, 70.5, 70.8, 130.5, 131.5, 131.7, 135.8, 138.2, 141.0, 141.1, 141.2, 141.2, 141.38, 141.41, 141.9, 142.1, 142.3, 142.8, 142.9, 143.0, 143.1, 144.2, 144.3, 144.7, 145.0, 145.1, 145.2, 145.3, 145.9, 146.0, 146.4, 146.9, 147.0, 148.2, 163.8 (C=O), 164.0 (C=O). MS (ESI +) *m/z* 1105 [M + Na^+]. The spectroscopic data of **(43)** and **(44)** match with that in the literature.[161]

Diethyl endo,endo-(*m*-phenylenedimethyl)-1,2:7,21-bis(methano)[60]fullerene -61,61, 62,62-tetracarboxylate (46)

A solution of C_{60} (300 mg, 0.42 mmol) in toluene (600 ml) was prepared by stirring at rt for 12 h. Then 1,3-bis{[(ethoxycarbonyl)acetoxy]methyl} benzene **(35)** (152 mg, 0.15 mmol), DBU (0.4 ml, 2.68 mmol) and I_2 (211 mg, 0.83 mmol) were added and the mixture was stirred at rt for 5 h. The solution was filtered through a short-plug of silica gel (15 cm), eluted with toluene (to remove unreacted C_{60}) and CH_2Cl_2 successively before being applied onto a chromatographic column (SiO_2) and eluted with CH_2Cl_2 /petroleum spirit (2:1). Recrystallisation from petroleum spirit/CH_2Cl_2 provided **(46)** (140.6 mg, 31%). Dark-red solid. IR: 2919 (C(sp^3)-H), 1743 (C=O), 1235 (C-O) cm^{-1}. ^{1}H-NMR ($CDCl_3$, 500 MHz): δ 1.34 (t, *J* = 7.0 Hz, 6H, 2 × CH_3), 4.35-4.45 (m, 4H, 2 × C$\underline{H_2}$$CH_3$), 5.16 (d, *J* = 12.9 Hz, 2H, ArCH_2O), 5.86 (d, *J* = 12.9 Hz, 2H, ArCH_2O), 7.28 (d, *J* = 7.5 Hz, 2H, 2 × ArH), 7.38 (t, *J* = 7.5 Hz, 1H,

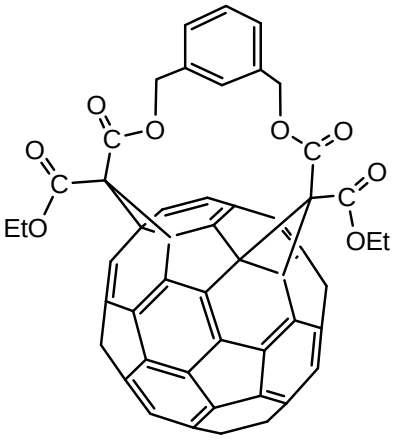

cis-2
(46)

ArH), 7.52 (s, 1H, ArH). ^{13}C-NMR ($CDCl_3$, 125 MHz): δ 14.2 (CH_3), 49.3, 63.3, 67.0, 67.4, 70.7, 123.7, 126.6, 128.7, 135.9, 136.3, 136.7, 137.6, 140.0, 141.1, 141.3, 142.4, 143.1, 143.3, 143.6, 143.8, 144.0, 144.2, 144.3, 144.5, 144.7, 145.1, 145.2, 145.4, 145.7, 145.76, 145.80, 146.12, 146.14, 147.4, 147.5, 147.6, 148.8, 162.9 (C=O), 163.0 (C=O). MS (ESI +) *m/z* 1105 [M + Na^+]. The spectroscopic data match with that in the literature.[161]

Tetraethyl 1,2:34,35-bis(methano)[60]fullerene-61,61,62,62-tetracarboxylate (47)

Compound **(43)** (68.1 mg, 0.06 mmol) was dissolved in THF/EtOH 1:1 (70 ml), and K_2CO_3 (695.3 mg, 5.03 mmol) was added. The mixture was then stirred at rt for 1.5 h, filtered and evaporated to remove solvent *in vacuo*. Elution through a chromatographic column (SiO_2) with toluene followed by elution with petroleum spirit yielded **(47)** (34.4 mg, 53%). Brown solid. ^{1}H-NMR ($CDCl_3$, 500 MHz): δ 1.42 (t, *J* = 7.1 Hz, 6H, 2 × CH_3), 1.47 (t, *J* = 7.1 Hz, 6H, 2 × CH_3), 4.43-4.50 (m, 4H, 2 × CH_2), 4.55 (q, *J* = 6.8 Hz, 4H, 2 × CH_2). MS (ESI +) *m/z* 1059 [M + Na^+]. This compound has been reported in the literature but no NMR spectral data was given.[129]

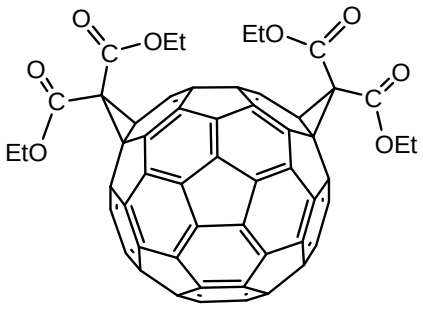

trans-4
(47)

Tetraethyl 1,2:18,36-bis(methano)[60]fullerene-61,61,62,62-tetracarboxylate (48)

Compound **(44)** (20.9 mg, 0.02 mmol) was dissolved in THF/EtOH 1:1 (25 ml), and K_2CO_3 (213.4 mg, 1.54 mmol) was added. The mixture was then stirred at rt for 1.5 h, filtered and evaporated to remove solvent *in vacuo*. Elution through a chromatographic column (SiO_2) with toluene followed by elution with petroleum spirit

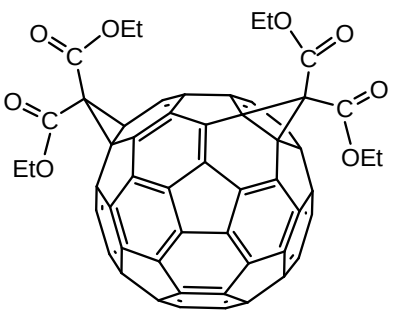

e
(48)

yielded **(48)** (6.2 mg, 31%). Dark-red solid. ^{1}H-NMR ($CDCl_3$, 500 MHz): δ 1.40 (t, J = 6.7 Hz, 6H, 2 × CH_3), 1.43 (t, J = 6.7 Hz, 6H, 2 × CH_3), 4.40-4.47 (m, 8H, 4 × CH_2). MS (ESI +) *m/z* 1059 [M + Na^+]. This compound has been reported in the literature but no NMR spectral data was given.[129]

Tetraethyl 1,2:7,21-bis(methano)[60]fullerene-61,61,62,62-tetracarboxylate (49)

Compound **(40)** (60.6 mg, 0.06 mmol) was dissolved in THF/EtOH 1:1 (80 ml), and K_2CO_3 (618.7 mg, 4.47 mmol) was added. The mixture was then stirred at rt for 1.5 h, filtered and evaporated to remove solvent *in vacuo*. Elution through a chromatographic column (SiO_2) with toluene followed by elution with petroleum spirit yielded **(49)** (13.1 mg, 23%). Brown solid. ^{1}H-NMR ($CDCl_3$, 500 MHz): δ 1.38 (t, J = 7.1 Hz, 6H, 2 × CH_3), 1.45 (t, J = 7.1 Hz, 6H, 2 × CH_3), 4.35-4.55 (m, 8H, 4 × CH_2). MS (ESI +) *m/z* 1059 [M + Na^+]. This compound has been reported in the literature but no NMR spectral data was given.[129]

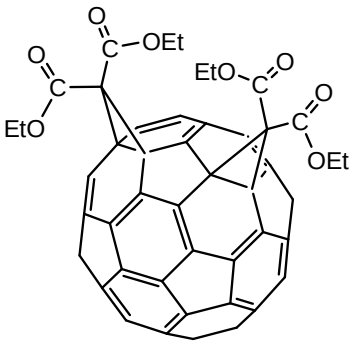

cis-2
(49)

Compound **(46)** (14.3 mg, 0.013 mmol) was dissolved in THF/EtOH 1:1 (20 ml), and K_2CO_3 (143.0 mg, 1.03 mmol) was added. The mixture was then stirred at rt for 1.5 h, filtered and evaporated to remove solvent *in vacuo*. Elution through a chromatographic column (SiO_2) with toluene followed by elution with petroleum spirit yielded **(49)** (7.1 mg, 53%). Dark-red solid. This compound had the same ^{1}H-NMR and MS data as **(49)** described above.

Tetraethyl 1,2:16,17-bis(methano)[60]fullerene-61,61,62,62-tetracarboxylate (50)

Compound **(41)** (24.4 mg, 0.022 mmol) was dissolved in THF/EtOH 1:1 (30 ml), and K_2CO_3 (243.7 mg, 1.76 mmol) was added. The mixture was then stirred at rt for 1.5 h,

filtered and evaporated to remove solvent *in vacuo*. Elution through a chromatographic column (SiO_2) with toluene followed by elution with petroleum spirit yielded **(50)** (9.8 mg, 43%). Brown solid. ^{1}H-NMR ($CDCl_3$, 500 MHz): 1.43 (t, J = 7.1 Hz, 12H, 4 × CH_3), 4.39-4.52 (m, 8H, 4 × CH_2). MS (ESI +) *m/z* 1059 [M + Na^+]. This compound has been reported in the literature but no NMR spectral data was given.[129]

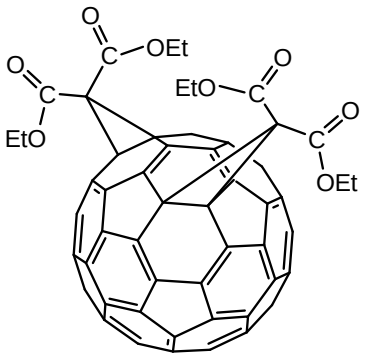

cis-3
(50)

Chapter 5: References

1. Kroto, H. W.; Heath, J. R.; O'Brien, S. C.; Curl, R. F.; Smalley, R. E. *Nature* **1985**, *318*, 162.
2. Kroto, H. W.; Allaf, A. W.; Balm, S. P. *Chem. Rev.* **1991**, *91*, 1213.
3. Hirsch, A.; Brettreich, M. *Fullerenes, Chemistry and Reactions* **2005**, WILEY-VCH, Weinheim.
4. Krätschmer, W.; Lamb, L. D.; Fostiropoulos, K.; Huffman, D. R. *Nature* **1990**, *347*, 354.
5. Schmalz, T. G.; Seitz, W. A.; Klein, D. J.; Hite, G. E. *Chem. Phys. Lett.* **1986**, *130*, 203.
6. Hirsch, A. *The Chemistry of the Fullerenes* **1994**, Thieme: Stuttgart.
7. Krätschmer, W.; Fostiropoulos, K.; Huffman D. R. *Nature* **1990**, *347*, 354.
8. Ajie, H., Alvarez M. M.; Anz, S. J.; Beck, R. D.; Diederich, F.; Fostiropoulos, K.; Huffman, R.; Krätschmer, W.; Rubin, Y.; Schriver, K. E.; Sensharma, D.; Whetten, R. L. *J. Phys. Chem.* **1990**, *94*, 8630.
9. Hare, J. P.; Kroto, H. W.; Taylor, R. *Chem. Phys. Lett.* **1991**, *177*, 394.
10. Kroto, M. *J. Mater. Chem.* **1997**, *7*, 1097.
11. Da Ros, T.; Prato, M. *Chem. Commun.* **1999**, *8*, 663.
12. Wudl, F. *Acc. Chem Res.* **1992**, *25*, 157.
13. Hirsch, A. *Synthesis* **1995**, 895.
14. Hirsch, A. *Angew. Chem. Int. Ed. Engl.* **1993**, *32*, 1138.
15. Diederich, F.; Isaacs, L.; Philp, D. *Chem Soc. Rev.* **1994**, *23*, 243.
16. Foote, C. S. *Top. Curr. Chem.* **1994**, *169*, 347.
17. Kasermann, F.; Kempf, C. *Antiviral Res.* **1997**, *34*, 65.
18. An, Y. Z.; Chen, C. H. B.; Anderson, J. L.; Sigman, D. S.; Foote, C. S.; Rubin, Y. *Tetrahedron* **1996**, *52*, 5179.
19. Tabata, Y.; Murakami, Y.; Ikada, Y. *Fullerene Sci. Technol.* **1997**, *5*, 989.
20. Friedman, S. H.; DeCamp; D. L.; Sijbesma, R. P.; Srdanov, G.; Wudl, F.; Kenyon, G. L. *J. Am. Chem. Soc.* **1993**, *115*, 6506.
21. Sijbesma, R.; Srdanov, G.; Wudl, F.; Castoro, J. A.; Wilkins, C.; Friedman, S. H.;

DeCamp, D. L.; Kenyon, G. L. *J. Am. Chem. Soc.* **1993**, *115*, 6510.

22. Nakamura, E.; Tokuyama, H.; Yamago, S.; Shiraki, T.; Sugiura, Y. *Bull. Chem. Soc. Jpn.* **1996**, *69*, 2143.
23. Roniolo, C.; Bianco, A.; Maggini, M.; Scorrano, G.; Prato, M.; Marastoni, M.; Tomatis, R.; Spisani, S.; Palù, G.; Blair, E. D. *J. Med. Chem.* **1994**, *37*, 4558.
24. Schuster, D. I.; Wilson, S. R.; Schinazi, R. F. *Bioorg. Med. Chem. Lett.* **1996**, *6*, 1253.
25. Dugan, L. L.; Turetsky, D. M.; Du, C.; Lobner, D.; Wheeler, M.; Almli, C. R.; Shen, C. K. F.; Luh, T, Y.; Choi, D. W.; Lin, T. S. *Proc. Natl. Acad. Sci. U.S.A.* **1997**, *94*, 9434.
26. Hsu, S. C.; Wu, C. C.; Luh, T. Y.; Chou, C. K.; Han, S. H.; Lai, M. Z. *Blood* **1998**, *91*, 2658.
27. Huang, Y. L.; Shen, C. K.; Luh, T. Y.; Yang, H. C.; Hwang, K. C.; Chou C. K. *Eur. J. Biochem.* **1998**, *254*, 38.
28. Tutt, L. W.; Kost, A. *Nature* **1992**, *356*, 225.
29. Kajzar, F.; Taliani, C.; Danieli, R.; Rossini, S.; Zamboni, R. *Chem. Phys. Lett.* **1994**, *217*, 418.
30. Haddon, R. C. *Acc. Chem. Res.* **1992**, *25*, 127.
31. Rosseinsky, M. J. *J. Mater. Chem.* **1995**, *5*, 1497.
32. Allemand, P. M.; Khemani, K. C.; Koch, A.; Wudl, F.; Holczer, K.; Donovan, S.; Gruner, G.; Thompson, J. D. *Science* **1991**, *253*, 301.
33. Dai, L.; Mau, A. W. H.; Griesser, H. J.; Spurling, T. H.; White, J. W. *J. Phys. Chem.* **1995**, *99*, 17302.
34. Hawker, C. J. *Macromolecules* **1994**, *27*, 4836.
35. Bunker, C. E.; Lawson, G. E.; Sun Y. P. *Macromolecules* **1995**, *28*, 3744.
36. Weis, C.; Friedeich, C.; Muelhaupt, R.; Frey, H. *Macromolecules* **1995**, *28*, 403.
37. Kojima, Y.; Matsuoka, T.; Takajashi, H.; Kurauchi, T. *Macromolecules* **1995**, *28*, 8868.
38. Nigam, A.; Shecharam, T.; Bharadwaj, T.; Giovanola, J.; Narang, S.; Malhotra, R. *J.*

Chem. Soc., Chem. Commun., **1995**, 1547.

39. Cao, T.; Webber, S. E. *Macromolecules* **1995**, *28*, 3741.
40. Ma, B.; Lawson, G. E.; Bunker, C. E.; Kitayforodskiy, A.; Sun, Y. P. *Chem Phys. Lett.* **1995**, *247*, 51.
41. Zhang, N.; Schricker, S. R.; Wudl, F.; Prato, M.; Maggini, M.; Scorrano, G. *Chem. Mater.* **1995**, *7*, 441.
42. Shi, S.; Li, Q.; Khemani, K. C.; Wudl, F. *J. Am. Chem. Soc.* **1992**, *114*, 10656.
43. Hawker, C. G.; Wooley, K. L.; Fréchet, J. M. *J. Chem. Soc., Chem Commun.* **1994**, 925.
44. Wooley, K. L.; Hawker, C. J.; Fréchet, J. M., Wudl, F.; Srdanov, G.; Shi, S.; Li, C.; Kao, M. *J. Am. Chem. Soc.* **1993**, *115*, 9836.
45. Chiang, L. Y.; Wang, L. Y.; Tseng, S. M.; Wu, J. S.; Hsieh, K. H. *J. Chem. Soc., Chem. Commun.* **1994**, 2675.
46. Chiang, L. Y.; Wang, L. Y.; Kuo, C. S. *Macromolecules* **1995**, *28*, 7574.
47. Chupa, J. A.; Xu, S.; Fischetti, R. F.; Strongin, R. M.; McCauley, J. P.; Smith, A. B.; Blasie, J. K.; Peticolas, L. J.; Bean, J. C. *J. Am. Chem. Soc.* **1993**, *115*, 4383.
48. Shi, X.; Caldwell, W. B.; Chen, K.; Mirkin, C. A. *J. Am. Chem. Soc.*, **1994**, *116*, 11598.
49. Guldi, D. M.; Maggini, M.; Scorrano, G.; Prato, M. *J. Am. Chem. Soc.* **1997**, *119*, 974
50. Sariciftci, N. S.; Smilowitz, L.; Heeger, A. J.; Wudl, F. *Science*, **1992**, *258*, 1474.
51. Morita, S.; Zakidov, A. A.; Yoshino, K. *Solid State Commun.*, **1992**, *82*, 249.
52. Matsuzawa, N.; Dixon, D. A.; Fukunaga, T. *J. Phys. Chem.* **1992**, *96*, 7594.
53. Haddon, R. C. *Science* **1993**, *261*, 1545.
54. Satpathy, S. *Chem. Phys. Lett.* **1986**, *130*, 545.
55. Hale, P. D. *J. Am. Chem. Soc.* **1986**, *108*, 6087.
56. Larsson, S.; Volosov, A.; Rosen, A. *Chem. Phys. Lett.* **1987**, *137*, 501.
57. Rosen, A.; Wastberg, B. *J. Chem. Phys.* **1989**, *90*, 2525.
58. Haddon, R. C.; Brus, L. E.; Raghavachari, K. *Chem. Phys. Lett.* **1986**, *125*, 459.

59. Xie, Q.; Perez-Cordero, E.; Echegoyen, L. *J. Am. Chem. Soc.* **1992**, *114*, 3978.

60. Haufler, R. E.; Conceicao, J.; Chibante, L. P. F.; Chai, Y.; Byrne, N. E.; Flanagan, S.; Haley, M. M.; O'Brian, S. C.; Pan, C.; Xiao, Z; Billups, W. E., Ciufolini, M. A.; Hauge, R. H.; Margrave, J. L.; Wilson, L. J.; Curl R. F.; Smalley, R. E. *J. Phys. Chem.* **1990**, *94*, 8634.

61. Allemand, P. M.; Koch, A.; Wudl, F.; Rubin, Y.; Diederich, F.; Alvarez, M. M.; Anz, S. J.; Whetten, R. L. *J. Am. Chem. Soc.* **1991**, *113*, 1050.

62. Dubois, D.; Kadish, K. M.; Flanagan, S.; Hauffer, R. E.; Chibante, L. P. F.; Wilson, L. J. *J. Am. Chem. Soc.* **1991**, *113*, 4364.

63. Dubois, D.; Kadish, K. M.; Flanagan, S.; Wilson, L. J. *J. Am. Chem. Soc.* **1991**, *113*, 7773.

64. Ohsawa, Y.; Saji, T. *J. Chem. Soc., Chem. Commun.* **1992**, 781.

65. Zhou, F.; Jehoulet, C.; Bard, A. J. *J. Am. Chem. Soc.* **1992**, *114*, 11004.

66. Koh, W.; Dubois, D.; Kutner, W.; Jones, M. T.; Kadish, K. M. *J. Phys. Chem.* **1992**, *96*, 4163.

67. Caron, C.; Subramanian, R.; D'Souza, F.; Kim, J.; Kutner, W.; Jones, M. T., Kadish, K. M. *J. Am. Chem. Soc.* **1993**, *115*, 8505.

68. Magdesieva, T. V.; Kravchuk, D. N.; Bashilov, V. V.; Kusnestova, I. V.; Sokolov, V. I.; Butin, K. P. *Russ. Chem. Bull.* **2002**, *51*, 1588.

69. Fullagar, W. K.; Gentle, I. R.; Heath, G. A.; White, J. W. *J. Chem. Soc., Chem. Commun.* **1993**, 525.

70. Bausch, J. W.; Prakash, G. K. S.; Olah, G. A.; Tse, D. S.; Lorents, D. C.; Bae, Y. K.; Malhorta, R. *J. Am. Chem. Soc.* **1991**, *113*, 3205.

71. Hebard, A. F.; Rosseinsky, M. J.; Haddon, R. C.; Murphy, D. W.; Glarum, S. H.; Palstra, T. T. M.; Ramirez, A. P.; Kortan, A. R. *Nature* **1991**, *350*, 600.

72. Holczer, K.; Klein, O.; Huang, S. M.; Kaner R. B.; Fu, K. J.; Whetten R. L.; Diederich, F. *Science* **1991**, *252*, 351.

73. Stephens, P. W.; Mihaly, L.; Lee, P. L.; Whetten, R. L.; Huang, S. M.; Kaner, R. B.; Diederich, F.; Holczer, K. *Nature* **1991**, 351.

74. Zhou, O, Fischer, J. E.; Coustel, N.; Kycia, S.; Zhu, Q.; McGhie, A. R.; Romanov, W. J.; McCauley, J. P.; Smith, A. B.; Cox, D. E. *Nature* **1991**, *351*, 462.

75. Kelty, S. P.; Chen, C. C.; Lieber C. M. *Nature* **1991**, 233.

76. Tanigaki, T.; Ebbesen T. W. *Nature* **1991**, *352*, 222.

77. Tanigaki, K.; Hirosawa, I.; Ebbesen, T. W.; Mizuki, J.; Shimakawa, Y.; Kubo, Y.; Tsai, J. S.; Kuroshima, S. *Nature*, **1992**, *356*, 419.

78. Boulas, P.; Subramanian, R.; Kutner, W.; Jones, M. T.; Kadish, K. M. *J. Electrochem. Soc.* **1993**, *140*, L130.

79. Stephens, P. W.; Cox, D.; Lauher, J. W.; Mihaly, L.; Wiley, J. B.; Allemand, P. M.; Hirsch, A.; Holczer, K.; Li, Q.; Thompson, J. D.; Wudl, F. *Nature* **1992**, *355*, 331.

80. Wudl, F.; Hirsch, A.; Khemani, K. C.; Suzuki, T.; Allemand, P. M.; Kosch, A.; Eckert, H.; Srdanov, G.; Webb, H. M. *ACS Symp. Ser.* **1992**, *481*, 161.

81. Hirsch, A.; Groesser, T.; Skiebe, A.; Soi, A. *Chem. Ber.* **1993**, *126*, 1061.

82. Fagan, P J.; Krusic, P. J.; Evans, D. H.; Lerke, S. A.; Johnston, E. *J. Am. Chem. Soc.* **1992**, *114*, 9697.

83. Champeil, E.; Crean, C.; Larraya, C.; Pescitelli, G.; Proni, G.; Ghosez, L. *Tetrahedron*, **2008**, *64*, 10319.

84. Bingel C. *Chem. Ber.* **1993**, *126*, 1957.

85. Patil, A. O.; Schriver, G. W.; Carstensen, B.; Lundberg, R. D. *Polym. Bull.* **1993**, *30*, 187.

86. Geckeler, K. E.; Hirsch, A. *J. Am. Chem. Soc.* **1993**, *115*, 3850.

87. Chen, K.; Caldwell, W. B.; Mirkin, C. A. *J. Am. Chem. Soc.* **1993**, *115*, 1193.

88. Caldwell, W. B.; Chen, K.; Mirkin, C. A.; Babinec, S. J. *Langmuir*, **1993**, 1324.

89. Li, J.; Takeuchi, A.; Ozawa, M.; Li, X.; Saigo, K.; Kitazawa, K. *J. Chem. Soc., Chem. Commun.* **1993**, 1784.

90. Tsuda, M.; Ishida, T.; Nogami, T.; Surono, S.; Ohashi, M. *J. Chem. Soc., Chem. Commun.* **1993**, 1296.

91. Schlueter, J. A.; Seaman, J. M.; Taha, S.; Cohen, H.; Lykke, K. R.; Wang, H. H.; Williams, J. M. *J. Chem. Soc., Chem. Commun.* **1993**, 972.

92. Prato, M.; Suzuki, T.; Foroudian, H.; Li, Q.; Khemani, K.; Wudl, F.; Leonetti, J.; Little, R. D.; White, T.; Rickborn, B.; Yamago, S.; Nakamura, E. *J. Am. Chem. Soc.* **1993**, *115*, 1594.

93. Belik, P.; Guegel, A.; Spikermann, J.; Muellen, K. *Angew. Chem. Int. Ed. Engl.* **1993**, *32*, 78.

94. Guegel, A.; Kraus, A.; Spikermann, J.; Belik P.; Muellen, K. *Angew. Chem. Int. Ed. Engl.* **1994**, *33*, 559.

95. Belik, P.; Guegel, A.; Kraus, A.; Spikermann, J.; Enkelmann, V.; Frank, G.; Muellen, K. *Adv. Mater.* **1993**, *5*, 854.

96. Rubin, Y.; Khan, S.; Freedberg, D. I.; Yeretzian, C. *J. Am. Chem. Soc.* **1993**, *115*, 344.

97. An, Y. Z.; Anderson, J. L.; Rubin, Y. *J. Org. Chem.* **1993**, *58*, 4799.

98. Suzuki, T.; Li, Q.; Khemani, K. C.; Wudl, F. *J. Am. Chem. Soc.* **1991**, *114*, 7301.

99. Smith, A. B.; Strongin, R. M.; Brard, L.; Furst, G. T.; Romanov, W. J. Owens, K. G.; King, R. C. *J. Am. Chem. Soc.* **1993**, *115*, 5829.

100. Wudl, F. *Acc. Chem. Res.* **1992**, *25*, 157.

101. Isaacs, L.; Wehrsig, A.; Diederich, F. *Helv. Chem. Acta* **1993**, *76*, 1231.

102. Skiebe, A.; Hirsch, A. *J. Chem. Soc., Chem. Commun.* **1994**, 335.

103. Tsuda, M.; Ishida, T.; Nogami, T.; Surono, S.; Ohashi, M. *Chem. Lett.* **1992**, 2333.

104. Hoke II, S. H.; Molstad, J.; Dilattato, D.; Jay, M. J.; Carlson, D.; Kahr, B.; Cooks, R. G. *J. Org. Chem.* **1992**, *57*, 5069.

105. Wilson, S. R.; Kaprinidis, N.; Wu, Y.; Schuster, D. I. *J. Am. Chem. Soc.* **1993**, *115*, 8495.

106. Prato, M.; Maggini, M.; Scorrano, G.; Lucchini, V. *J. Org. Chem.* **1993**, *58*, 3613.

107. Zhang, X.; Romero, A.; Foote, C. S. *J. Am. Chem. Soc.* **1993**, *115*, 11024.

108. Morton, J. R.; Preston, K. F.; Krusic, P. J.; Hill, S. A.; Wasserman, E. *J. Phys. Chem.* **1992**, *96*, 3576.

109. Morton, J. R.; Preston, K. F.; Krusic, P. J.; Hill, S. A.; Wasserman, E. *J. Am. Chem. Soc.* **1992**, *114*, 5454.

110. Morton, J. R.; Preston, K. F.; Krusic, P. J.; Wasserman, E. *J. Chem. Soc., Trans. 2* **1992**, 1425.

111. Krusic, P. J.; Roe, D. C.; Johnston, E.; Morton, J. R.; Preston, K. F. *J. Phys. Chem.* **1993**, *97*, 1736.

112. Zhang, S.; Brown, T. L.; Du, Y.; Shapley, J. R. *J. Am. Chem. Soc.* **1993**, *115*, 6705.

113. Hirsch, A.; Groesser, T.; Skiebe, A.; Soi, A. *Chem. Ber.* **1993**, *126*, 1061.

114. Brizzolara, D.; Ahlemann, J. T.; Roesky, H. W.; Keller, K. *Bull. Soc. Chim Fr.* **1993**, *130*, 745.

115. Greegan, K. M.; Robbins, J. L.; Robbins, W. K.; Millar, J. M.; Sherwood, R. D.; Tindall, P. J.; Cox, D. M.; Smith, A. B.; McCauley, J. P.; Jones, D. R.; Gallagher, R. T. *J. Am. Chem. Soc.* **1992**, *114*, 1103.

116. Escobedo, J. O.; Frey, A. E.; Strongin, R. M. *Tetrahedron lett.* **2002**, *43*, 6117.

117. Balch, A. L.; Costa, D. A.; Noll, B. C.; Olmstead, M. M. *J. Am. Chem. Soc.* **1995**, *117*, 8926.

118. Tajima, Y.; Takeuchi, K. *J. Org. Chem.* **2002**, *67*, 1696.

119. Hawkins, J. M.; Lewis, T. A.; Loren, S. D.; Meyer, A.; Heath, L. R.; Shibato, Y.; Saykally, R. J. *J. Org. Chem.* **1990**, *55*, 6250.

120. Hawkins, J. M.; Meyer, A.; Lewis, T. A.; Loren, S.; Hallander, F. J. *Science* **1991**, *252*, 312.

121. Hawkins, J. M.; Loren, S.; Meyer, A.; Nunlist, R. *J. Am. Chem. Soc.* **1991**, *113*, 7770.

122. Hawkins, J. M. *Acc. Chem. Soc.* **1992**, *25*, 150.

123. Hawkins, J. M.; Meyer, A.; Lewis, T. A.; Bunz, U.; Nunlist, R.; Ball, G. E.; Ebbesen, T. W.; Tanigaki, K. *J. Am. Chem. Soc.* **1992**, *114*, 7954.

124. Olah, G. A.; Bucsi, I.; Aniszfeld, R.; Prakash, G. K. S. *Carbon* **1992**, *30*, 1203.

125. Olah, G. A.; Bucsi, I.; Ha, D. S.; Aniszfeld, R.; Lee, C. S.; Prakash, G. K. S.

Fullerene Sci. Technol. **1997**, *5*, 389.

126. Kitagawa, T.; Lee, Y.; Hanamura, M.; Sakamoto, H.; Konno, H.; Takeuchi, K. I.; Komatsu, K. *Chem. Commun.* **2002**, 3062.
127. Kitagawa, T.; Sakamoto, H.; Takeuchi, K. I. *J. Am. Chem. Soc.* **1999**, *121*, 4298.
128. Kitagawa, T.; Takeuchi, K. I. *Bull. Chem. Soc. Jpn.* **2001**, *74*, 785.
129. Hirsch, A.; Lamparth, I.; Karfunkel, H. R. *Angew. Chemie, Int. Ed. Engl.* **1994**, *33*, 437.
130. Thilgen, C.; Herrmann, A.; Diederich, F. *Helv. Chim. Acta* **1997**, *80*, 183.
131. Burley, G. A. *PhD Thesis*, University of Wollongong, **2002**
132. Camps, X.; Hirsch, A. *J. Chem. Soc., Perkin Trans.* 1. **1997**, 1595
133. Ball, G. E.; Burley, G. A.; Chaker, L.; Hawkins, B. C.; Williams, J. R.; Keller, P. A.; Pyne, S. G. *J. Org. Chem.* **2005**, *70*, 8572.
134. Diederich, F.; Thilgen, C. *Science*, **1996**, *271*, 317.
135. Diederich, F.; Kessinger, R. *Acc. Chem. Res.* **1999**, *32*, 537.
136. Djojo, F.; Herzog, A.; Lamparth, I.; Hampel, F.; Hirsch, A. *Chem. Eur. J.* **1996**, *2*, 1537.
137. Burley, G. A.; Keller, P. A.; Pyne, S. G.; Ball, G. E. *J. Org. Chem.* **2002**, *67*, 8316.
138. Ishii, T.; Shinkai, S. *Tetrahedron* **1999**, *55*, 12515.
139. Ishii, T.; Iguchi, R.; Shinkai, S. *Tetrahedron* **1999**, *55*, 3883.
140. Ishii, T.; Nakashima, K.; Shinkai, S.; Ikeda, A. *J. Org. Chem.* **1999**, *64*, 984.
141. Kessinger, R.; Gómez-López, M.; Boudon, C.; Gisselbrecht, J-P.; Gross, M.; Echegoyen, L.; Diederich, F. *J. Am. Chem. Soc.* **1998**, *120*, 8545.
142. Collins, D. C.; Lee, M. L. *Anal. Bioanal. Chem.* **2002**, *372*, 66.
143. Stach, J.; Baumbach, J. I. *IJIMS* 5 **(2002)** *1*, 1.
144. Karpas, Z.; Stimac, R. M.; Rappoport, R. *Int. J. Mass Spectrom Ion Proc.* **1998**, *83*, 163.
145. Eiceman, G. W. *Critical Rev. Anal. Chem.* **1991**, *22*, 471.
146. Guevremont, K. W.; Siu, K. W. M.; Wang, J.; Ding, L. *Anal. Chem.* **1997**, *69*, 3959.

147. Clemmer, D. E.; Yansheng, L. *Anal. Chem.* **1997**, 69, 2504.

148. Hoaglund, C. H.; Valentine, S. J.; Clemmer, D. E. *Anal. Chem.* **1997**, 69, 4156.

149. Shelimov, K. B.; Clemmer, D. E.; Hudgins, R. R.; Janold, M. F. *J. Am. Chem. Soc.* **1997**, *119*, 2240.

150. Dugourd, Ph.; Hudgins, R. R.; Clemmer, D. E.; Janold, M. F. *Rev. Sci. Instrum.* **1997**, *68*, 1122.

151. Valentine, S. J.; Counterman, A. E.; Hoaglund, C. S.; Reilly, J. P.; Clemmer, D. E. *J. Am. Soc. Mass. Spectrom* **1998**, *9*, 1213.

152. Hoaglund, C. S.; Valentine, S. J.; Sporleder, C. R.; Reilly, J. P.; Clemmer, D. E. *Anal. Chem.* **1998**, *70*, 2236.

153. Henderson, S. C.; Valentine, S. J.; Counterman, A. E.; Clemmer, D. E. *Anal. Chem.* **1999**, *71*, 291.

154. Srebalus, C. A.; Li, J.; Marshall, W. S.; Clemmer, D. E. *Anal. Chem.* **1999**, *71*, 3918.

155. Valentine, S. J.; Counterman, A. E.; Clemmer, D. E. *J. Am. Soc. Mass. Spectrom* **1999**, *10*, 1188.

156. Hoaglund-Hyzer, C. S.; Li, J.; Clemmer, D. E. *Anal. Chem*. **2000**, *72*, 2737.

157. Srebalus, C. A.; Li, J.; Marshall, W. S.; Clemmer, D. E. *J. Am. Soc. Mass. Spectrom.* **2000**, *11*, 352.

158. Srebalus Barnes, C. A.; Clemmer, D. E. *Anal. Chem.* **2001**, *73*, 424.

159. Hoaglund-Hyzer, C. S.; Clemmer, D. E. *Anal. Chem.* **2001**, *73*, 177.

160. Kanu, Abu B.; Dwivedi, P.; Tam, M.; Matz, L.; Herbert, H. *J. Mass. Spectrom.* **2008**, *43*, 1.

161. Nierengarten, J.-F.; Habicher, T.; Kessinger, R.; Cardullo, F.; Diederich, F. *Helv Chem Acta*, **1997**, *80*, 2238.

162. Mash, E.A.; Nelson, K.A.; van Deusen, S.; Hemperly S.B. *Organic Syntheses*, **1993**, *8*, 155.

Appendix I

Summary of Reactions

1. Synthesis of tethered bismalonates (36), (34) and (35) by linking ethyl 3-chloro-3-oxopropanoate (39) to dimethanols (38), (42) and (45)

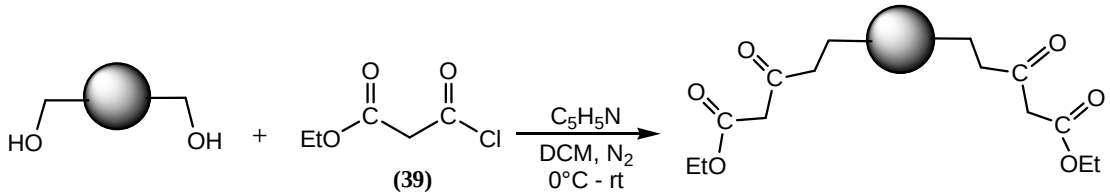

Diol	Tethered Bismalonates	Yield	Ref.[161]
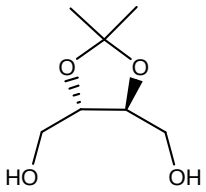 (+)-(4*R*,5*R*)-bis{[(ethoxycarbonyl) acetoxy]methyl-2,2-dimethyl-1,3-dioxolane **(38)**	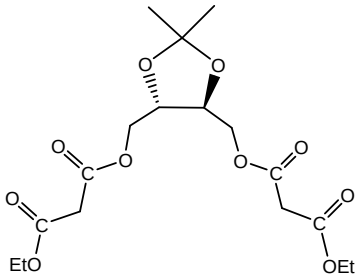 **(36)**	68%	61%
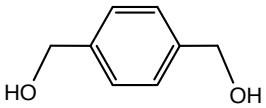 1,4-bis{[(ethoxycarbonyl) acetoxy]methyl}benzene **(42)**	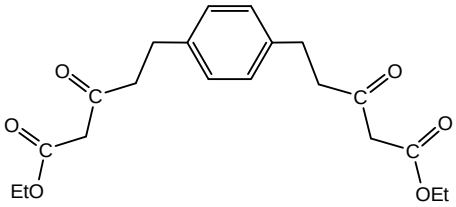 **(34)**	72%	65%
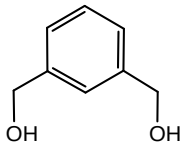 1,3-bis{[(ethoxycarbonyl) acetoxy]methyl}benzene **(45)**	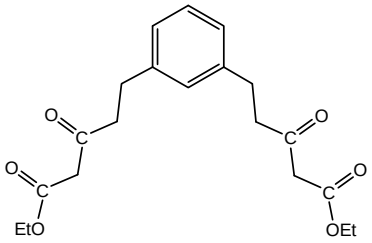 **(35)**	75%	81%

2. Bingel additions to [60]fullerene by tethered malonates (36), (34) and (35) and comparision of the yields of products to the corresponding ones reported by Nierengarten *et al*.

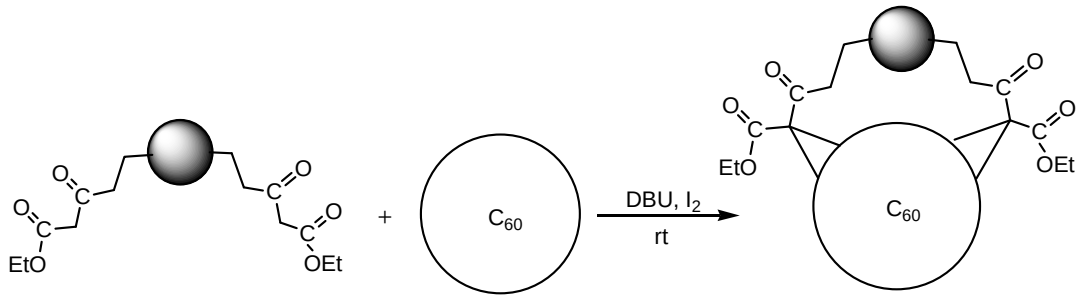

Tethered bismalonates	Resulted bisadduct(s)				
	Structure	Regio-isomerism	Symmetry Operation	Yield	Ref.[161]
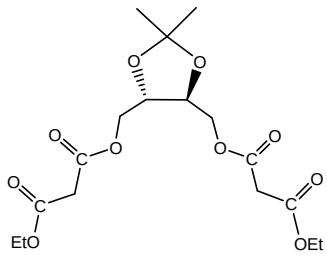 **(36)**	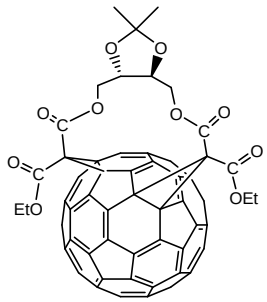 **(40)**	*cis-2*	*C1*	10%	21%
	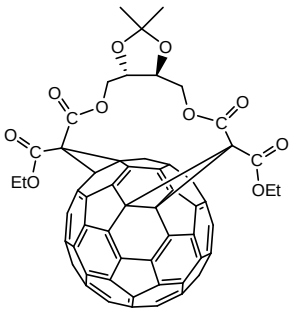 **(41)**	*cis-3*	*C2*	6%	15%

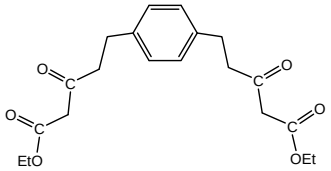 **(34)**	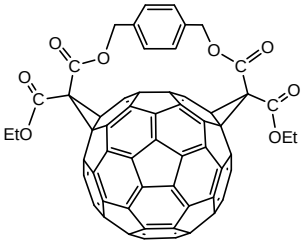 **(43)**	*trans-4*	*Cs*	30%	33%
	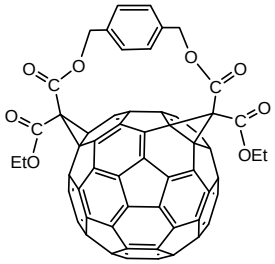 **(44)**	*e*	*C1*	10%	8%
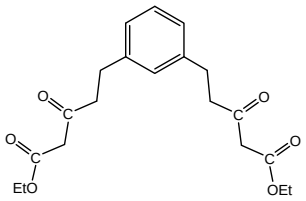 **(35)**	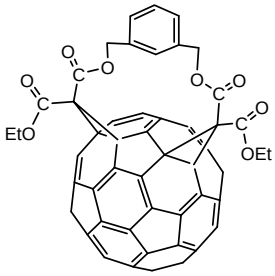 **(46)**	*cis-2*	*Cs*	31%	32%

3. Transesterification of bisadducts to form regioisomeric bismethanofullerenyl tetraethylesters

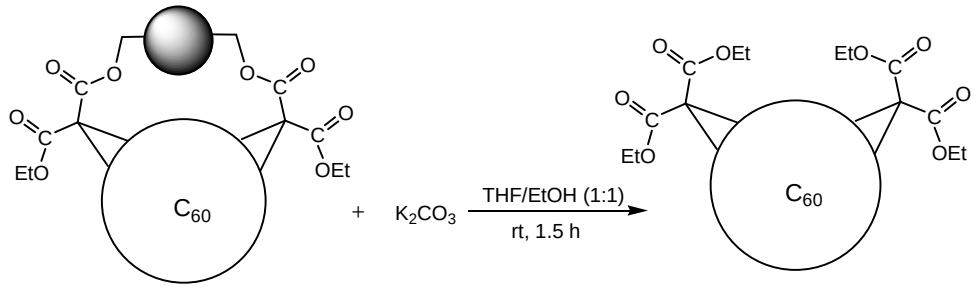

Material Bisadduct	Regio-isomerism	Resulted Tetraethylester	Yield	Ref.[161]
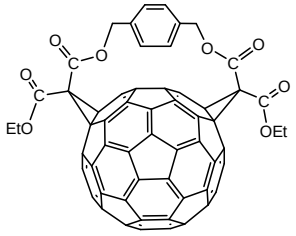 **(43)**	*trans-4*	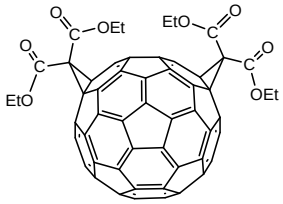 **(47)**	53%	N/A
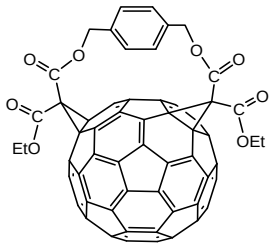 **(44)**	*e*	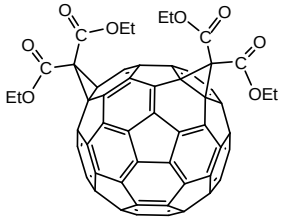 **(48)**	31%	N/A
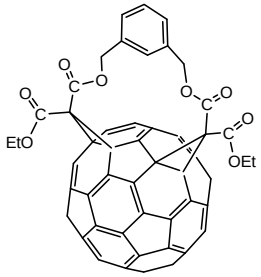 **(46)**	*cis-2*	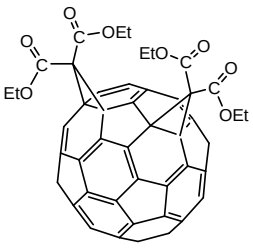 **(49)**	23%	N/A

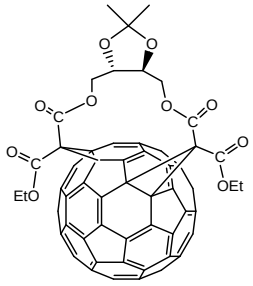 **(40)**	*cis-2*	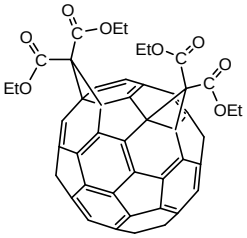 **(49)**	53%	N/A
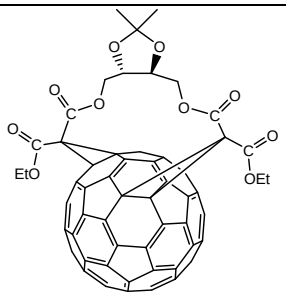 **(41)**	*cis-3*	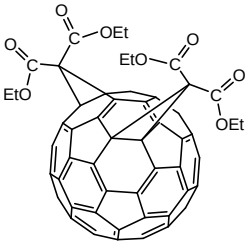 **(50)**	43%	83%

Appendix II

Nuclear Magnetic Resonance (NMR) spectra of malonate tethers, tethered bismethano[60]fullerenyl adducts and tetraethyl bismethano[60]fullerenyl tetracarboxylate

1. 2,3-*O*-Isopropylidene-l-threitol (38)

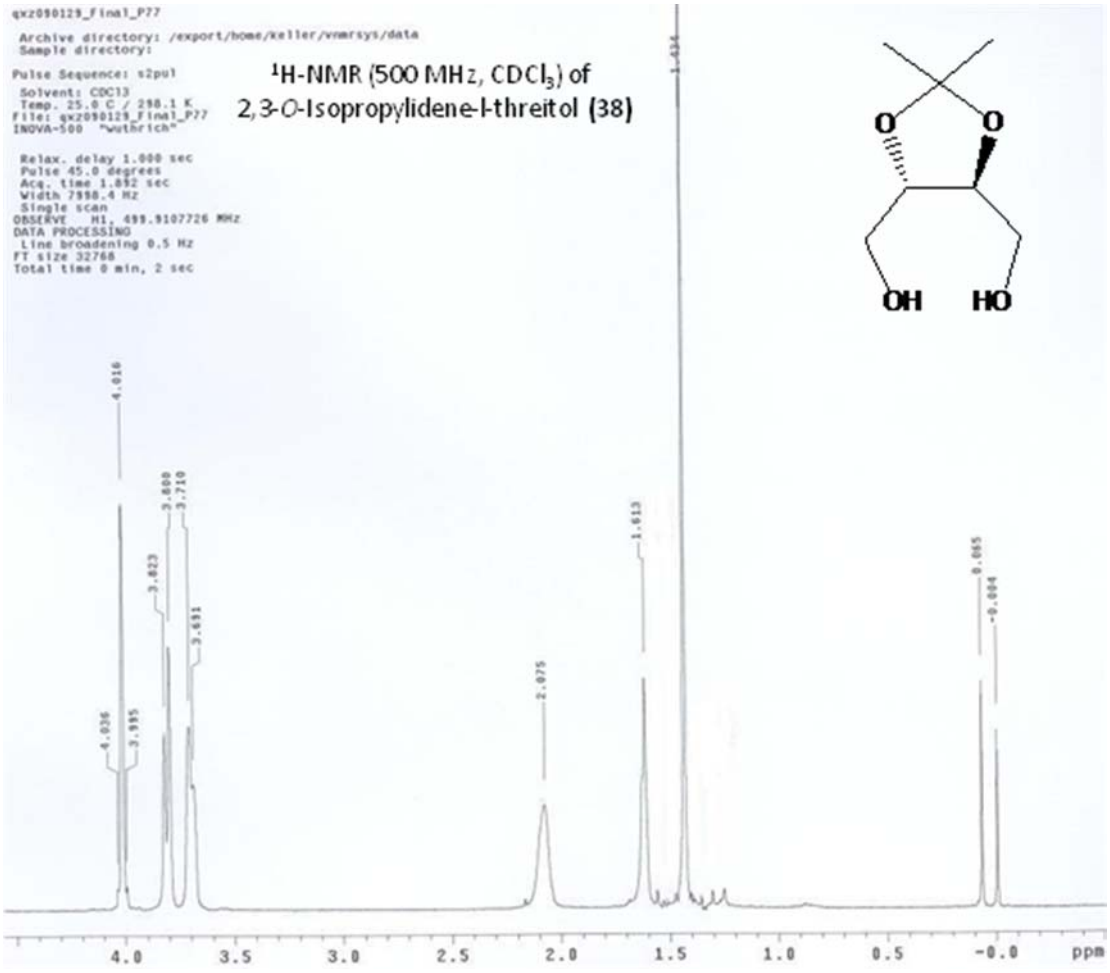

	Results from this study			Reported[162]		
	Chemical shift (ppm)	Multi-plicity	Coupling constant (Hz)	Chemical shift (ppm)	Multi-plicity	Coupling constant (Hz)
CH_3	1.43	s	-	1.42	s	-
OH	2.08	s	-	3.73	m	-
CH_2	3.71	d	9.3			
CH_2	3.82	d	11.7			
CH	4.02	t	10.3	3.94	m	-

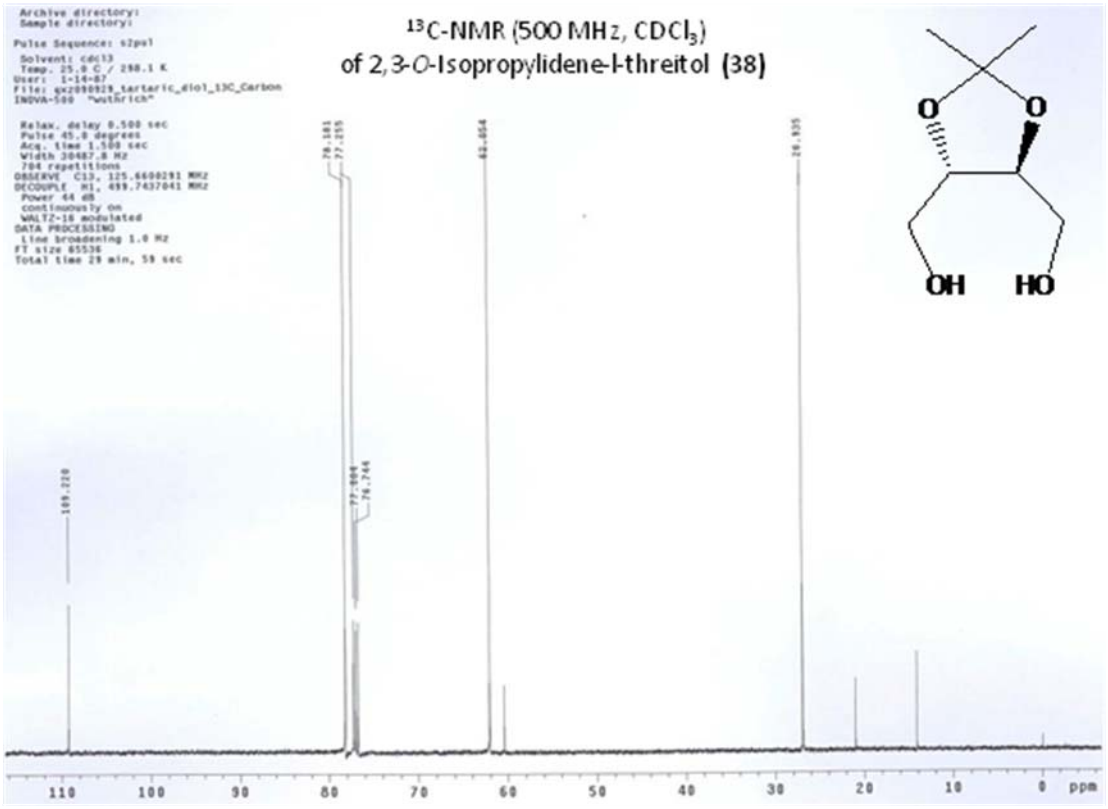

Reported by Mash *et al.*[162]	26.8	62.1	78.3	109.1
This study	26.9	62.1	78.2	109.2
Group	CH_3	CH_2	CH	CMe_2

2. (+)-(*4R,5R*)-bis{[(ethoxycarbonyl)acetoxy]methyl}-2,2-dimethyl-l,3-dioxolane (36)

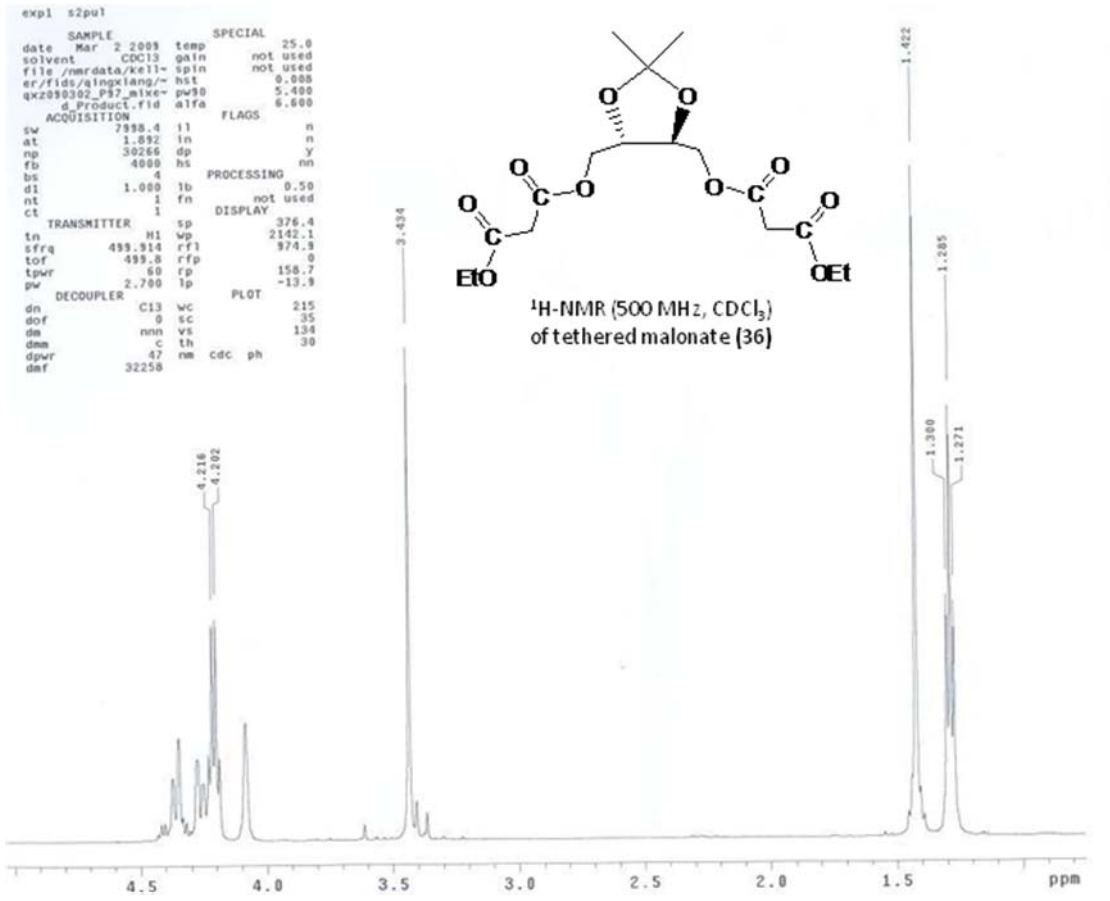

	Results from this study			Reported[161]		
	Chemical shift (ppm)	Multi-plicity	Coupling constant (Hz)	Chemical shift (ppm)	Multi-plicity	Coupling constant (Hz)
$CH_2C\underline{H}_3$	1.28	t	7.0	1.25	t	7.0
$O_2C(CH_3)_2$	1.42	s	-	1.38	s	-
$COCH_2CO$	3.43	s	-	3.40	s	-
CH	4.09	s	-	4.05	t	2.5
$C\underline{H}_2CH_3$	4.21	q	7.0	4.17	q	7.0
$CHC\underline{H}_2O$	4.25-4.40	m	-	4.20-4.35	m	-

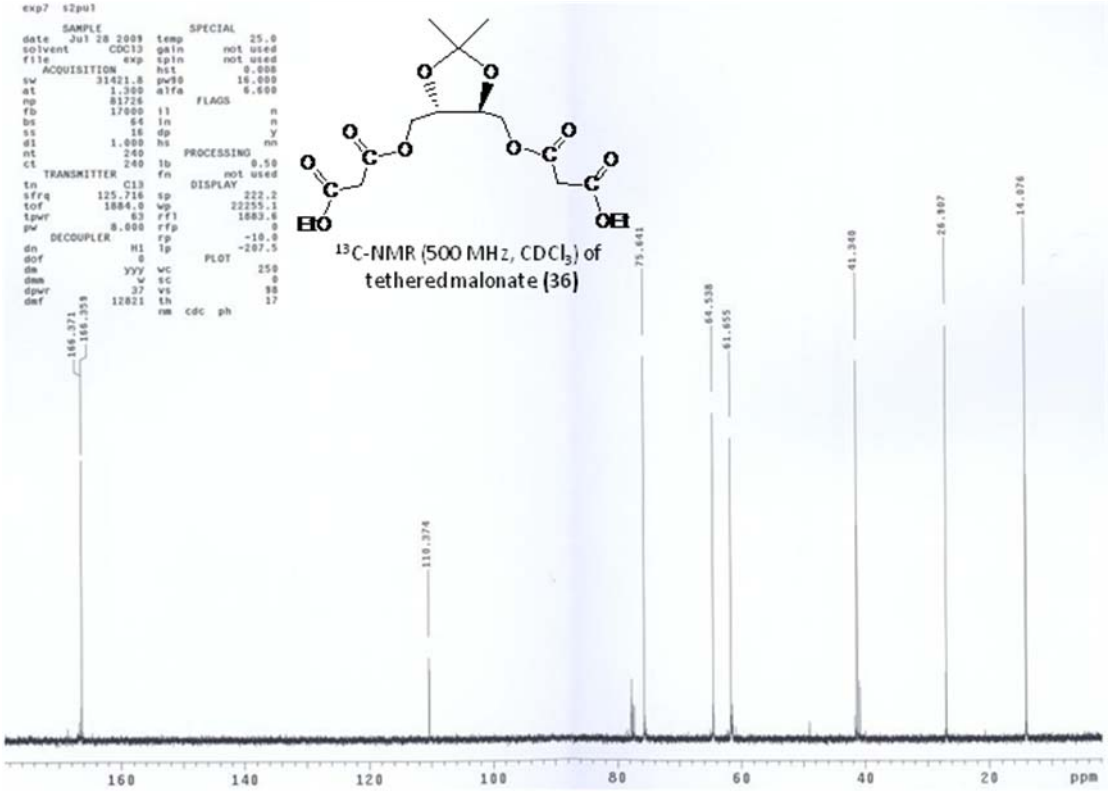

	Chemical shift (ppm)				
Ref.[161]	13.99	26.81	41.26	61.67	64.53
This study	14.07	26.90	41.34	61.65	64.53
Group	$CH_2\underline{C}H_3$	$O_2C(\underline{C}H_3)_2$	$\underline{C}H_2CH_3$	$CH\underline{C}H_2O$	$CO\underline{C}H_2CO$
	Chemical shift (ppm)				
Ref.[161]	75.54	110.43	166.24	166.30	
This study	75.64	110.37	166.35	166.37	
Group	CH	CMe_2	C=O	C=O	

3. Diethyl endo-endo-[(*4R,5R*)-(2,2-dimethyl-1,3-dioxolane-4,5-diyl)dimethyl]-1,2:7,21-bis(methano)[60]fullerene-61,61,62,62-tetracarboxylate (40)

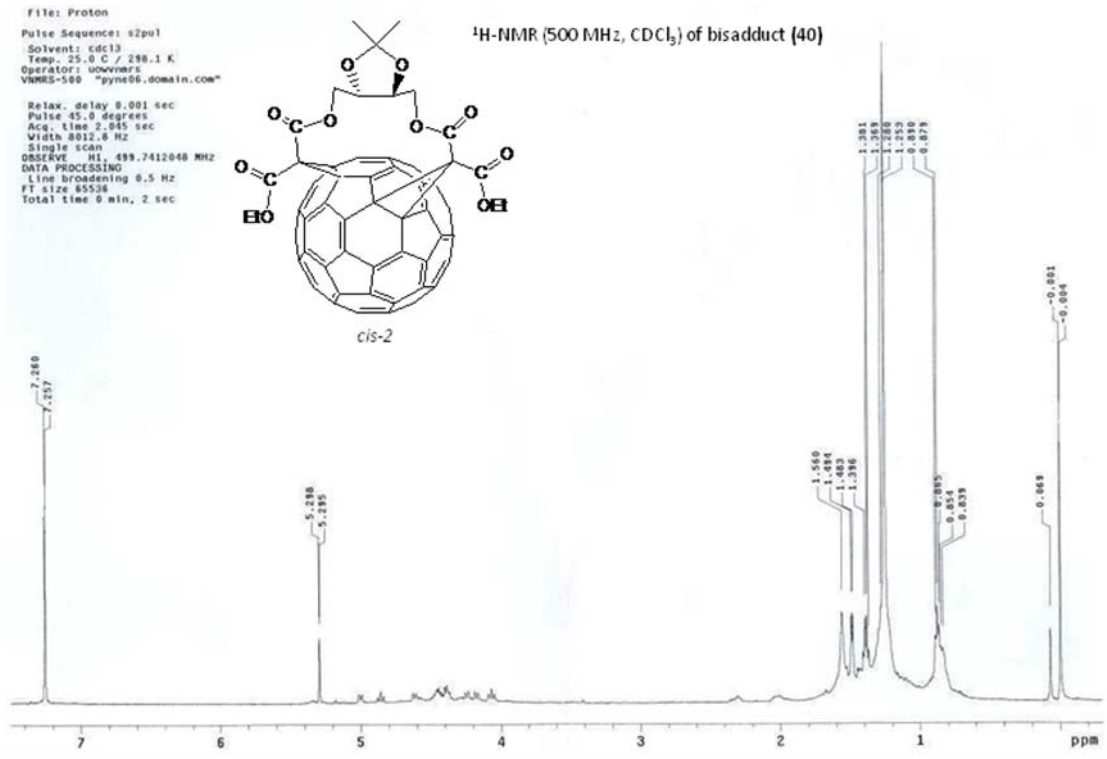

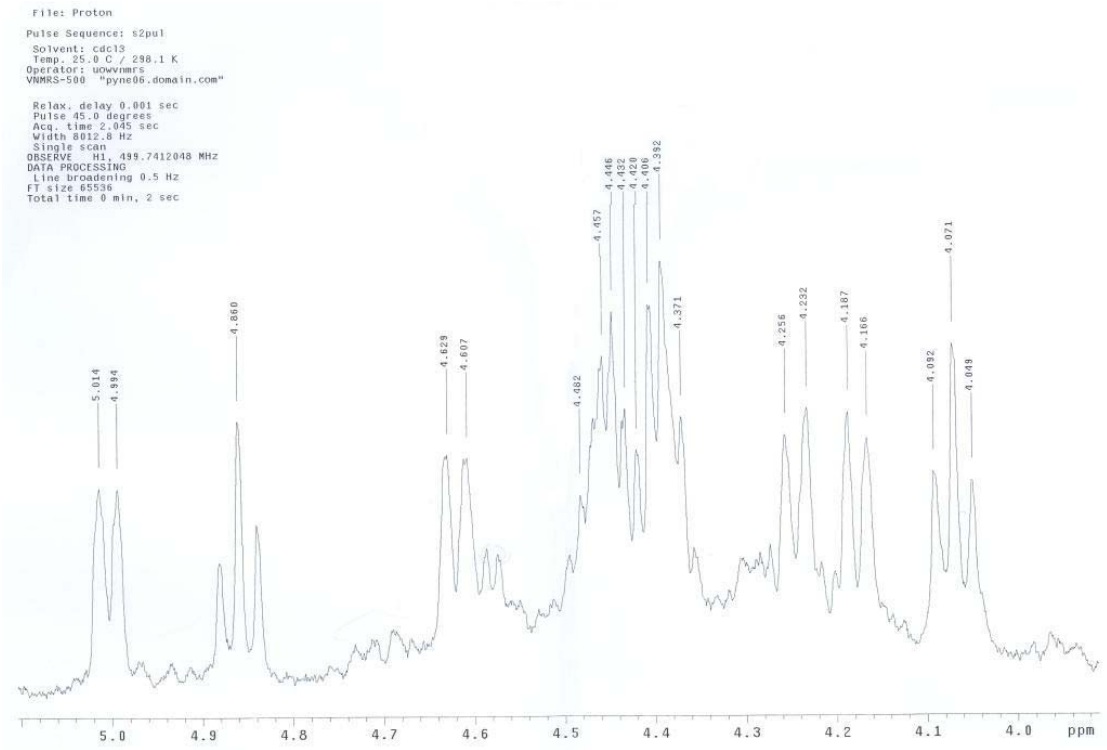

	Results from this study			Reported[161]		
	Chemical shift (ppm)	Multiplicity	Coupling constant (Hz)	Chemical shift (ppm)	Multiplicity	Coupling constant (Hz)
$CH_2C\underline{H}_3$	1.38	t	6.7	1.36	t	7.1
$CH_2C\underline{H}_3$	1.39	t	6.6	1.37	t	7.1
$O_2C(CH_3)_2$	1.48	s	-	1.46	s	-
$O_2C(CH_3)_2$	1.49	s	-	1.47	s	-
CH	4.07	t	10.5	4.05	t	10.5
$CHC\underline{H}_2O$	4.17	d	10.1	4.15	dd	10.5, 2.6
$CHC\underline{H}_2O$	4.24	d	11.0	4.22	dt	10.5, 2.6
$C\underline{H}_2CH_3$	4.34-4.48	m	-	4.33-4.47	m	-
$CHC\underline{H}_2O$	4.61	d	10.7	4.60	dt	10.5, 2.6
CH	4.86	t	10.1	4.84	t	10.5
$CHC\underline{H}_2O$	5.00	d	8.0	4.98	dd	10.5, 2.6

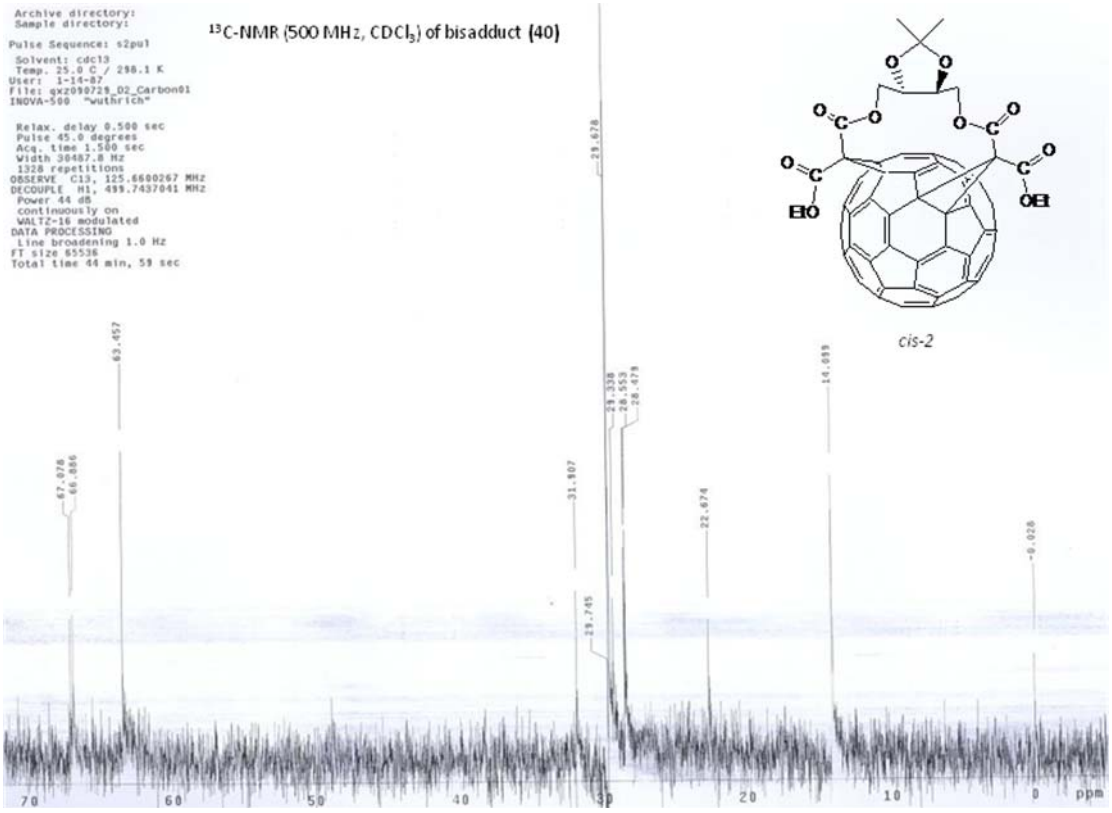

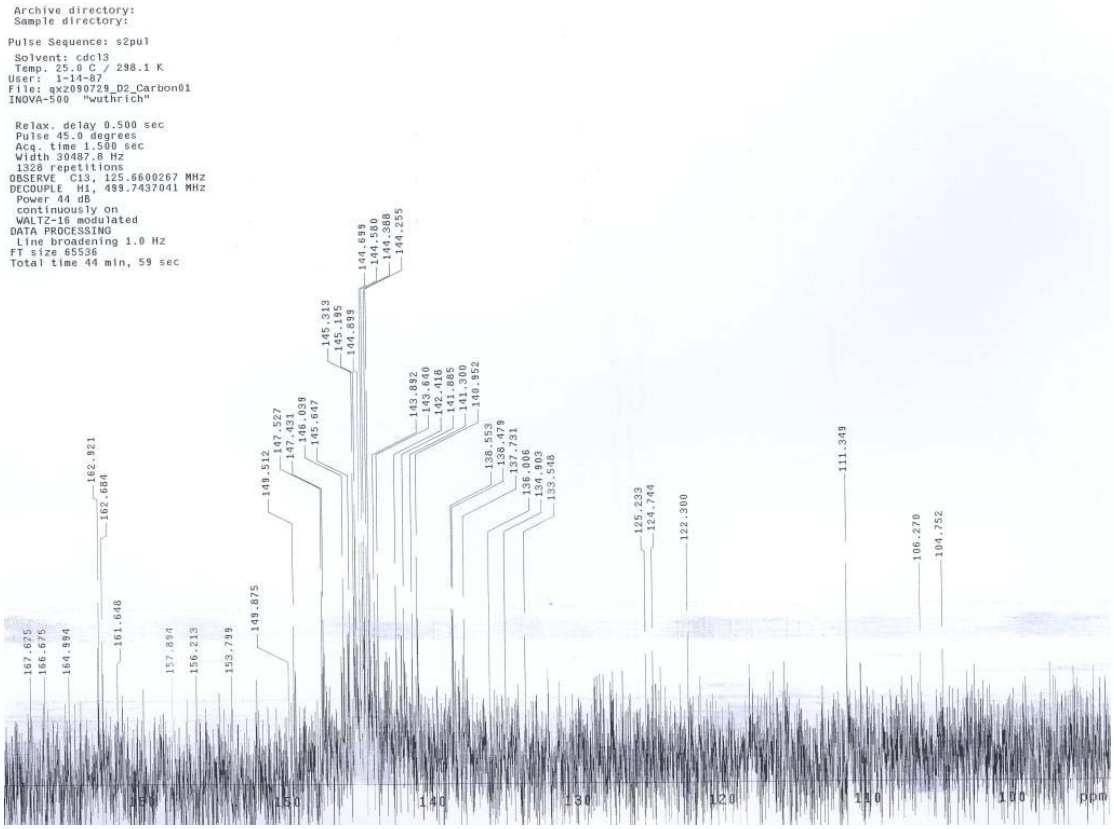

	Chemical shift (ppm)								
Ref.[161]	14.12	14.13	28.48	28.55	48.90 (2×)	63.46 (2×)	66.89	67.08 (2×)	67.16
This study	14.10	-	18.48	28.55	-	63.46	66.88	67.08	-
Ref.[161]	70.10	70.17	78.25	78.29	111.35	133.55	137.55	137.73	137.83
This study	-	-	-	-	111.35	133.55	-	137.73	-
Ref.[161]	138.06	138.33	138.48	138.55	140.92	140.95	141.30	141.33	141.89
This study	-	-	138.48	138.55	-	140.95	141.30	-	141.88
Ref.[161]	142.09	142.42	142.45	143.15	143.20	143.64	143.66	143.89	143.94
This study	-	142.42	-	-	-	143.64	-	143.89	-
Ref.[161]	144.19	144.25	144.39	144.57	144.58	144.69	144.72	144.90	145.03
This study	-	144.25	144.39	-	144.58	144.70	-	144.90	-
Ref.[161]	145.18	145.19	145.21	145.27	145.32	145.33	145.35	145.64	145.71
This study	-	145.19	-	-	145.31	-	-	145.65	-
Ref.[161]	145.75	145.77	146.00	146.04	146.15	146.19	147.33	147.43	147.53
This study	-	-	-	146.04	-	-	-	147.43	147.53
Ref.[161]	149.38	149.51	162.63	162.68	162.92	162.99			
This study	-	149.51	-	162.68	162.92	-			

4. Diethyl endo-endo-[(*4R,5R*)-(2,2-dimethyl-1,3-dioxolane-4,5-diyl)dimethyl]-1,2:16,17-bis(methano)[60]fullerene-61,61,62,62-tetracarboxylate (41)

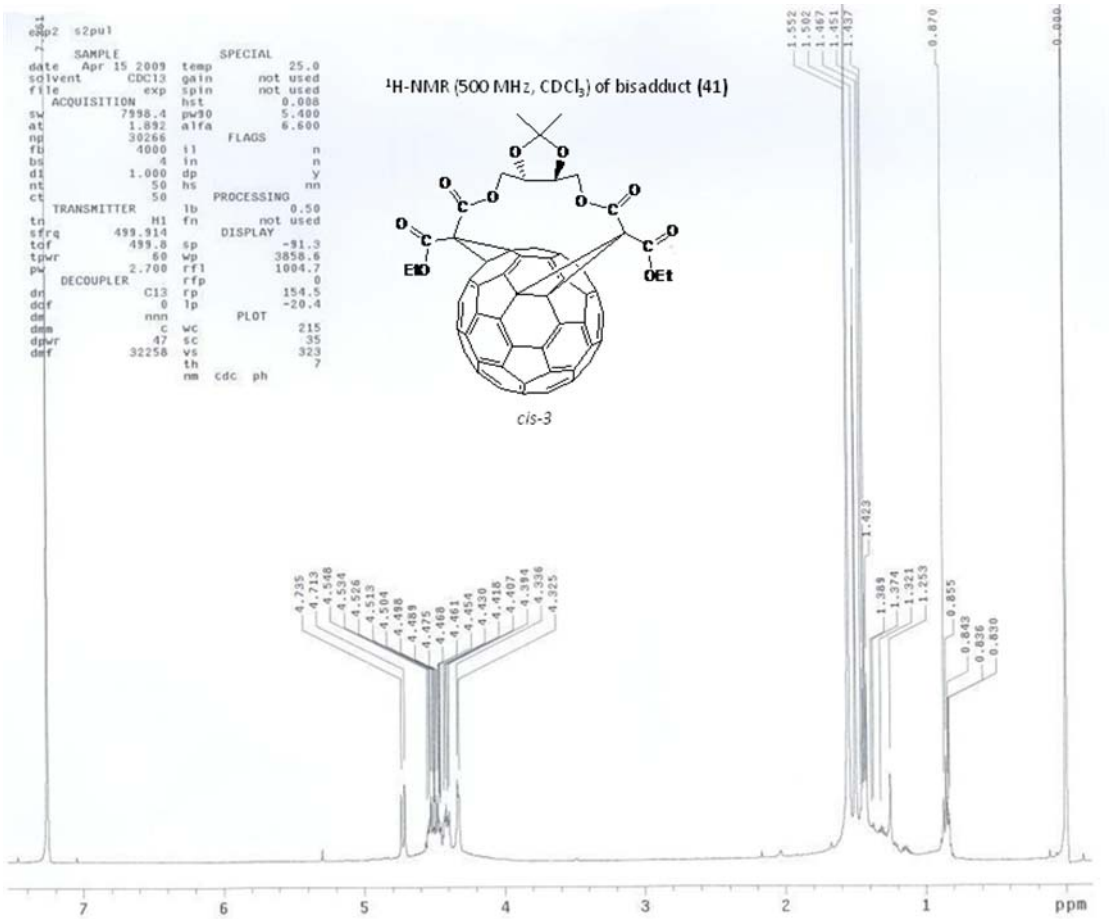

	Results from this study			Reported[161]		
	Chemical shift (ppm)	Multi-plicity	Coupling constant (Hz)	Chemical shift (ppm)	Multi-plicity	Coupling constant (Hz)
$CH_2C\underline{H}_3$	1.43	t	7.1	1.44	t	7.1
$O_2C(CH_3)_2$	1.50	s	-	1.50	s	-
$CHC\underline{H}_2O$	4.31-4.36	m	-	4.31-4.36	m	-
$CHC\underline{H}_2O$	4.39-4.44	m	-	4.39-4.44	m	-
$C\underline{H}_2CH_3$	4.44-4.57	m	-	4.44-4.57	m	-
CH	4.70-4.75	m	-	4.70-4.75	m	-

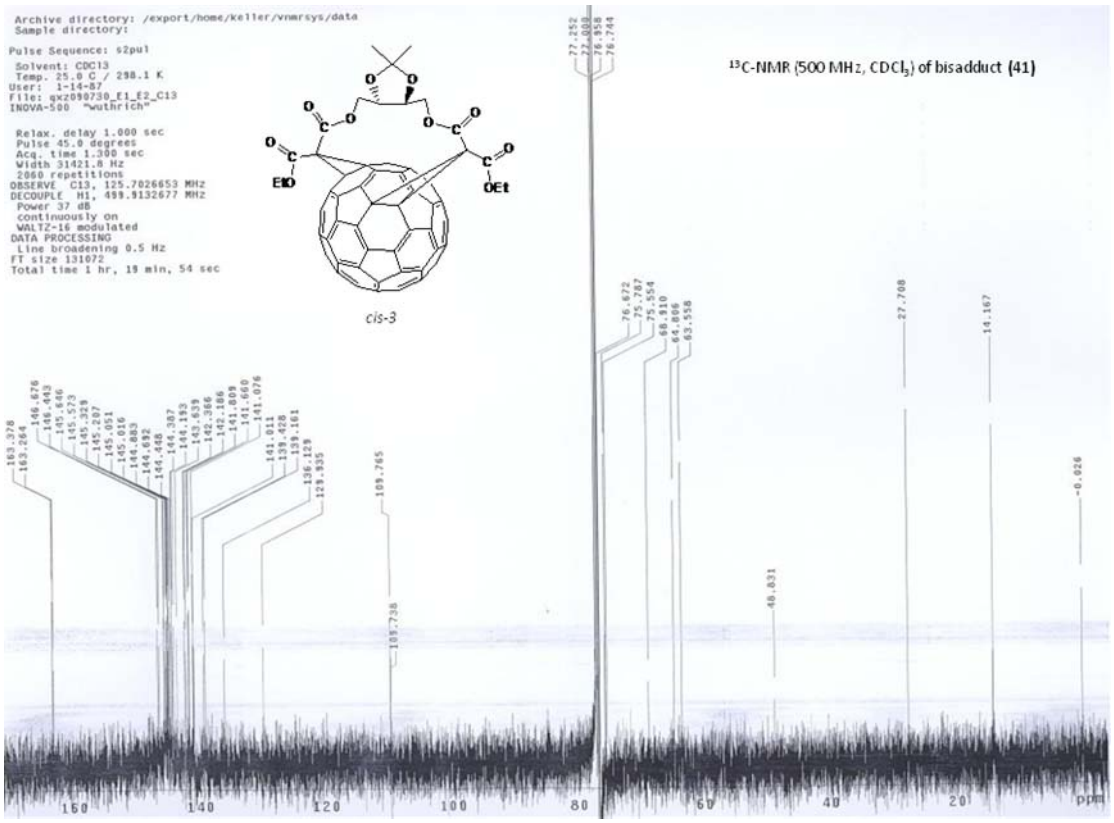

	Chemical shift (ppm)								
Ref.[161]	14.22	27.79	48.92	63.71	64.95	69.05	71.91	75.95	109.99
This study	14.16	27.71	48.83	63.56	64.81	68.91	-	75.79	109.76
Ref.[161]	130.20	136.41	139.45	139.73	141.27	141.30	141.36	141.96	142.11
This study	129.93	136.13	139.16	139.43	141.01	141.07	141.66	141.81	142.18
Ref.[161]	142.48	142.66	143.92	144.48	144.68	144.74	144.99	145.18	145.31
This study	142.37	-	143.64	144.45	144.69	144.88	145.01	145.20	145.33
Ref.[161]	145.35	145.50	145.63	145.88	145.94	146.75	146.98	163.61	163.72
This study	-	145.57	145.64	-	-	146.44	146.67	163.26	163.38

5. 1,4-Bis{[(ethoxycurbonyl)acetoxy]methyl}benzene (34)

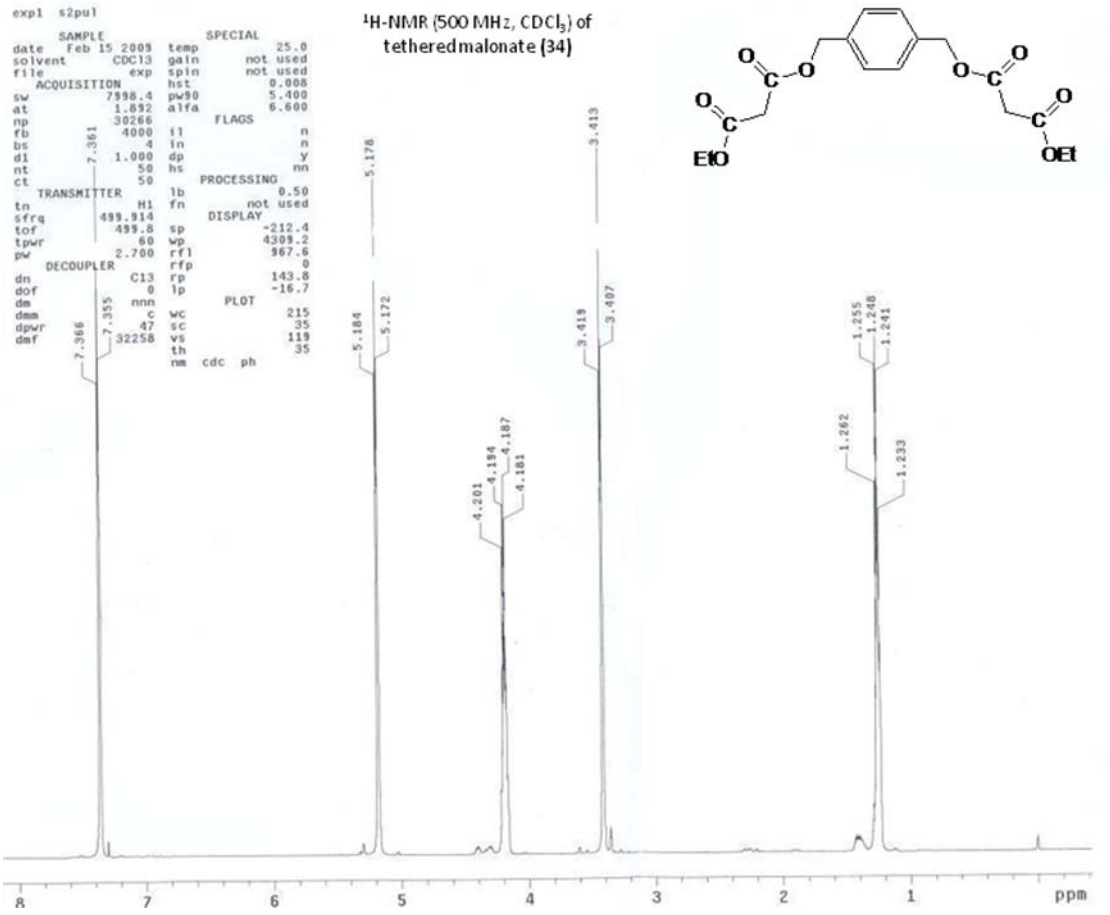

	Results from this study			Reported[161]		
	Chemical shift (ppm)	Multi-plicity	Coupling constant (Hz)	Chemical shift (ppm)	Multi-plicity	Coupling constant (Hz)
CH_3	1.24	t	7.1	1.19	t	7.1
$COCH_2CO$	3.41	s	-	3.36	s	-
$C\underline{H}_2CH_3$	4.19	q	7.0	4.13	q	7.1
$ArCH_2O$	5.17	s	-	5.12	s	-
ArH	7.36	s	-	7.30	s	-

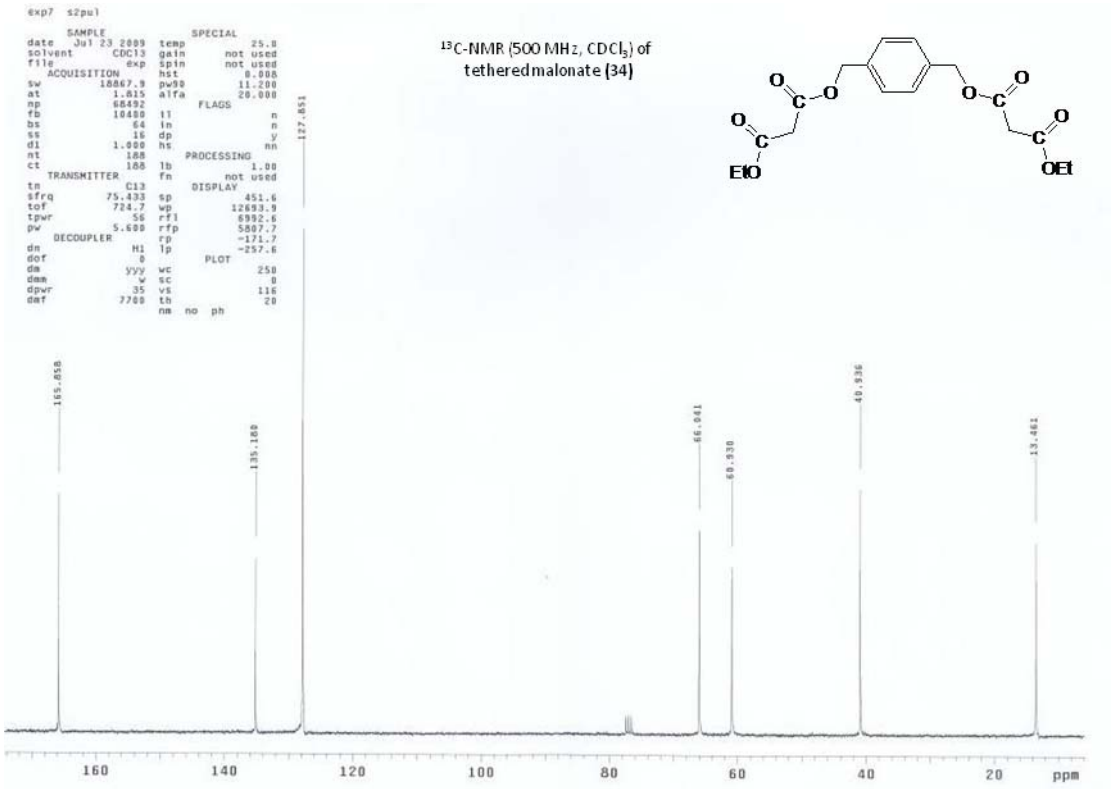

	Chemical shift (ppm)			
Ref.[161]	13.70	41.22	61.23	66.34
This study	13.46	40.93	60.93	66.04
Group	CH_3	$\underline{C}H_2CH_3$	$ArCH_2O$	$CO\underline{C}H_2CO$
	Chemical shift (ppm)			
Ref.[161]	128.09	135.27	166.02 (2×)	
This study	127.85	135.18	165.85	
Group	ArC	ArC	C=O	

6. Diethylendo,endo-(*p*-phenylenedimethyl)-1,2:34,35-bis(methano)[60]fullerene -61,61, 62,62-tetracarboxylate (43)

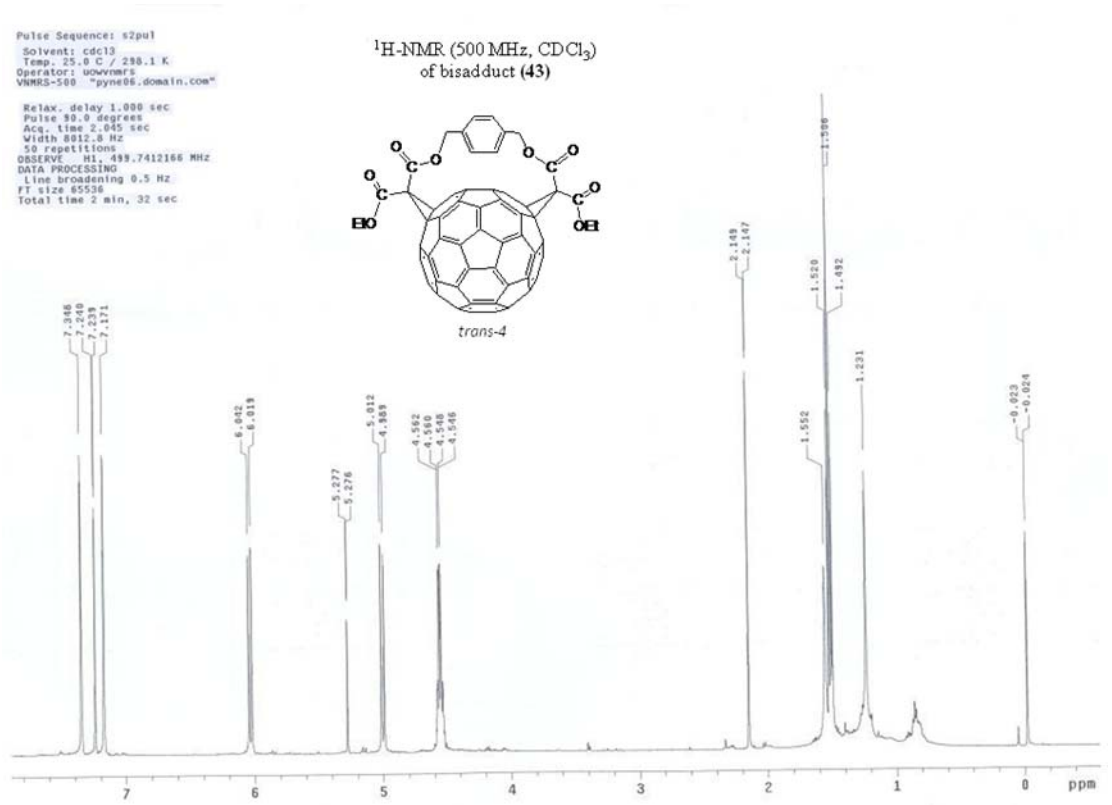

	Results from this study			Reported[161]		
	Chemical shift (ppm)	Multiplicity	Coupling constant (Hz)	Chemical shift (ppm)	Multiplicity	Coupling constant (Hz)
CH_3	1.50	t	7.1	1.50	t	7.1
$C\underline{H}_2CH_3$	4.52-4.58	m	-	4.52-4.58	m	-
$ArCH_2O$	5.00	d	11.0	5.00	d	11.3
$ArCH_2O$	6.02	d	11.2	6.02	d	11.3
ArH	7.17	s	-	7.16	d	1.8
ArH	7.34	s	-	7.52	d	1.8

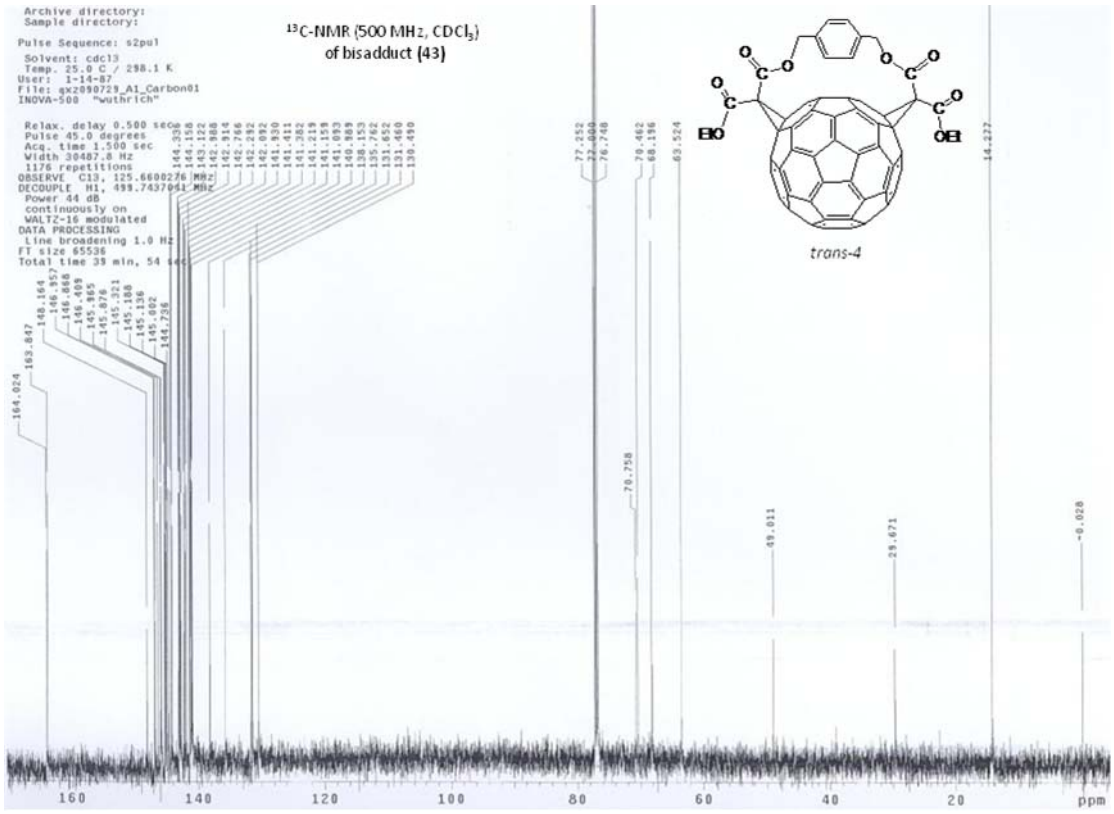

	Chemical shift (ppm)								
Ref.[161]	14.27	49.01	63.51	68.18	70.45	70.75	130.48	131.45	131.65
This study	14.27	49.01	63.52	68.19	70.46	70.75	130.49	131.46	131.65
Ref.[161]	135.75	138.15	140.97	141.08	141.15	141.20	141.37	141.39 (2×)	141.91
This study	135.76	138.15	140.99	141.09	141.16	141.22	141.38	141.41	141.93
Ref.[161]	142.07	142.28	142.75	142.90	142.97	143.11	144.15	144.32	144.72
This study	142.09	142.29	142.76	142.91	142.99	143.12	144.16	144.33	144.73
Ref.[161]	144.98	145.12	145.17	145.30	145.32	145.86	145.95	146.40	146.85
This study	145.00	145.13	145.19	-	145.32	145.87	145.96	146.41	146.87
Ref.[161]	146.94	148.15	163.82	164.00					
This study	146.95	148.16	163.84	164.02					

7. (±)-diethy1endo,endo-(*p*-phenylenedimethyl)-1,2:18,36-bis(methano)[60] fullerene-61,61,62,62-tetracarboxylate (44)

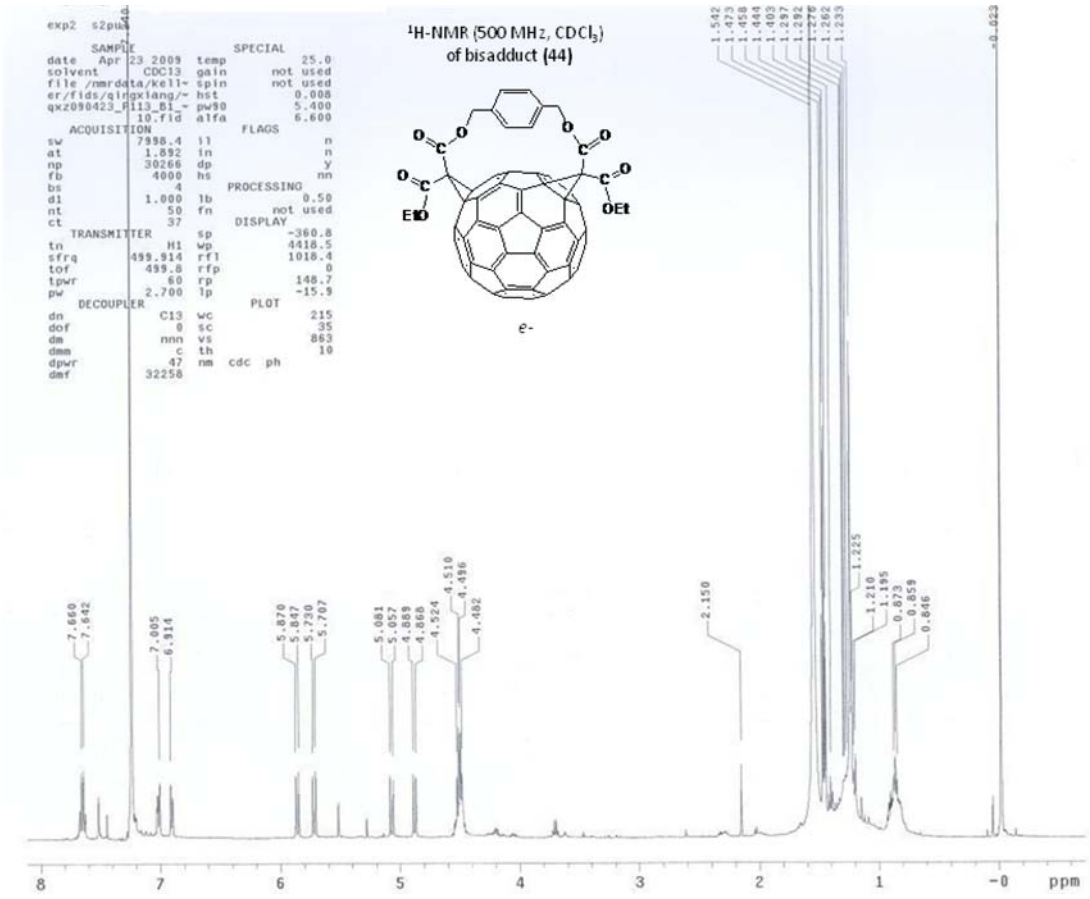

	Results from this study			Reported[161]		
	Chemical shift (ppm)	Multiplicity	Coupling constant (Hz)	Chemical shift (ppm)	Multiplicity	Coupling constant (Hz)
CH_3	1.45	t	7.1	1.45	t	7.1
CH_3	1.45	t	7.1	1.46	t	7.1
$C\underline{H}_2CH_3$	4.46-4.55	m	-	4.46-4.55	m	-
$ArCH_2O$	4.88	d	11.0	4.88	d	11.3
$ArCH_2O$	5.07	d	11.7	5.07	d	11.8
$ArCH_2O$	5.72	d	11.6	5.72	d	11.8
$ArCH_2O$	5.86	d	11.0	5.86	d	11.3
ArH	6.91	d	7.7	6.90	dd	7.5, 1.5
ArH	7.00	d	7.7	7.01	dd	7.5, 1.5
ArH	7.64	d	7.8	7.63	dd	8.0, 1.5
ArH	7.66	d	8.0	7.66	dd	8.0, 1.5

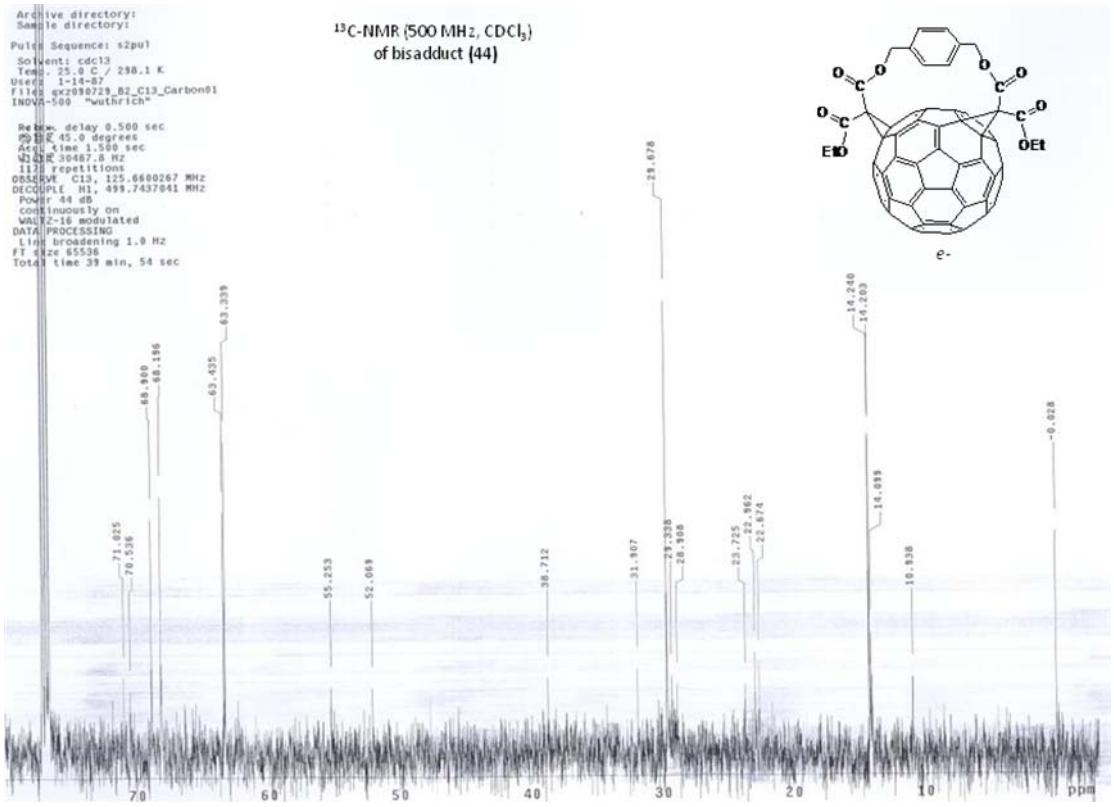
Archive directory:
Sample directory:
Pulse Sequence: s2pul
Solvent: cdcl3
Temp. 25.0 C / 298.1 K
User: 1-14-87
File: gx2090729_B2_C13_Carbon01
INOVA-500 "wuthrich"
Relax. delay 0.500 sec
Pulse 45.0 degrees
Acq. time 1.500 sec
Width 30487.8 Hz
1176 repetitions
OBSERVE C13, 125.6600267 MHz
DECOUPLE H1, 499.7437041 MHz
Power 44 dB
continuously on
WALTZ-16 modulated
DATA PROCESSING
Line broadening 1.0 Hz
FT size 65536
Total time 39 min, 54 sec
13C-NMR (500 MHz, CDCl3)
of bisadduct (44)
OEt
OEt
e-
ppm

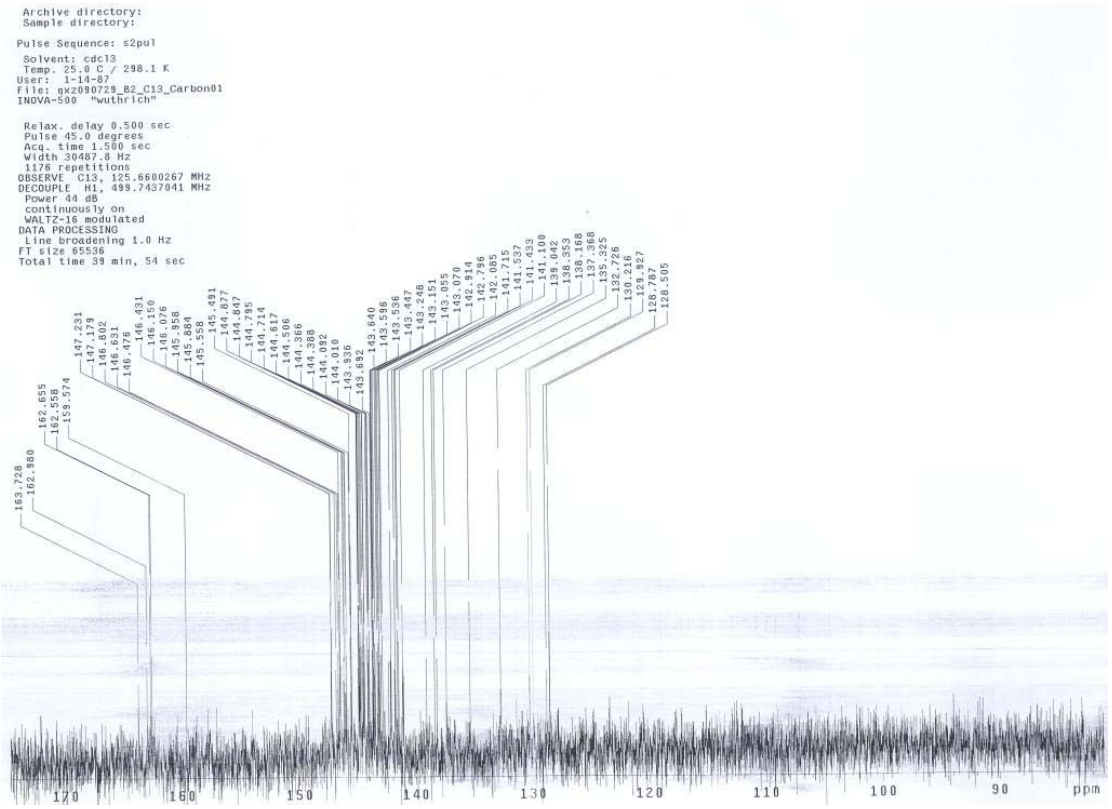
Archive directory:
Sample directory:
Pulse Sequence: s2pul
Solvent: cdcl3
Temp. 25.0 C / 298.1 K
User: 1-14-87
File: gx2090729_B2_C13_Carbon01
INOVA-500 "wuthrich"
Relax. delay 0.500 sec
Pulse 45.0 degrees
Acq. time 1.500 sec
Width 30487.8 Hz
1176 repetitions
OBSERVE C13, 125.6600267 MHz
DECOUPLE H1, 499.7437041 MHz
Power 44 dB
continuously on
WALTZ-16 modulated
DATA PROCESSING
Line broadening 1.0 Hz
FT size 65536
Total time 39 min, 54 sec
ppm

	Chemical shift (ppm)								
Ref.[161]	14.21	14.25	52.09	52.78	63.34	63.44	68.20	68.90	70.55
This study	14.20	14.24	52.07	-	63.34	63.44	68.20	68.90	70.53
Ref.[161]	70.83	71.04	71.88	128.51	129.93	130.23	132.73	135.34	137.38
This study	-	71.02	-	128.50	129.93	130.21	132.73	135.32	137.37
Ref.[161]	138.17	138.36	139.05	141.04	141.09	141.11	141.44	141.54	141.72
This study	138.17	138.35	139.04	-	141.10	-	141.43	141.54	141.72
Ref.[161]	141.78	142.09	142.12	142.30	142.80	142.92	143.07	143.12	143.15
This study	-	142.09	-	-	142.79	142.91	143.07	143.12	143.15
Ref.[161]	143.26	143.46	143.54	143.60	143.64	143.70	143.95	144.02	144.10
This study	143.25	143.44	143.53	143.60	143.64	143.69	143.94	144.01	144.10
Ref.[161]	144.38	144.39	144.46	144.51	144.63	144.72	144.76	144.80	144.85
This study	144.39	-	144.46	144.50	144.62	144.71	-	144.79	144.84
Ref.[161]	144.88	145.50	145.56	145.89	145.96	146.08	146.16	146.42	146.44
This study	144.87	145.50	145.56	145.88	145.96	146.07	146.15	146.43	-
Ref.[161]	146.48	146.65	146.81	147.18	147.24	162.56	162.66	162.98	163.73
This study	146.47	146.63	146.80	147.18	147.23	162.56	162.65	162.98	163.73

8. 1,3-Bis{[(ethoxycurbonyl)acetoxy]methyl}benzene (35)

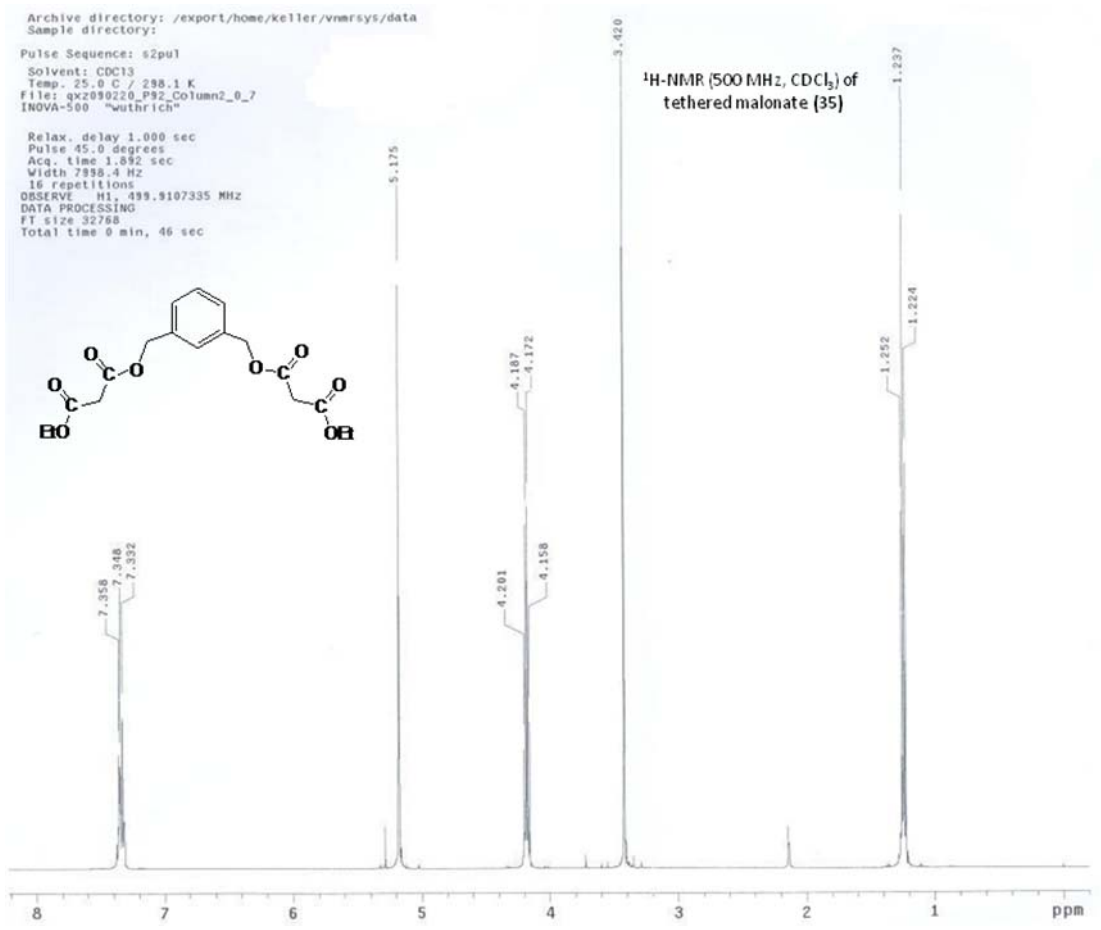

	Results from this study			Reported[161]		
	Chemical shift (ppm)	Multi-plicity	Coupling constant (Hz)	Chemical shift (ppm)	Multi-plicity	Coupling constant (Hz)
CH_3	1.23	t	7.1	1.22	t	7.1
$COCH_2CO$	3.42	s	-	3.39	s	-
$C\underline{H}_2CH_3$	4.18	q	7.1	4.16	q	7.1
$ArCH_2O$	5.17	s	-	5.15	s	-
ArH	7.34	m	-	7.31	br. s	-

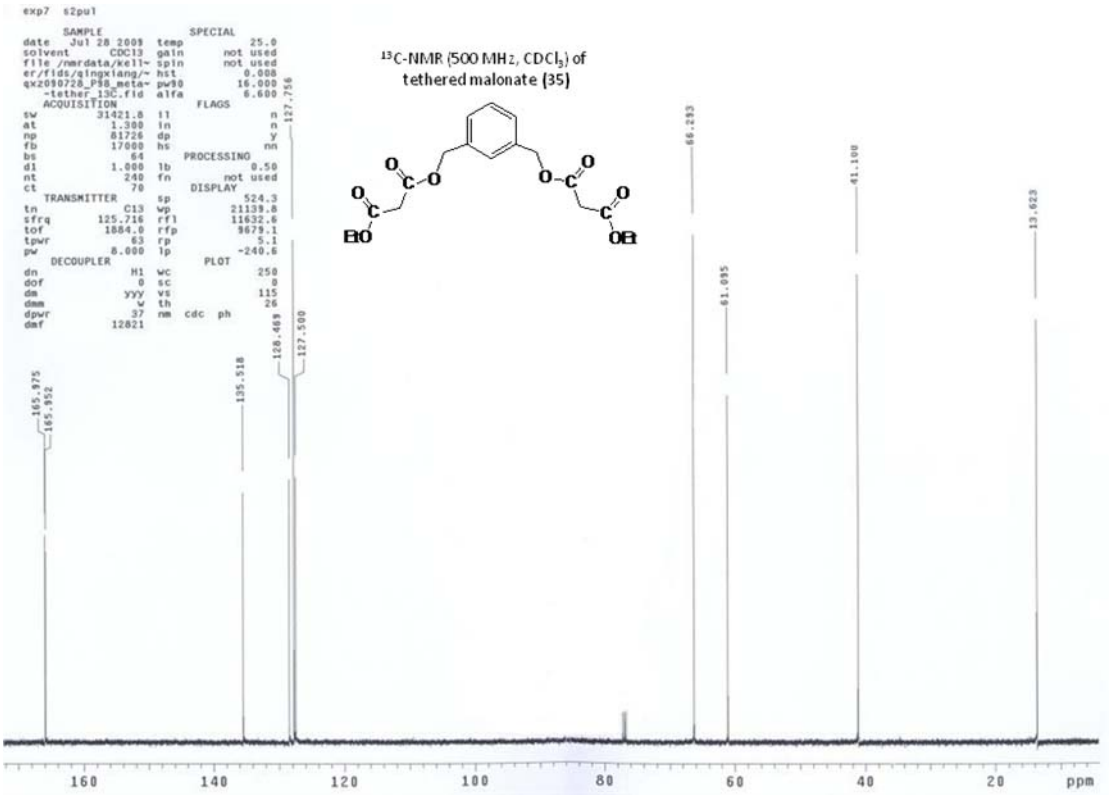

	Chemical shift (ppm)				
Ref.[161]	13.73	41.25	61.27	66.47	127.65
This study	13.62	41.10	61.09	66.29	127.50
Group	CH_3	$\underline{C}H_2CH_3$	$ArCH_2O$	$CO\underline{C}H_2CO$	ArC
	Chemical shift (ppm)				
Ref.[161]	127.91	128.58	135.48	166.06 (2×)	
This study	127.75	128.46	135.51	165.95 165.97	
Group	ArC	ArC	ArC	C=O	

9. Diethyl endo, endo-(*m*-Phenylenedimethyl)-1,2:7,21-Bis(methano) [60]fu11erene -61,61,62,62-tetracarboxylate (46)

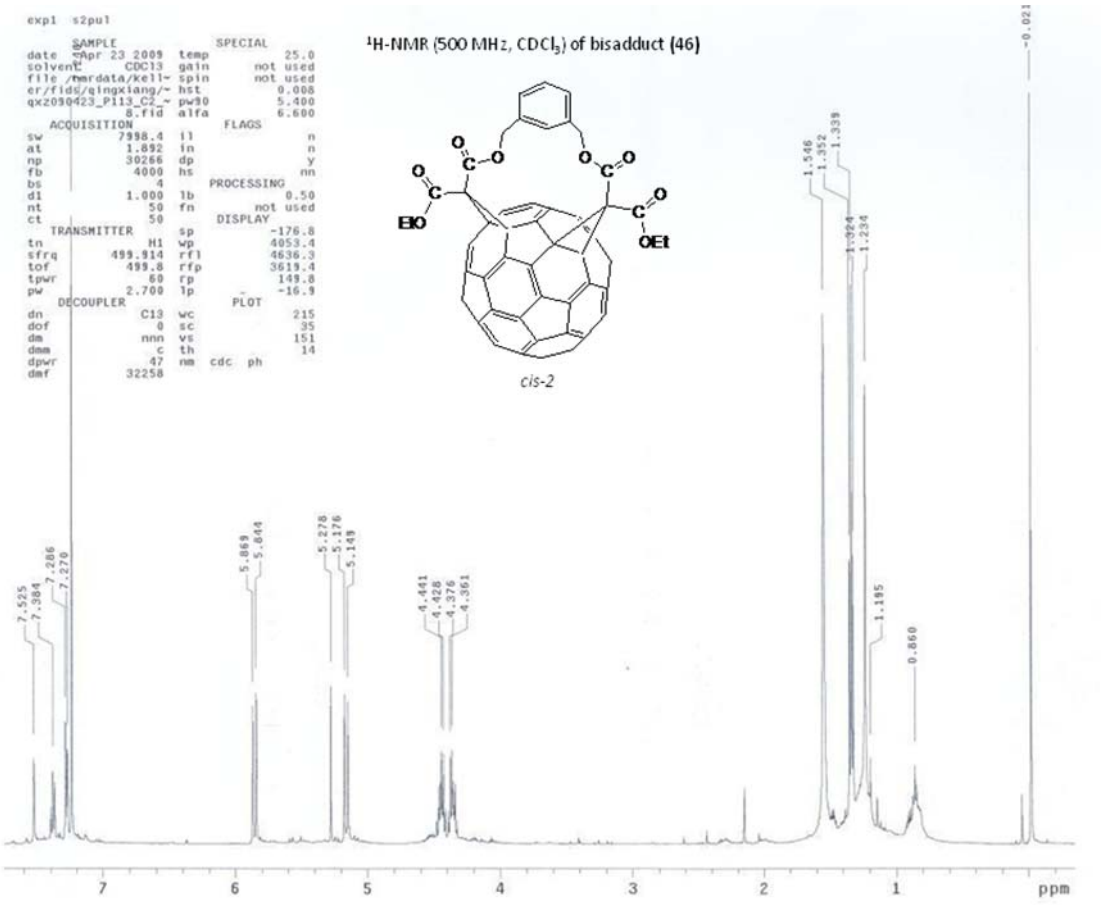

	Results from this study			Reported[161]		
	Chemical shift (ppm)	Multiplicity	Coupling constant (Hz)	Chemical shift (ppm)	Multiplicity	Coupling constant (Hz)
CH_3	1.34	t	7.0	1.34	t	7.1
$C\underline{H}_2CH_3$	4.35-4.45	m	-	4.34-4.46	m	-
$ArCH_2O$	5.16	d	12.9	5.16	d	12.8
$ArCH_2O$	5.86	d	12.9	5.86	d	12.8
ArH	7.28	d	7.5	7.27	dd	7.5, 1.5
ArH	7.38	d	7.5	7.38	t	7.5
ArH	7.52	s	-	7.52	t	1.5

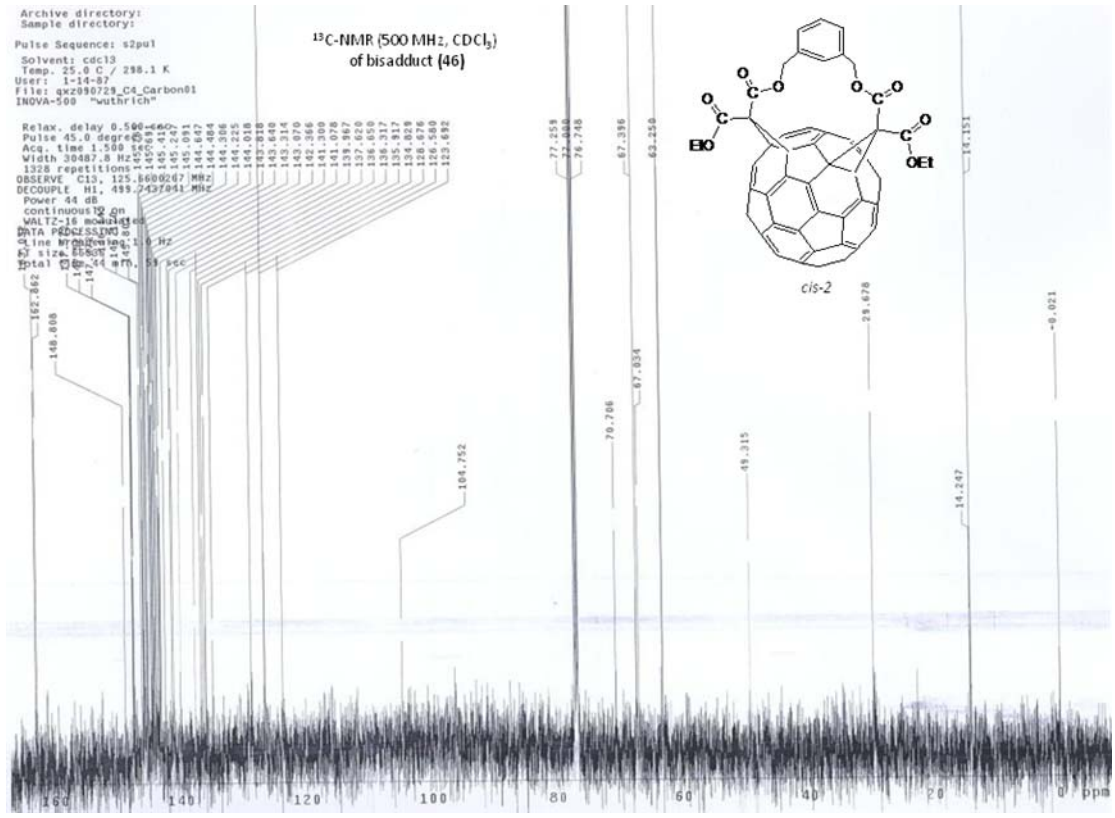
Archive directory:
Sample directory:
Pulse Sequence: s2pul
Solvent: cdcl3
Temp. 25.0 C / 298.1 K
User: 1-14-07
File: qxz090729_C4_Carbon01
INOVA-500 "wuthrich"
Relax. delay 0.500 sec
Pulse 45.0 degrees
Acq. time 1.500 sec
Width 30487.8 Hz
1328 repetitions
OBSERVE C13, 125.6600267 MHz
DECOUPLE H1, 499.7437041 MHz
Power 44 dB
continuously on
WALTZ-16 modulated
DATA PROCESSING
Line broadening 1.0 Hz
FT size 65536
Total time 44 min, 59 sec
13C-NMR (500 MHz, CDCl3)
of bisadduct (46)
EtO
OEt
cis-2
ppm

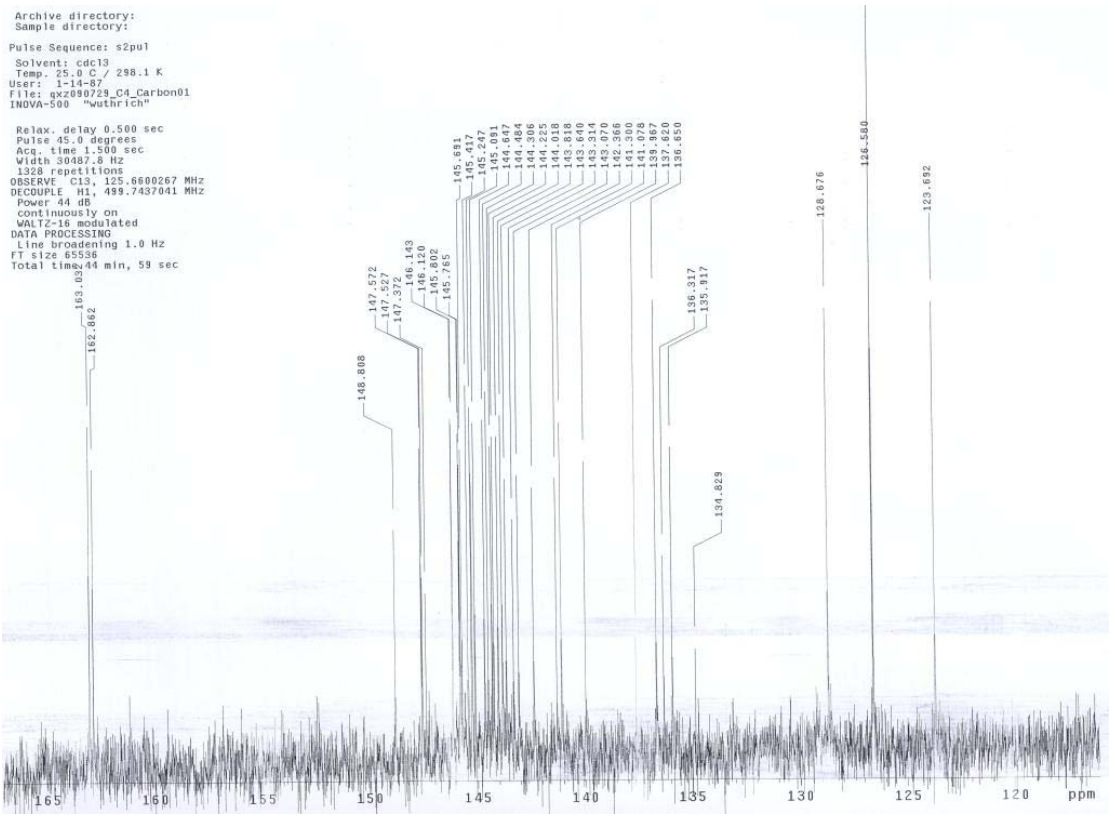
Archive directory:
Sample directory:
Pulse Sequence: s2pul
Solvent: cdcl3
Temp. 25.0 C / 298.1 K
User: 1-14-07
File: qxz090729_C4_Carbon01
INOVA-500 "wuthrich"
Relax. delay 0.500 sec
Pulse 45.0 degrees
Acq. time 1.500 sec
Width 30487.8 Hz
1328 repetitions
OBSERVE C13, 125.6600267 MHz
DECOUPLE H1, 499.7437041 MHz
Power 44 dB
continuously on
WALTZ-16 modulated
DATA PROCESSING
Line broadening 1.0 Hz
FT size 65536
Total time 44 min, 59 sec
ppm

	Chemical shift (ppm)								
Ref.[161]	14.15	49.36	63.25	67.07	67.41	70.74	123.73	126.59	128.68
This study	14.15	49.31	63.25	67.03	67.40	70.70	123.69	126.58	128.68
Ref.[161]	135.93	136.33	136.67	137.63	139.98	141.10	141.31	142.39	143.09
This study	135.92	136.32	136.65	137.62	139.97	141.08	141.30	142.37	143.07
Ref.[161]	143.33	143.66	143.84	144.03	144.24	144.32	144.50	144.66	145.11
This study	143.31	143.64	143.82	144.02	144.22	144.31	144.48	144.65	145.09
Ref.[161]	145.24	145.26	145.43	145.71	145.78	145.82	146.14	146.17	147.39
This study	145.24	-	145.42	145.69	145.76	145.80	146.12	146.14	147.37
Ref.[161]	147.54	147.59	148.83	162.87	163.04				
This study	147.53	147.57	148.81	162.86	163.03				

10. Tetraethyl-1,2:34,35-bis(methano)[60]fullerene-61,61,62,62-tetracarboxylate (47)

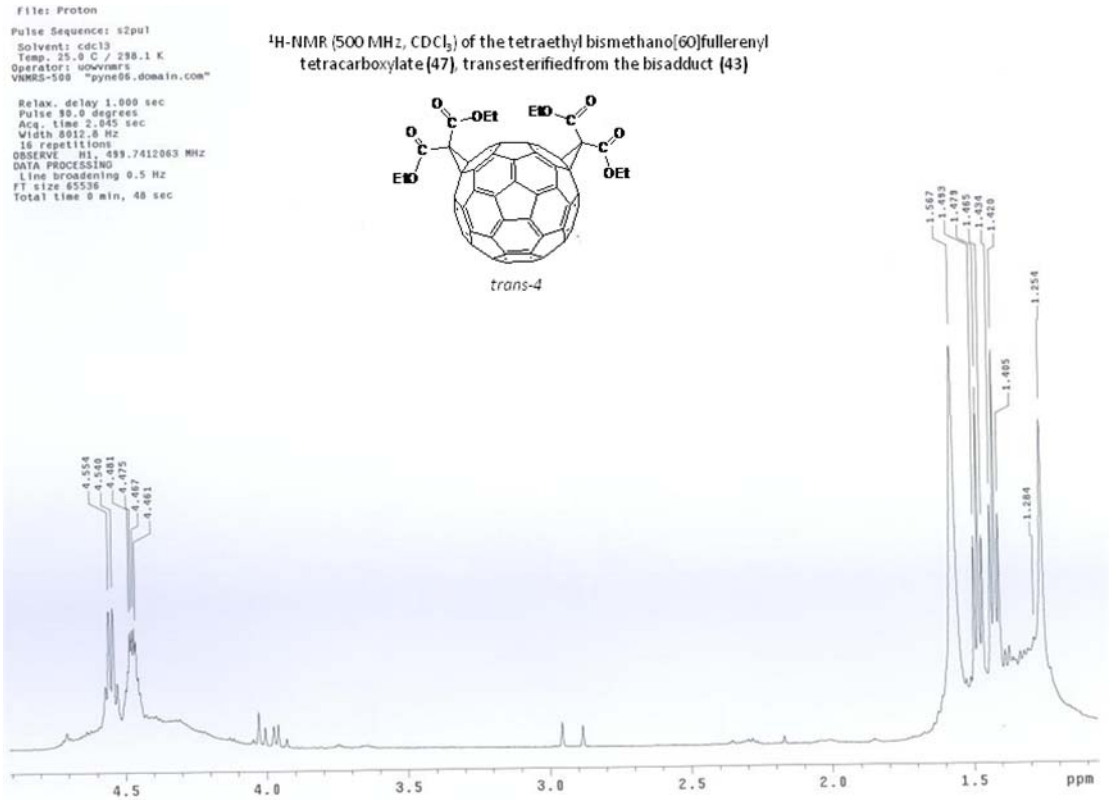

	Chemical shift (ppm)	Multiplicity	Coupling constant (Hz)
CH_3	1.42	t	7.1
CH_3	1.47	t	7.1
CH_2	4.43-4.50	m	-
CH_2	4.55	q	6.8

11. Tetraethyl-1,2:18,36-bis(methano)[60]fullerene-61,61,62,62-tetracarboxylate (48)

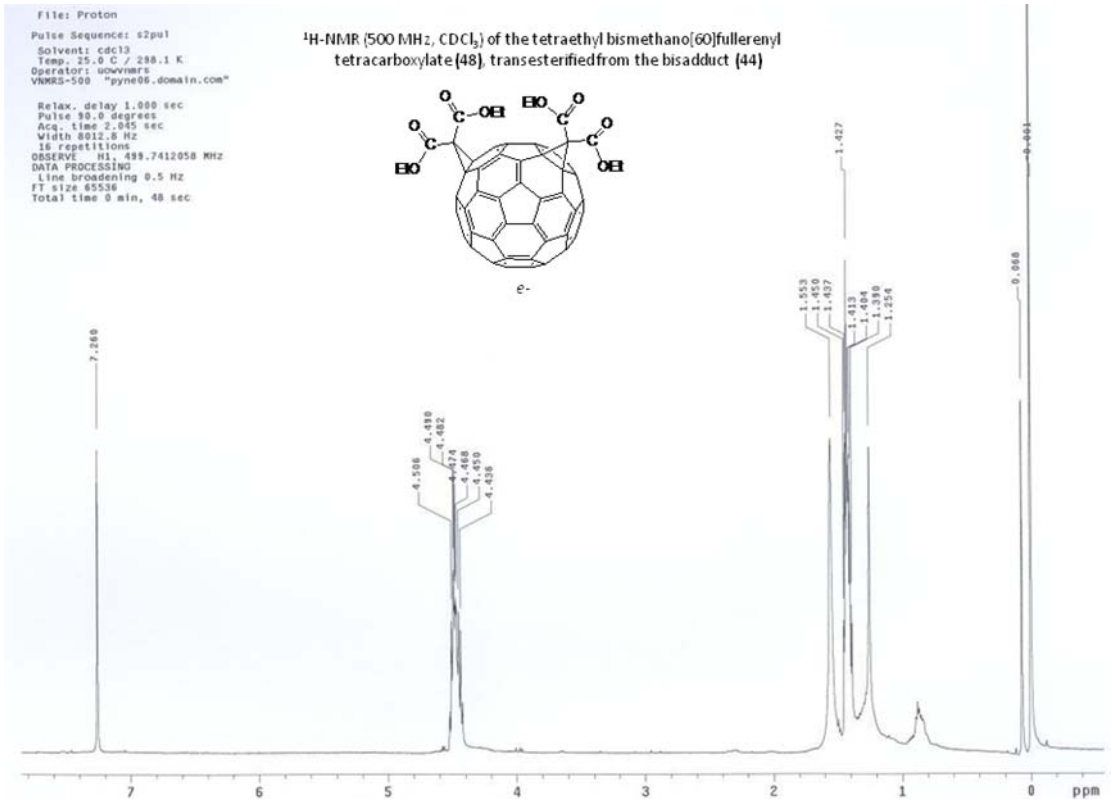

	Chemical shift (ppm)	Multiplicity	Coupling constant (Hz)
CH_3	1.40	t	6.7
CH_3	1.43	t	6.7
CH_2	4.40-4.47	m	-

12. Tetraethyl-1,2:7,21-bis(methano)[60]fullerene-61,61,62,62-tetracarboxylate (49)

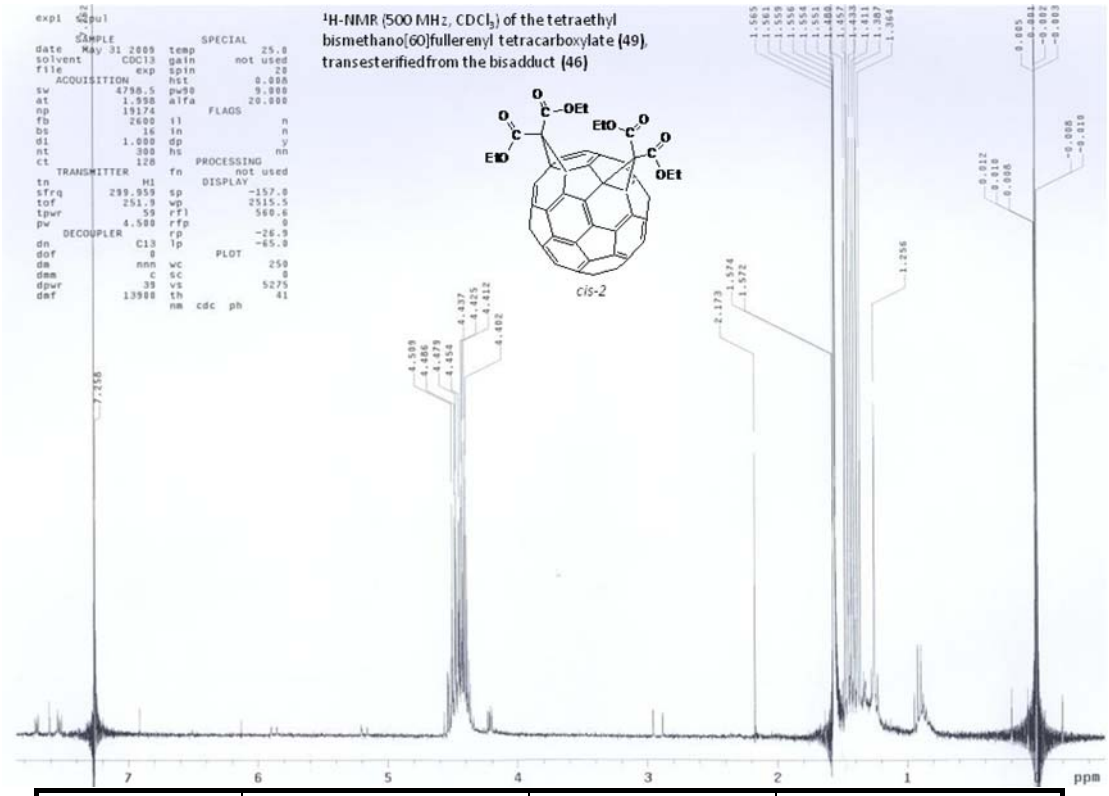

	Chemical shift (ppm)	Multiplicity	Coupling constant (Hz)
CH_3	1.38	t	7.1
CH_3	1.45	t	7.1
CH_2	4.35-4.55	m	-

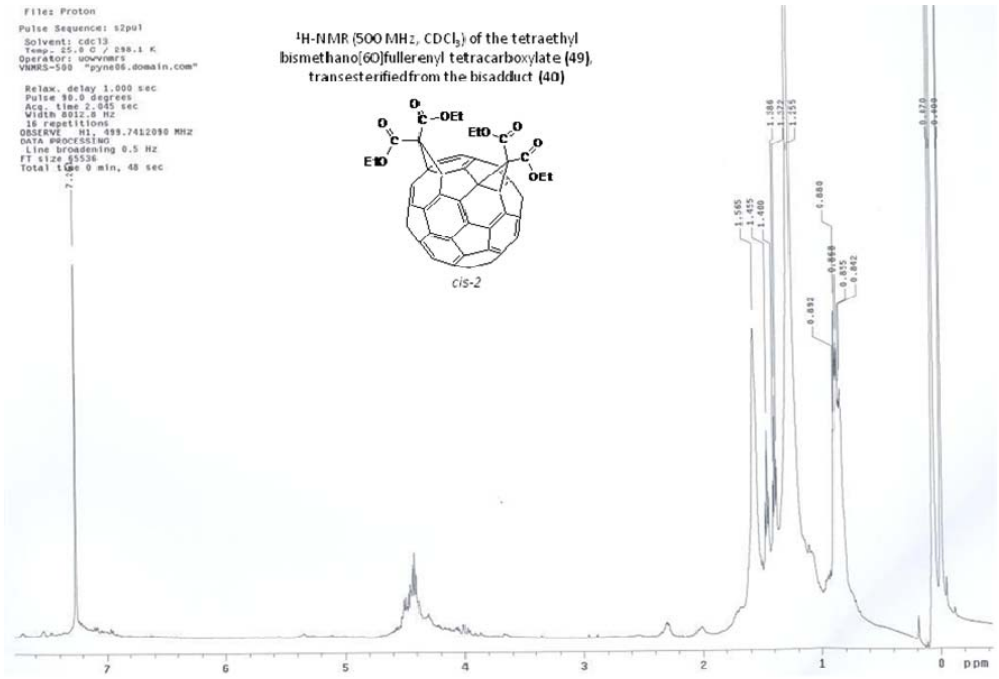

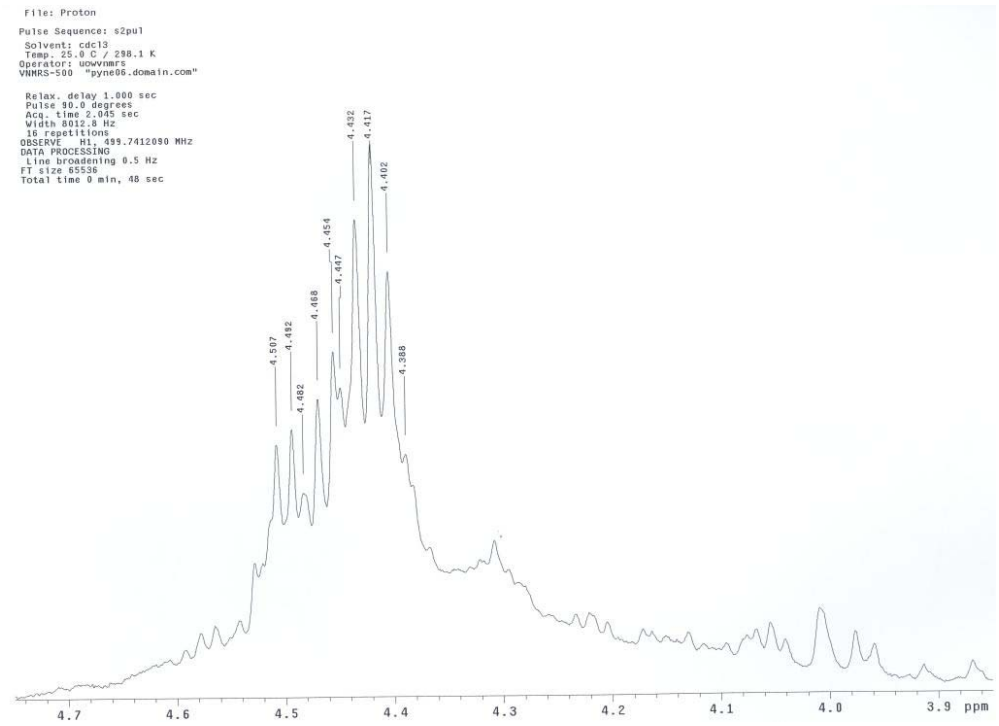

	Chemical shift (ppm)	Multiplicity	Coupling constant (Hz)
CH_3	1.38	t	7.1
CH_3	1.45	t	7.1
CH_2	4.36-4.53	m	-

13. Tetraethyl-1,2:16,17-bis(methano)[60]fullerene-61,61,62,62-tetracarboxylate (50)

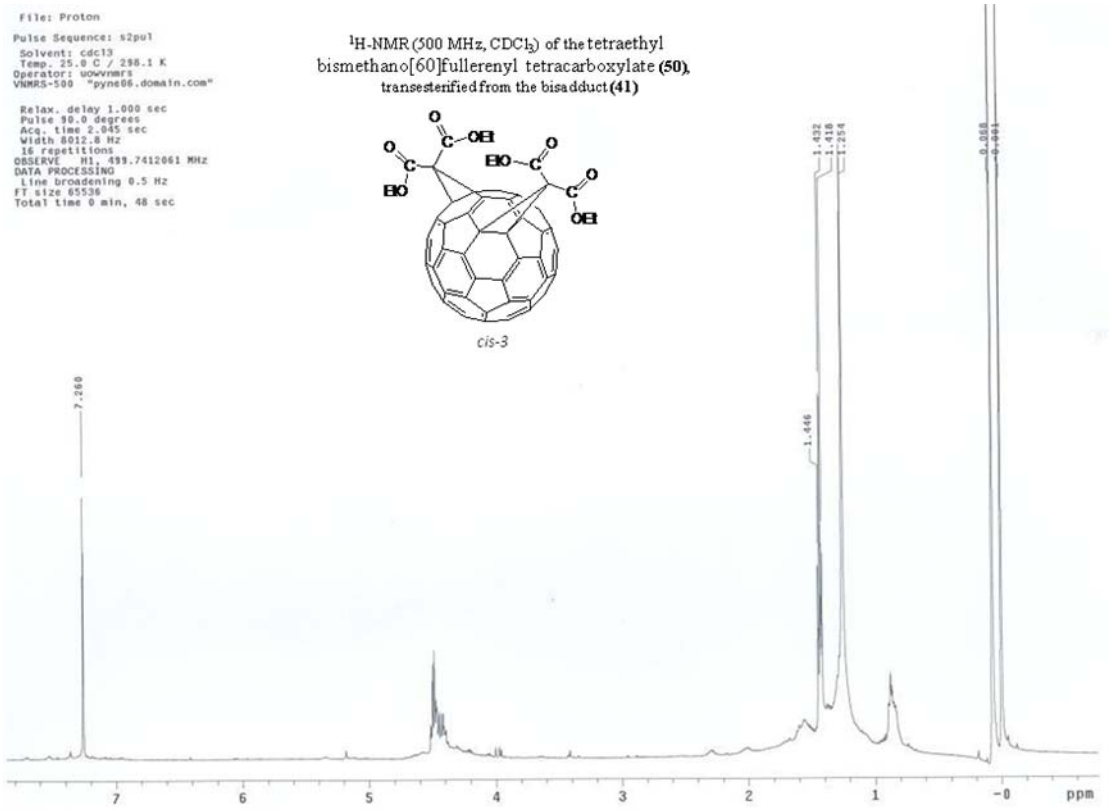

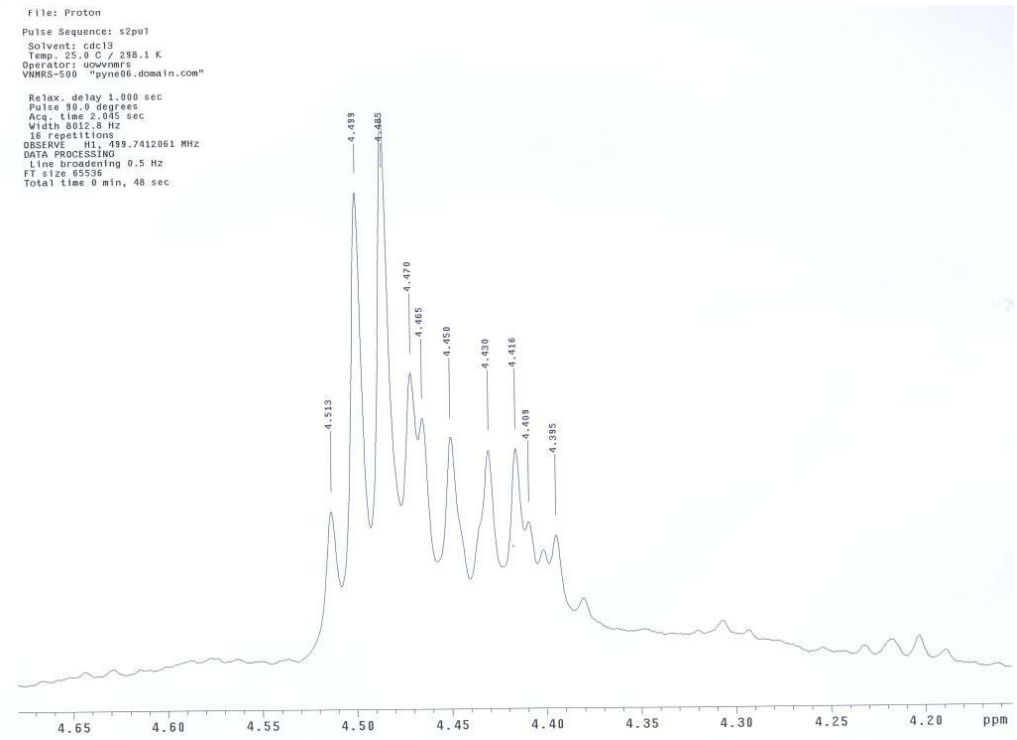

	Chemical shift (ppm)	Multiplicity	Coupling constant (Hz)
CH_3	1.43	t	7.1
CH_3	4.39-4.52	m	-

Appendix III

Infrared (IR) spectra of malonate tethers and bismethano[60]fullerenyl adducts

1. (+)-(*4R,5R*)-bis{[(ethoxycarbonyl)acetoxy]methyl}-2,2-dimethyl-l,3-dioxolane (36)

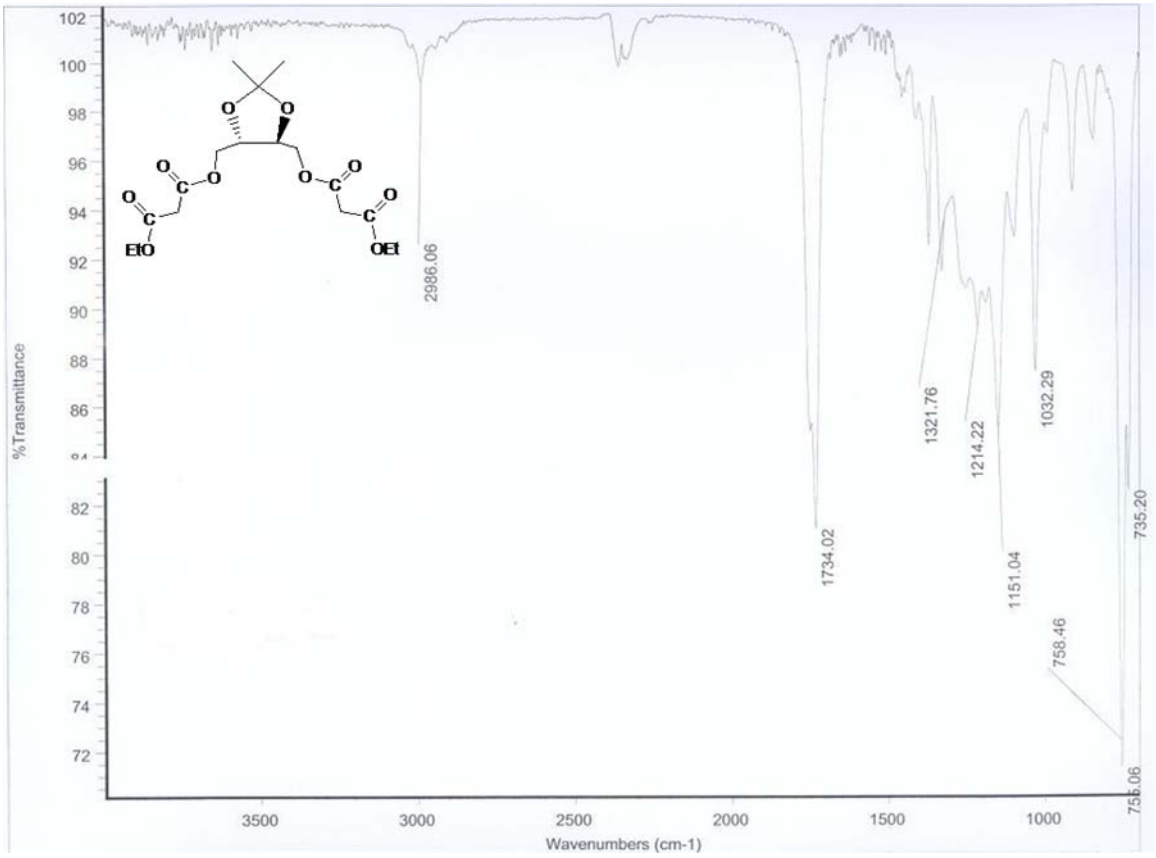

	Wavenumbers (cm^{-1})	
	Results from this study	Reported[161]
$C(sp^3)$-H	2986	-
C=O	1734	1734
C-O	1151	-

2. Diethyl endo-endo-[(*4R,5R*)-(2,2-dimethyl-1,3-dioxolane-4,5-diyl)dimethyl]-1,2:7,21-bis(methano)[60]fullerene-61,61,62,62-tetracarboxylate (40)

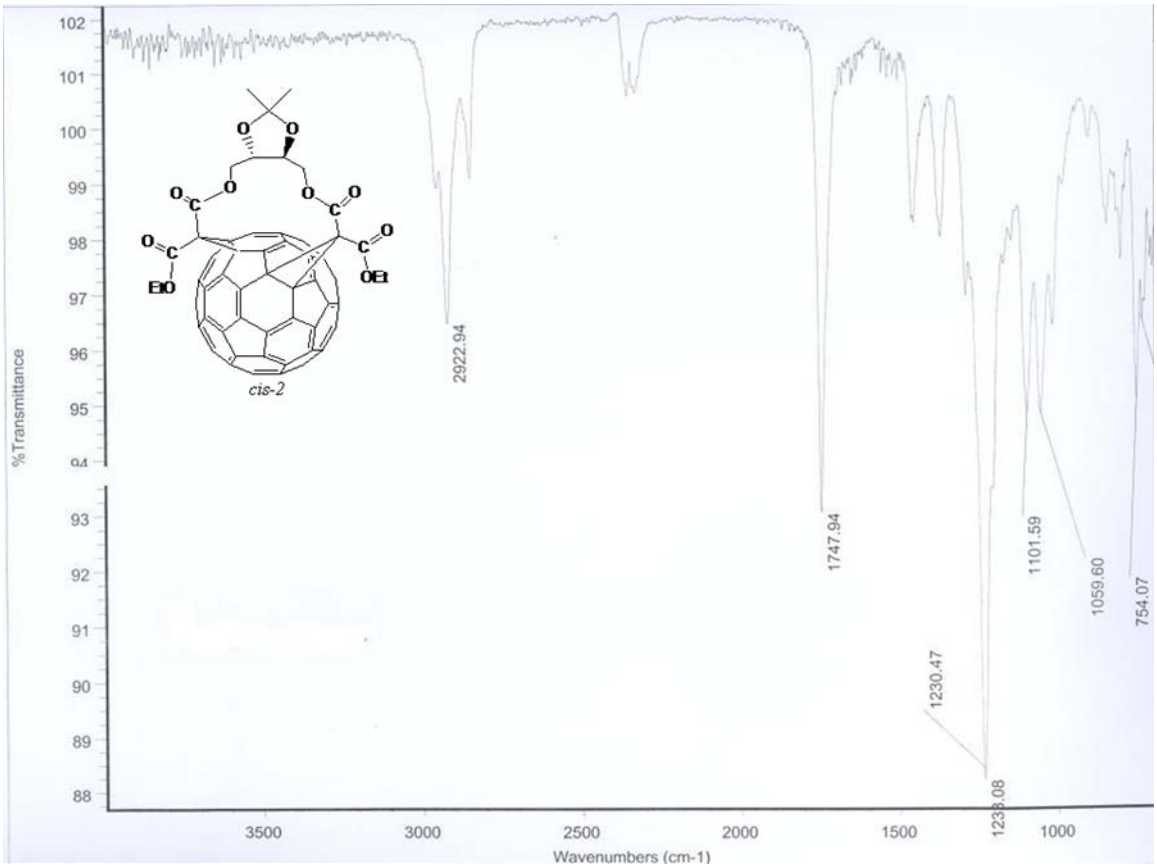

	Wavenumbers (cm^{-1})	
	Results from this study	Reported[161]
$C(sp^3)$-H	2922	-
C=O	1747	1746
C-O	1230	-

3. Diethyl endo-endo-[(*4R,5R*)-(2,2-dimethyl-1,3-dioxolane-4,5-diyl)dimethyl]-1,2:16,17-bis(methano)[60]fullerene-61,61,62,62-tetracarboxylate (41)

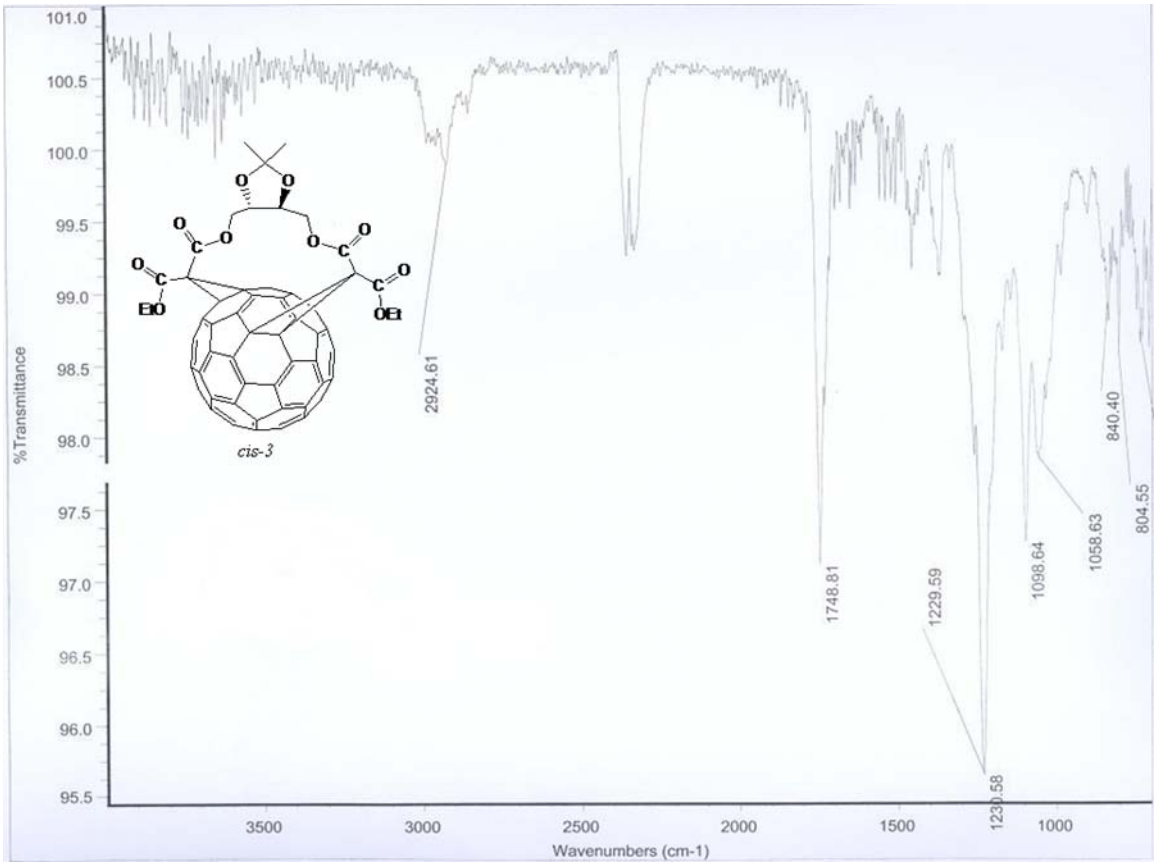

	Wavenumbers (cm^{-1})	
	Results from this study	Reported[161]
$C(sp^3)$-H	2924	-
C=O	1748	1747
C-O	1230	-

4. 1,4-Bis{[(ethoxycurbonyl)acetoxy]methyl}benzene (34)

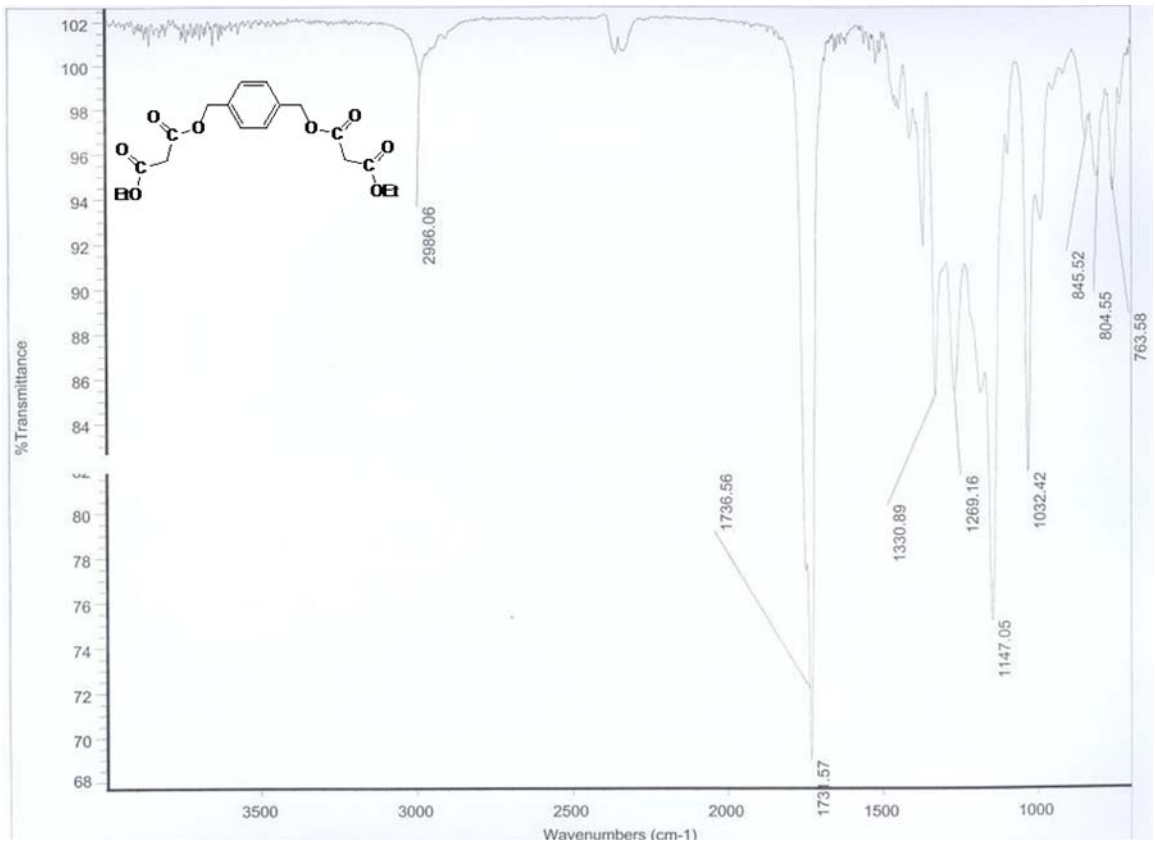

	Wavenumbers (cm^{-1})	
	Results from this study	Reported[161]
$C(sp^3)$-H	2986	-
C=O	1736	1735
C-O	1147	-
C(Ar)	804, 763	-

5. Diethyl endo,endo-(*p*-phenylenedimethyl)-1,2:34,35-bis(methano) [60]fullerene-61,61,62,62-tetracarboxylate (43)

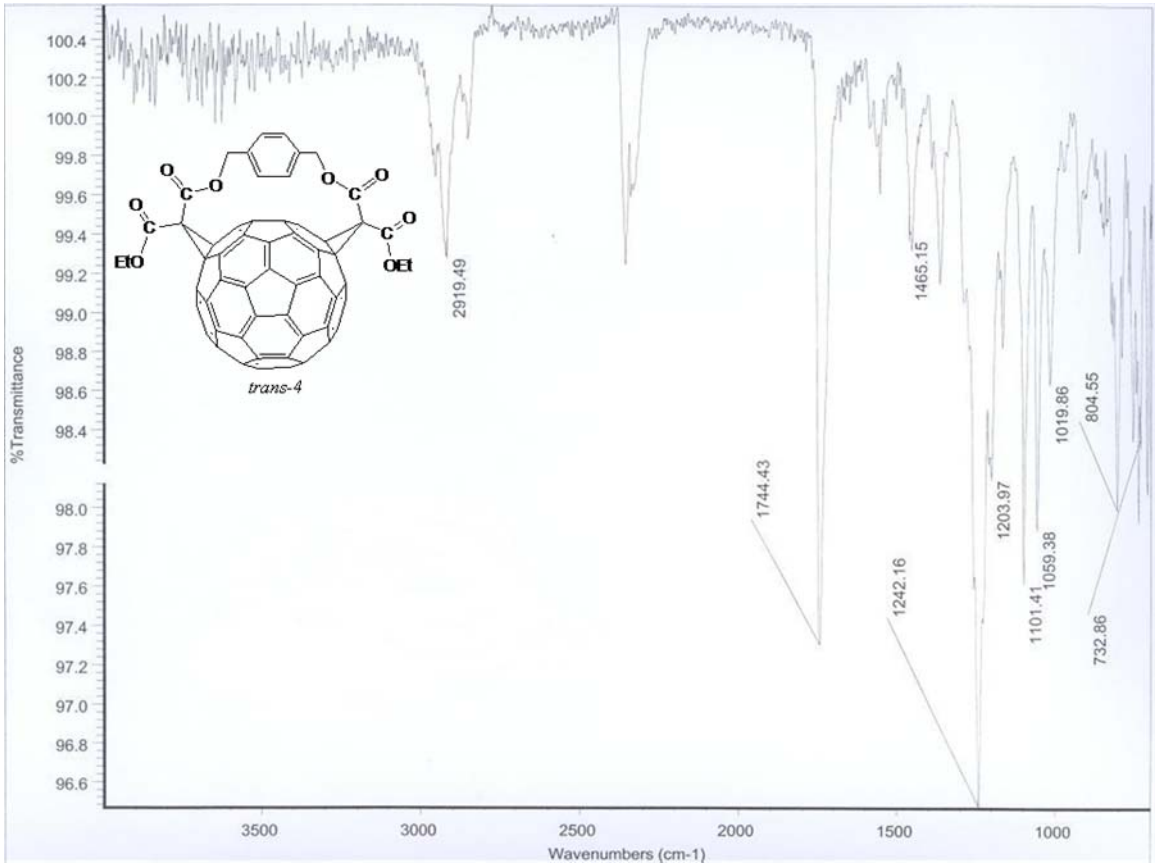

	Wavenumbers (cm^{-1})	
	Results from this study	Reported[161]
$C(sp^3)$-H	2919	-
C=O	1744	1743
C-O	1242	-
C(Ar)	804, 732	-

6. (±)-diethy1endo,endo-(*p*-phenylenedimethyl)-1,2:18,36-bis(methano) [60]fullerene-61,61,62,62-tetracarboxylate (44)

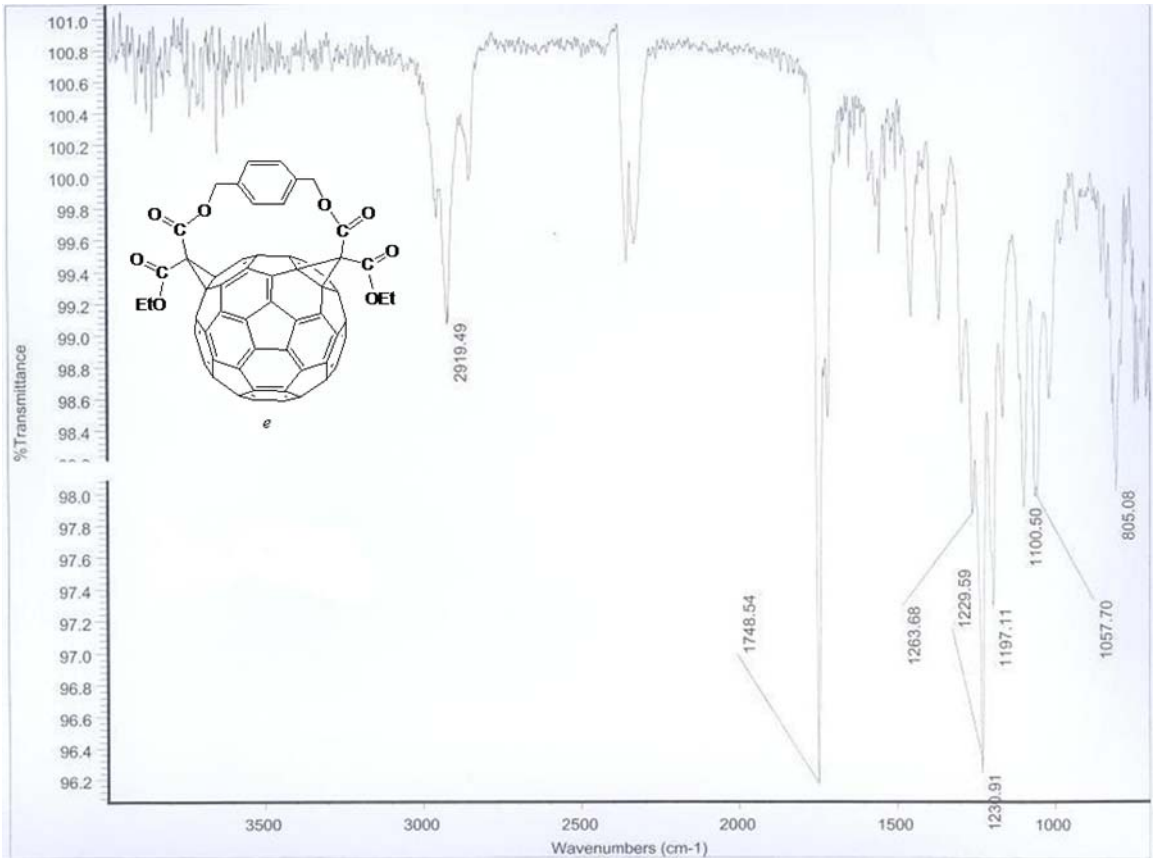

	Wavenumbers (cm^{-1})	
	Results from this study	Reported[161]
$C(sp^3)$-H	2919	-
C=O	1748	1747
C-O	1230	-
C(Ar)	805	-

7. 1,3-Bis{[(ethoxycurbonyl)acetoxy]methyl}benzene (35)

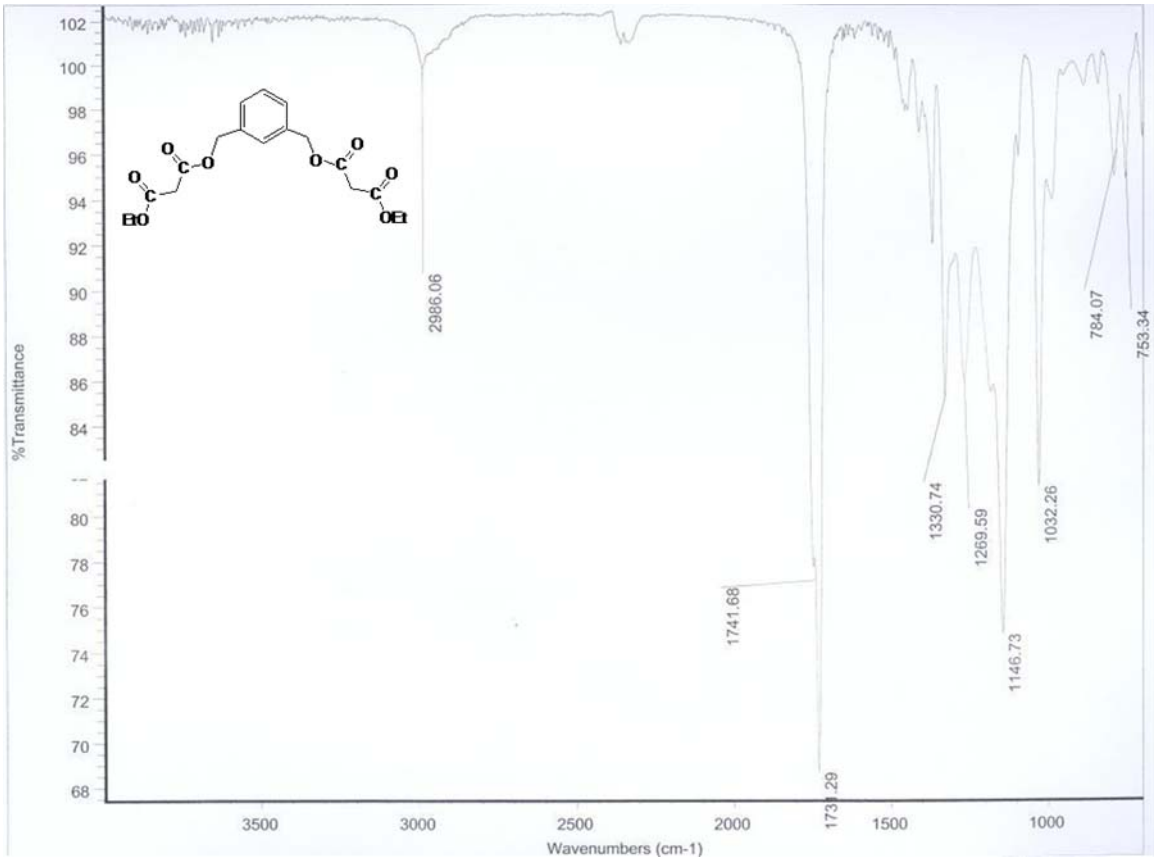

	Wavenumbers (cm^{-1})	
	Results from this study	Reported[161]
$C(sp^3)$-H	2986	-
C=O	1731	1737
C-O	1146	-
C(Ar)	784, 753	-

8. Diethyl endo,endo-(*m*-Phenylenedimethyl)-1,2:7,21-Bis(methano) [60]fu11erene-61,61, 62,62-tetracarboxylate (46)

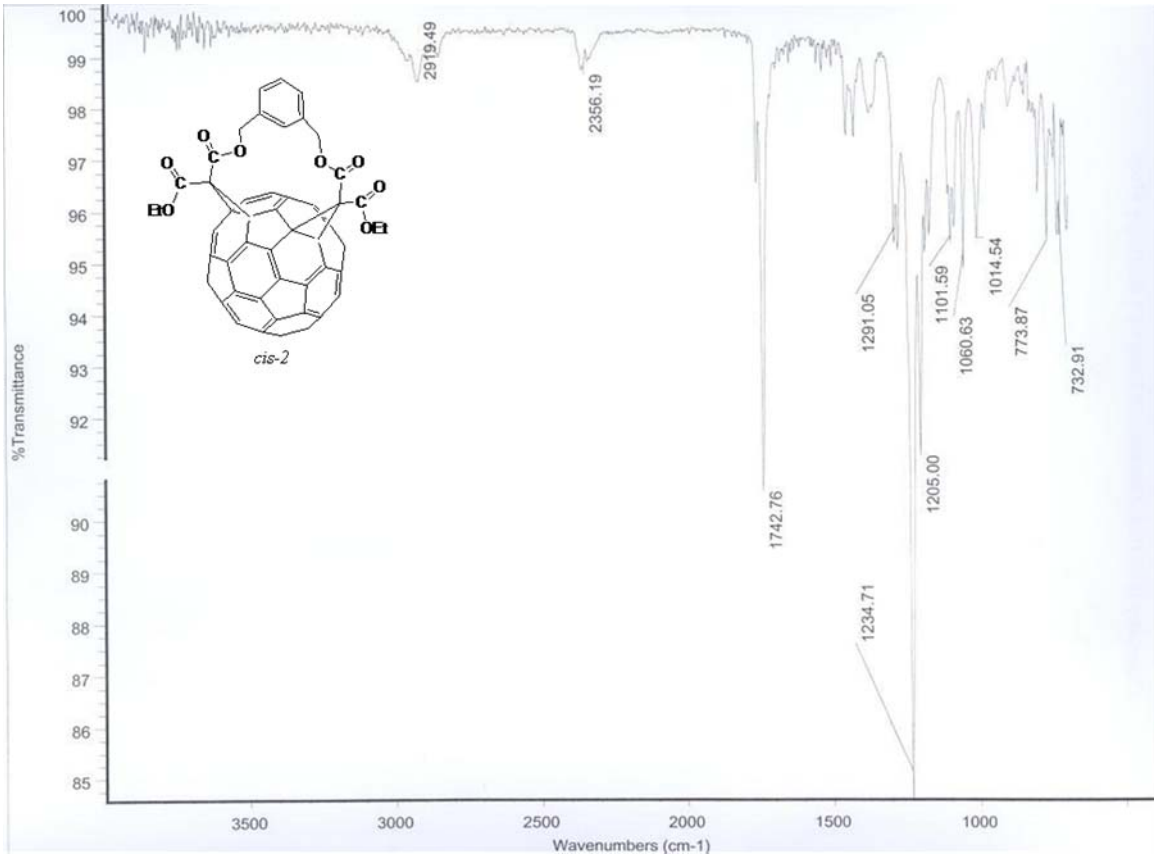

	Wavenumbers (cm^{-1})	
	Results from this study	Reported[161]
$C(sp^3)$-H	2919	-
C=O	1742	1742
C-O	1234	-
C(Ar)	773, 732	-

Appendix IV

Mass Spectra of tethered bismethano[60]fullerenyl adducts and tetraethyl bismethano[60]fullerenyl tetracarboxylate in the positive and negative ion modes

1. Tethered bisadducts (43), (44), (46), (40) and (41), ESI + ([M + Na]$^+$)

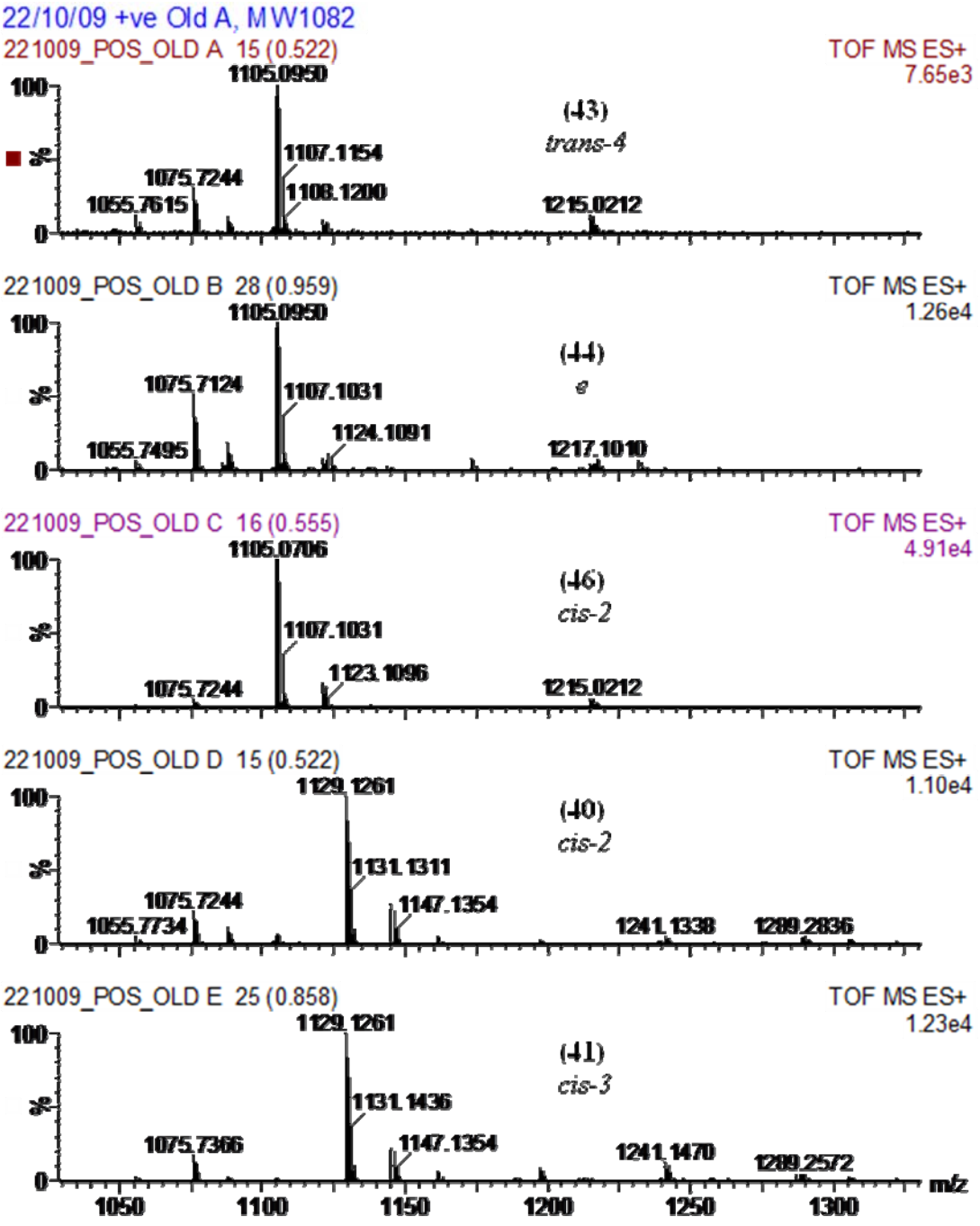

2. Tethered bisadducts (43), (44), (46), (40) and (41), ESI - ([M + H]⁻)

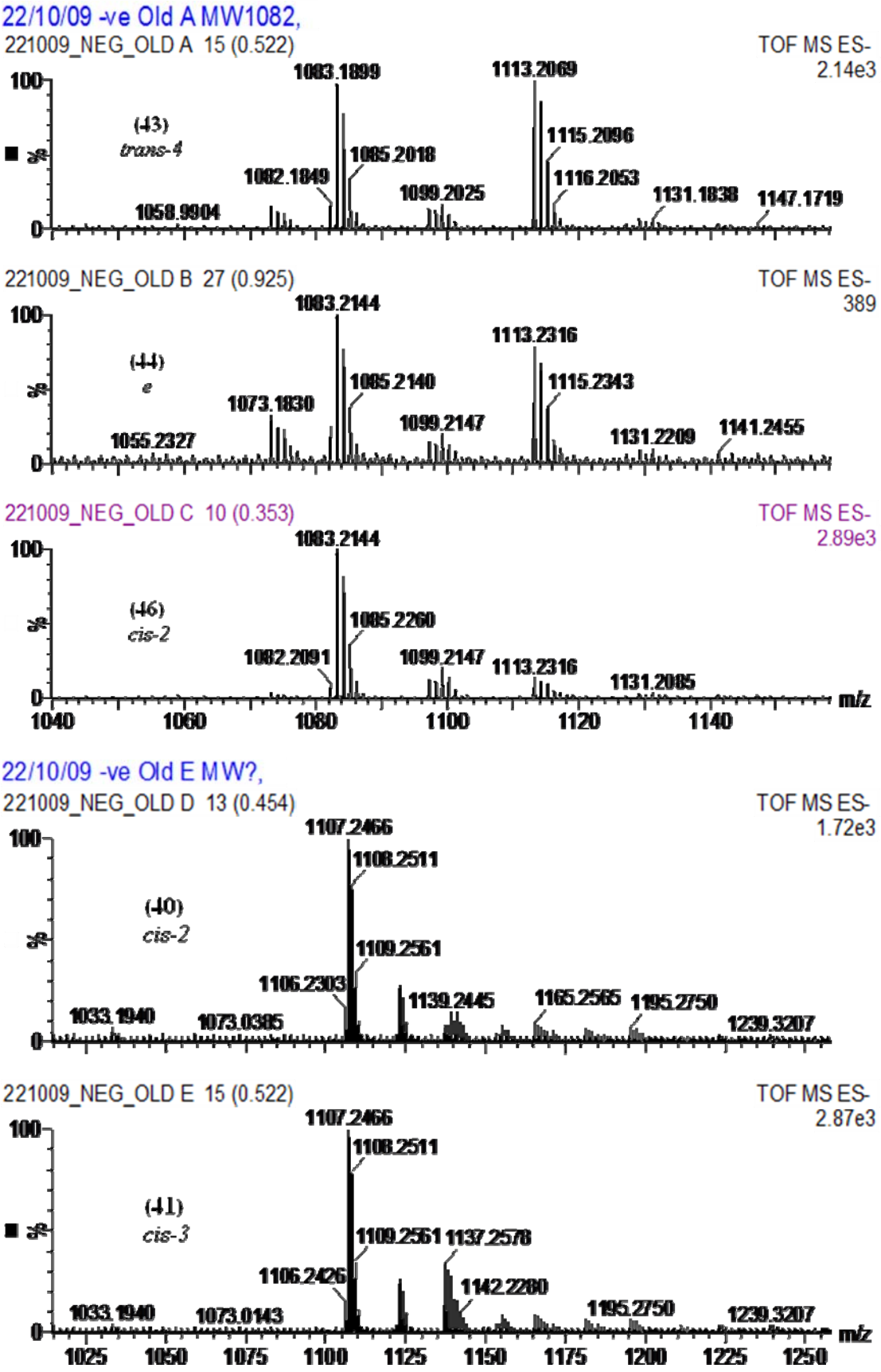

3. MeOH adducted tethered bisadducts, ESI – ([M + H]$^-$ and [M + Me + O]$^-$)

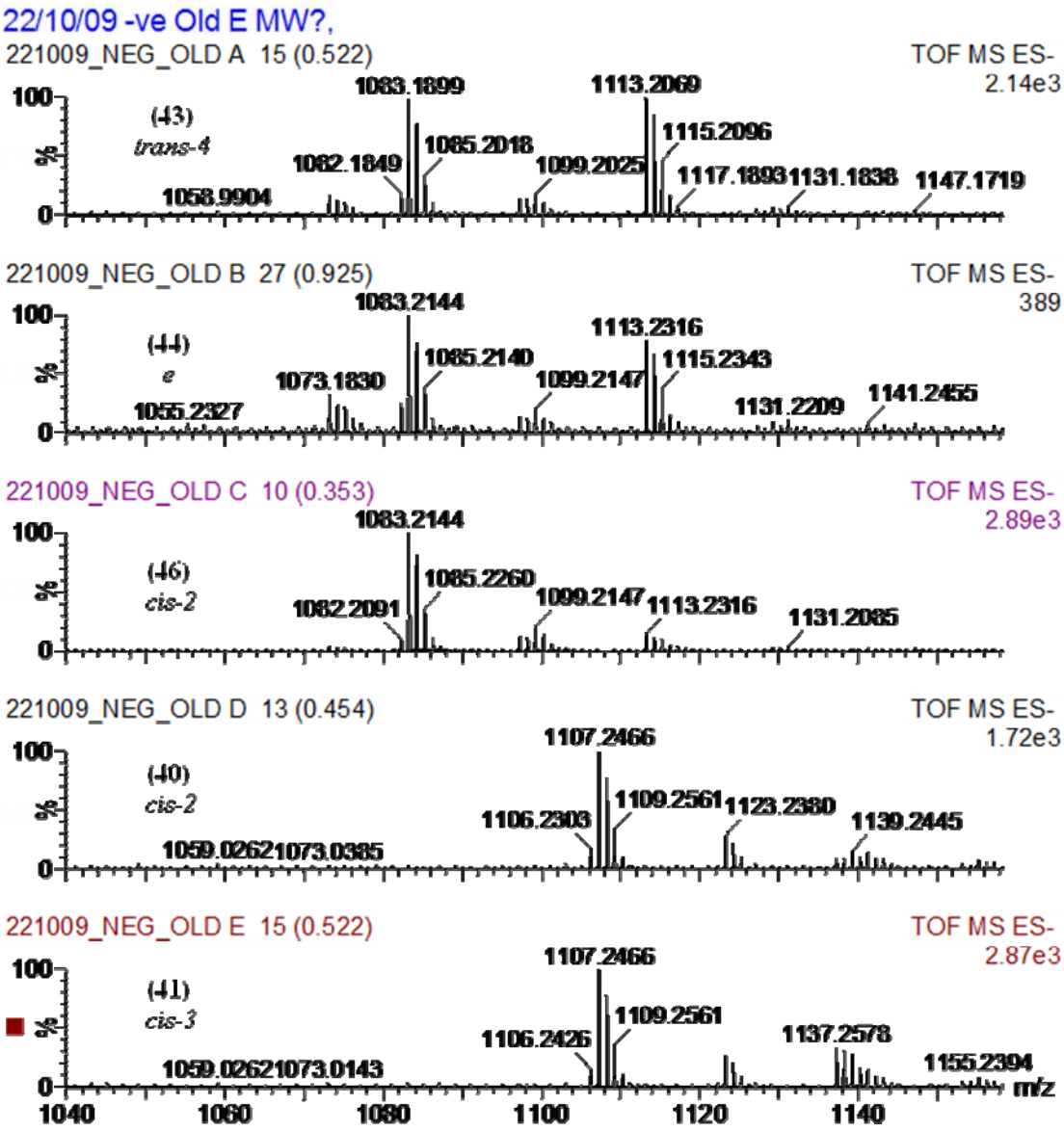

4. Non-tethered bisadducts (47) – (50), ESI + ($[M + Na]^+$)

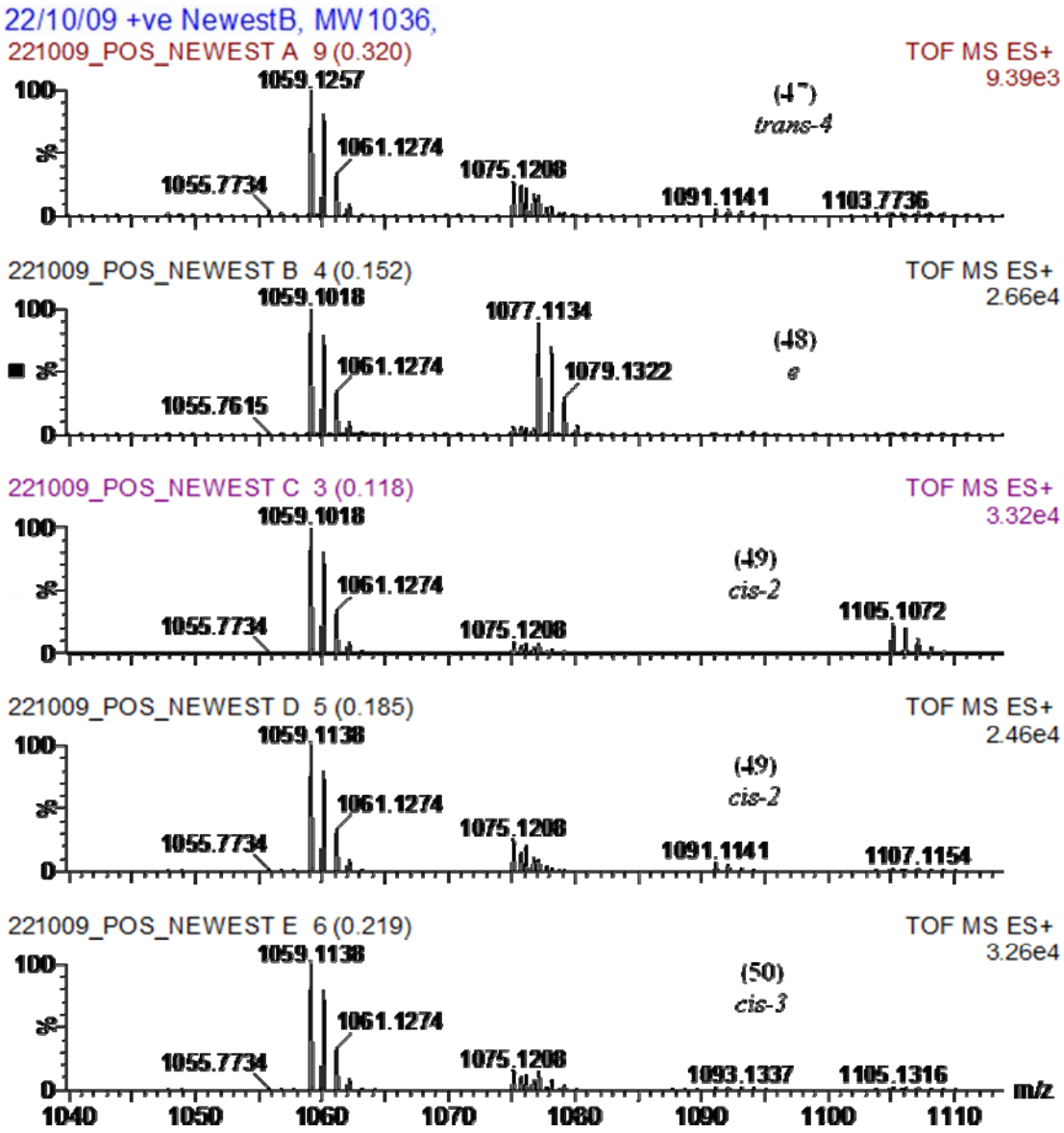

5. Non-tethered bisadducts (47) – (50), ESI - ([M + H]$^-$)